THERMAL-MODELLING OF EXTENSIONAL TECTONICS

by

Carolyn Denise Ruppel

SUBMITTED TO THE DEPARTMENT OF EARTH,
ATMOSPHERIC, AND PLANETARY SCIENCES IN
PARTIAL FULFILLMENT OF THE REQUIREMENTS
FOR THE DEGREE OF

MASTER OF SCIENCE

at the

MASSACHUSETTS INSTITUTE OF TECHNOLOGY

May 1986

Signature of Author _____
Department of Earth, Atmospheric, and Planetary Sciences
May 22, 1986

Certified by _____
Professor Leigh H. Royden
Thesis Supervisor

Accepted by _____
Chairman
Department Committee on Graduate Students

THERMAL-MODELLING OF EXTENSIONAL TECTONICS

by

Carolyn Denise Ruppel

Submitted to the Department of Earth, Atmospheric, and Planetary Sciences on May 22, 1986 in partial fulfillment of the requirements for the degree of Master of Science.

Abstract

This study focuses on the development of a FORTRAN program that generates forward models for the pressure-temperature-time paths of metamorphic rocks in extensional settings. Extension of the lithosphere occurs through three principal mechanisms: pure shear thinning, normal faulting along a single large-scale detachment zone in the crust, and movement along a series of imbricate normal faults. The program written for this study models the thermal effects of each kind of extension, but the emphasis is placed on the process of normal faulting along one discrete fault.

The effects of systematic variations in the angle of fault dip and the rate of lateral movement were tested by monitoring the depth-temperature-time paths of rock particles in the footwall of the normal fault that are initially at the same depth relative to the detachment and relative to the surface. Varying the angle of dip of the fault between 6° and 17°, while holding the rate of lateral displacement constant at 5 mm/yr, does not produce differences in depth-temperature-time paths large enough to cause detectable changes in the textures or mineralogy of metamorphic rocks. When the angle of dip of the fault is varied, but the unroofing rate (unroofing rate equals rate of lateral displacement times tangent of angle of fault dip) is held constant at 0.5 mm/yr, the depth-temperature-time paths for rocks originating at the same level are almost exactly the same. It is therefore not possible to distinguish between the depth-temperature-time paths of rocks that are unroofed at the same rate below detachment surfaces dipping at different angles.

The effects of varying the lateral displacement rate of the hanging wall between 2 mm/yr and 7.5 mm/yr were studied by monitoring the depth-temperature-time conditions of rock particles in the footwall of a normal fault dipping at 11°. At faster rates of displacement, rocks do not experience as much syntectonic cooling as they do when the hanging wall is displaced more slowly, but they undergo a larger drop in temperature once they have reached their final depths. The comparison of depth-temperature-time paths for rocks at different depths relative to the detachment surface shows that, for particles close to the detachment level, different rates of movement will not produce significant differences in the depth-temperature

curves. For rocks more than about 20 km below the detachment level, the depth-temperature paths show greater variation for different rates of lateral displacement of the hanging wall.

The depth-temperature-time paths for rocks uplifted from 15 km to 10 km as a result of pure shear thinning of the lithosphere were compared to those unroofed by movement along a normal fault surface. For the pure shear case, rocks undergo isothermal uplift followed by isobaric cooling through a relatively large change in temperature. At 100 Ma, these rocks have not yet reached the background steady-state temperature. A particle at the same initial and final depths, but unroofed as a result of movement along a normal fault, experiences a significant syntectonic cooling effect and continues to cool isobarically through a small temperature interval for about 20 my following the end of displacement along the fault. After the completion of this interval of post-tectonic cooling (at about 40 Ma for the case studied here), the rock remains at the same temperature. The particle in the pure shear terrain, on the other hand, experiences its greatest temperature changes during the post-tectonic interval.

Thesis Supervisor: Professor Leigh H. Royden
Title: Assistant Professor of Geophysics

Table of Contents

Chapter 1

Introduction

Two fundamental tectonic processes have been proposed to explain how rocks metamorphosed at intermediate crustal levels are uplifted to the Earth's surface. Compressional tectonics provides a mechanism by which the lithosphere is thickened, setting the stage for subsequent erosion during isostatic readjustment. Although uplift induced by an initial crustal thickening event is clearly an important process in some tectonic settings, extensional faulting also appears to be an important mechanism for uplift and tectonic denudation in some orogenic belts.

An important problem in the study of extensional tectonics is characterizing ways in which thinning of the lithosphere occurs. Although geologists have proposed several mechanisms -- including normal faulting and pure shear thinning of the lithosphere -- to explain how extension occurs, a principle difficulty still remains quantifying the various parameters that describe extension of the lithosphere. In the case of normal faulting, for example, the stratigraphic throw is often known, but parameters that describe the dip of the detachment surface and the rate of movement along the fault must often be inferred from sketchy field data. Metamorphic rocks in extensional terrains, however, provide an accurate record of the pressure-temperature conditions to which they have been subjected and often include minerals suitable for isotopic dating. If the information in metamorphic rocks can be extracted and the pressure-temperature-time path reconstructed, it should be possible to determine the rate at which uplift occurred and the approximate depth and temperature of the particle at specific times in the metamorphic history of a rock. Metamorphic rocks, then, probably hold the key to

understanding how extension occurs and at what rates rocks are uplifted in various tectonic settings.

Reconstruction of the pressure-temperature-time paths of metamorphic rocks defines an inverse problem; the metamorphic history is inferred on the basis of information stored in the chemistry of the rock. Royden and Hodges (1984) devised a method to invert the pressure-temperature paths of rocks in thrust terrains, and, theoretically, a similar technique could be employed to infer the complete pressure-temperature history of a suite of rocks from extensional terrains. Once the metamorphic history of a rock can be determined, however, it is nearly impossible to interpret the pressure-temperature-time path in terms of uplift rate, fault dip angle, or mechanism of uplift (pure shear vs. normal faulting) without theoretical models that test the effects of varying extensional parameters on the depth-temperature-time paths of metamorphic rocks. This study attempts to establish some of the theoretical models necessary for the interpretation of reconstructed metamorphic paths through the use of a computer program that generates forward models for the thermal history of a thinning lithosphere. The focus of this study is primarily on testing the effects of systematic variation in the extensional parameters on the pressure-temperature-time paths of rocks at various structural levels in terrains being thinned by either pure shear or normal faulting processes.

1.1 Extensional Processes in Metamorphic Terrains

Extension in a lithospheric plate may be accomodated by normal faulting and ductile stretching, processes that bring progressively deeper crustal layers nearer to the surface through tectonic denudation and pure shear thinning. In geophysical modelling, ductile stretching (pure shear) of the entire lithospheric column has traditionally been favored (Hamilton and Myers, 1966; Stewart, 1971) since it

provides a simplified view of extension as a process in which all particles of the lithosphere change position uniformly relative to one another. A more complicated, and perhaps more geologically-realistic model, explains extension as a process of differential mass transfer: material in the footwall of a major normal fault moves upward along a master detachment or a series of imbricate fault surfaces, and progressively deeper footwall rocks are extracted from beneath the hanging wall. In this model, the original spatial relationship of particles across the detachment surface is completely altered. Though both the footwall and hanging wall of the normal fault are involved in the sort of extension described by this model, it is primarily the footwall rocks that experience the most drastic temperature and pressure changes as tectonic denudation occurs.

The precise role of normal faulting in extension of the lithosphere is not completely understood. Wernicke (1981, 1985) proposed that major low-angle detachments root into the base of the lithosphere, making possible large lateral displacements across a single normal fault zone. High-angle normal faults that either penetrate to deep crustal levels or root into major detachment surfaces are also important in extending the lithosphere. Small movements along a series of these faults can result in more localized thinning of the lithosphere and the rotation of blocks of crustal material. High-angle faults penetrating to deep crustal levels may also play an important role in the extension of the footwall following its extraction from beneath the hanging wall along a major low-angle detachment. Listric normal faulting, low-angle faulting in which the detachment surface is non-planar and extension occurs through movement along a series of hanging wall imbricate faults, has been proposed as another way of accomodating lithospheric extension. The geometric complications introduced by the listric model, however, render it unsuited to the application of simple physical and mathematical

techniques, and the model is ignored in the discussion that follows. Instead, this study focusses primarily on extension resulting from movement on one low-angle detachment.

In the Cordilleran orogenic belt, metamorphic core complexes, uplifted "domes" of metamorphic rock that form the footwall of major Cenozoic detachments, provide a fine laboratory for the investigation of the extensional uplift of rocks from intermediate crustal levels. Metamorphic core complexes are structural features consisting of a mylonitized core flanked by metasediments (Eskola, 1948; Davis and Coney, 1979; Coney, 1980). A warped master decollement surface separates non-metamorphosed hanging wall slices from ductilely-deformed metamorphic rocks in the footwall. In core complexes north of Arizona, at least two distinct phases of deformation have been recognized. Regional metamorphism related to compression in the Sevier fold and thrust belt first affected a large region of the Cordillera in Jurassic-Cretaceous time. This event was followed by a period of rapid uplift and extension that accompanied widespread plutonism during Cenozoic time (Coney, 1979). Where plutonism did not play a locally significant role, previously metamorphosed rocks underwent retrograde metamorphism in response to decompression and cooling associated with uplift. Rocks close to intrusive bodies, however, experienced prograde metamorphism, and their textures and chemical compositions record the thermal changes associated with the intrusion of hotter material.

Core complexes generally comprise a region's highest topography, and exposed footwall metasediments often yield metamorphic pressures corresponding to depths of 10 to 15 km or more. The substantial uplift of these rocks from mid-crustal levels was probably accomplished through a combination of processses: in a purely mechanical sense, erosion during the entire history of the orogenic belt probably

plays an important role in unroofing deeply-buried rocks and, when coupled with tectonic denudation resulting from movement along a normal fault, acts to expose lower plate rocks very rapidly. On the scale of the entire lithosphere, density changes caused by the intrusion of hot peraluminous granite and isostatic reequilibration in response to tectonic unloading may also contribute significantly to the overall uplift of the core complex structure, but a mechanical process like erosion is still required to unroof rocks from intermediate and deep crustal depths.

The role of ductile stretching processes in carrying deeply buried metamorphic rocks to higher crustal levels remains poorly understood. The pure shear model has been used to simplify the analysis of regions as large as the Basin and Range Province of the Western Cordillera (Stewart, 1971) and the Pannonian Basin System of southeastern Europe (Royden et al., 1983), and it is tempting to apply the model to extension related to core complex uplift as well. The importance of metamorphic complexes, however, is that, theoretically, the metasediments of the footwall carry an accurate record of pressure-temperature changes during the processes of uplift, and these decompression and cooling paths should distinguish between normal-fault movement and pure shear thinning as the primary mechanism of uplift. For the reconstructed uplift paths of metamorphic rocks to have maximal usefulness and validity, a quantitative understanding of the relationship between extensional tectonics and the thermal structure of the lithosphere must be established. This study endeavors to examine the effects of extension on geothermal regimes and to establish quantitative models for pressure-temperature-time histories of rocks at various structural levels in extensional terrains.

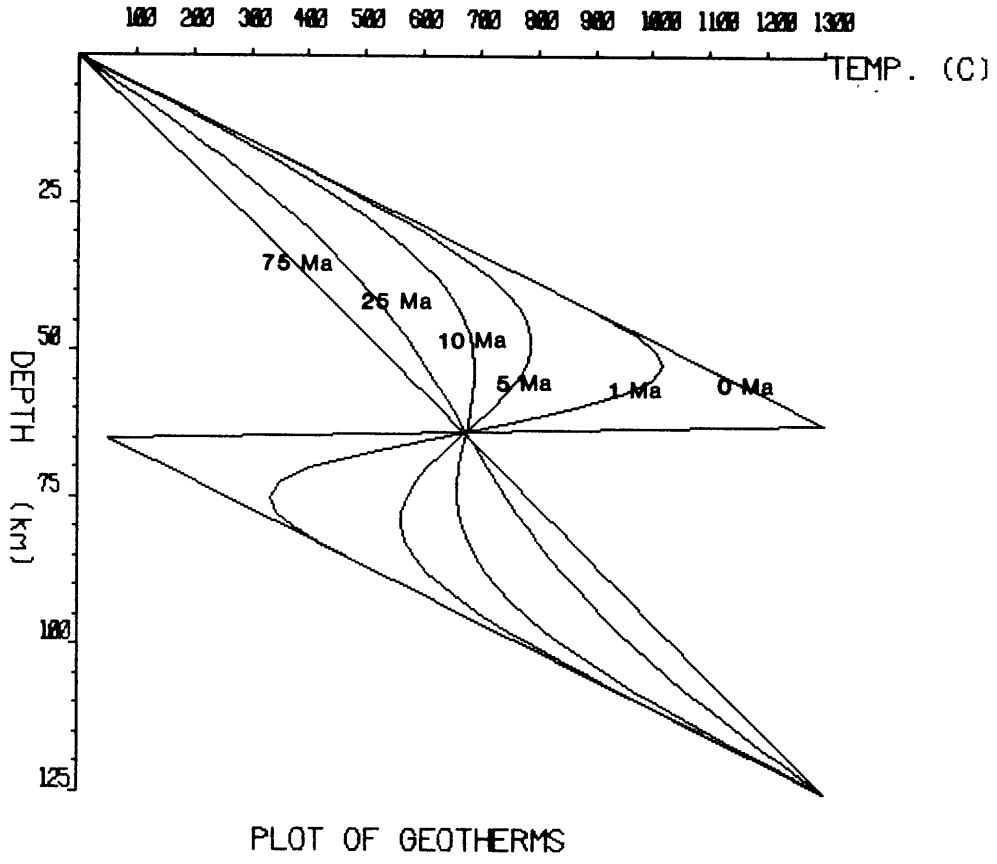

Figure 1-1: The relaxation of a sawtooth geotherm produced by doubling the crustal thickness in an instantaneous compressional event. Reequilibrating geotherms are given for 0, 1, 5, 10, 25, and 75 Ma.

1.2 Forward-Modelling

Forward-modelling of geothermal relaxation in various extensional settings provides a basis not only for the interpretation of uplift in core complexes, but also for understanding the pressure and temperature histories of rocks on a larger and more general scale. The problems of geotherm relaxation and prediction of theoretical pressure-time paths of metamorphic rocks were first solved for compressional models by Oxburgh and Turcotte (1959). Furlong and Londe (in

press) have recently used a finite difference technique to develop similar models for Basin and Range extension. In the idealized case, thrust faulting instantaneously doubles the thickness of the lithosphere, creating a sawtooth geotherm with a discontinuity where the bottom of the hot upper plate meets the top of the cool lower plate. As the geotherm reequilibrates, cooling of upper plate rocks and heating in the lower plate produce, respectively, retrograde and prograde metamorphism. Fig. 1-1 shows the reequilibration of a sawtooth geotherm created by instantanous doubling of the elastic thickness of the lithosphere for times 0 Ma, 1 Ma, 5 Ma, 10 Ma, 25 Ma, and 75 Ma. The stationary point at 62.5 km and 650°C is an artifact of the special case chosen for this analysis.

A similar model can be applied in areas undergoing extension by means of movement on a normal fault surface. In this case, cool upper plate rocks move onto hotter lower plate rocks, producing a steplike discontinuity in the geotherm. Reequilibration of the geotherms, shown in Fig. 1-2, involves heating of the relatively thin hanging wall and cooling in the thick stationary footwall, thermal adjustments that may cause prograde metamorphism of upper plate rocks and slow retrogression in the lower plate. The pure shear model, in contrast to the compressional and extensional scenarios, does not involve mechanical movement along discrete normal faults and therefore creates no discontinuities in the geotherm. Instantaneous stretching leaves each particle of the lithosphere at its original temperature but closer to the surface. Assuming that the geotherm then re-equilibrates to the level of the pre-stretching lithospheric thickness as shown in Figure 1-3, all rocks must undergo net cooling and therefore retrograde metamorphism.

The next chapters will introduce a computer technique that can be used to generate quantitative models for the relaxation of geotherms perturbed by extension

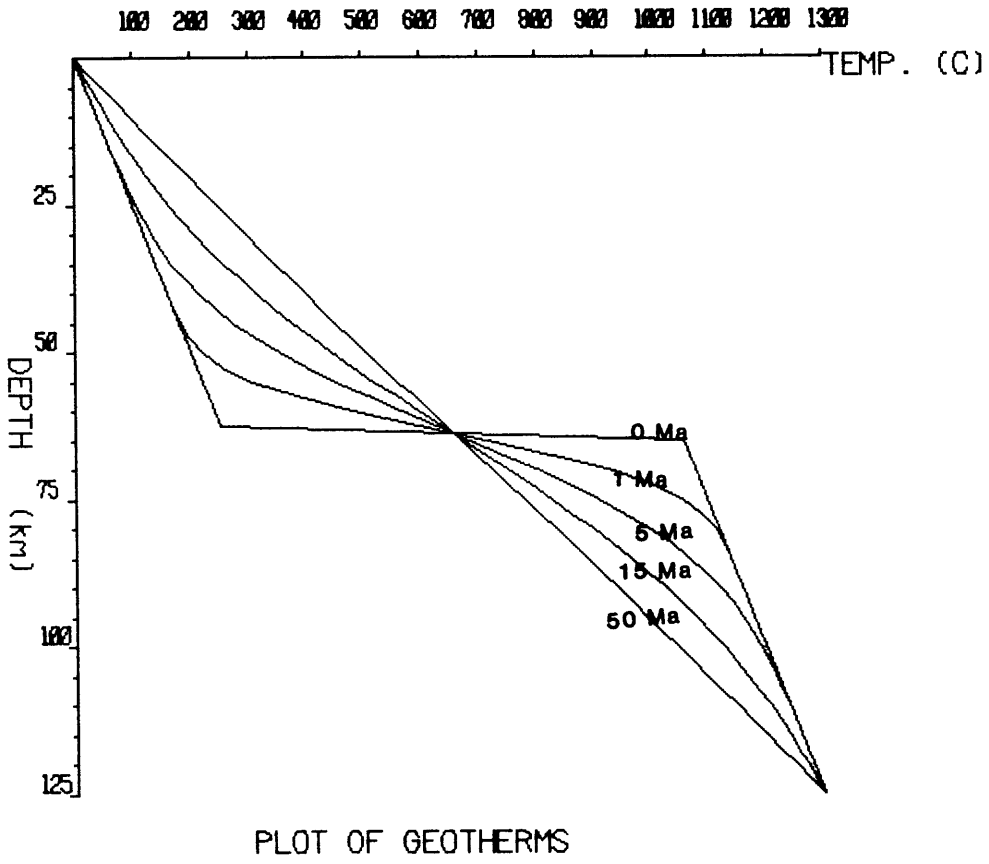

Figure 1-2: Relaxation of step discontinuity in a geotherm produced by instantaneous extension of the crust through movement along a normal fault surface. Reequilibrating geotherms are shown for times 0, 1, 5, 15, and 50 Ma. Stationary point at 62.5 km and 650°C is a result of special conditions used in this problem.

of the lithosphere. The focus will be placed on understanding how changing the geometry of a normal fault or the rate of movement along the detachment surface affects the depth-time-temperature paths of metamorphic rocks in the footwall. Finally, the relative effects of thinning the lithosphere through pure shear extension and tectonic denudation above a normal fault surface will be discussed through the comparison of depth-temperature-time paths generated by the forward modelling computer program.

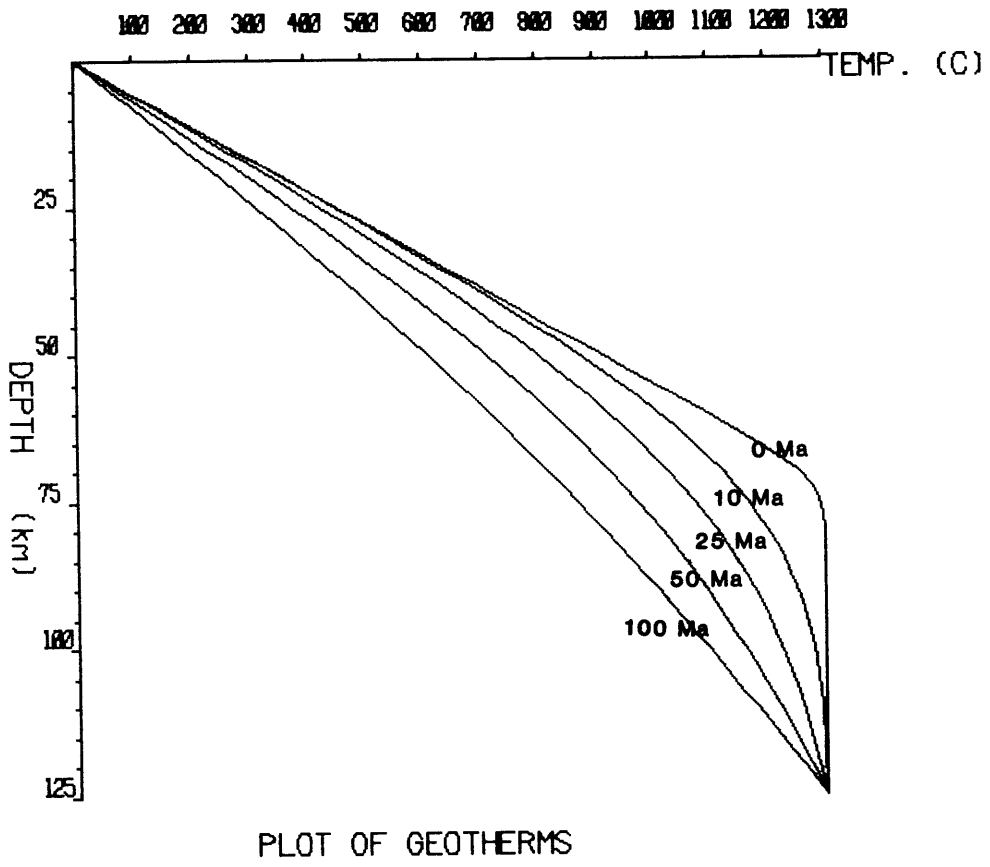

Figure 1-3: Relaxation of a geotherm perturbed by pure shear extension of the lithosphere with $\beta = \gamma = 1.75$ (75% extension of the entire lithosphere). Curves are given for times 0 Ma (end of instantaneous stretching episode) and 10, 25, 50 and 100 Ma.

Chapter 2

Quantitative Modelling

The development of a quantitative model for cooling and uplift paths of rocks in extending terrains requires the use of a mathematical technique that can be applied repeatedly and accurately over long time periods. Flexibility and ease of calculation are also important considerations, and the functional relationship employed must hold for all initial conditions. Even with the use of high-speed computers, certain mathematical techniques, particularly those involving the calculation and summation of many terms, are particularly cumbersome and difficult to check with a hand-held calculator. Fourier analysis is traditionally used to calculate the evolution of various geotherms, but the repeated calculation of sine and cosine coefficients and the necessity of summing over a large number of terms in the time intervals immediately following a thermal perturbation renders the uniform application of this technique undesirable. The error function provides a good alternative to lengthy Fourier summation for calculations during the several million years postdating a thermal disturbance, but combining the techniques -- using the more convenient error function for the initial stages of re-equilibration and switching to the more accurate Fourier summations once the length of the expressions becomes manageable -- introduces a functional discontinuity into the analysis. Numerical analysis, on the other hand, can be applied continuously from the beginning of a problem without the necessity of changing to a more manageable functional relationship after some initial period of time and provides a flexible technique suitable to the introduction of faults in the lithosphere.

2.1 Forward Modelling with Finite Difference Methods

Finite difference iteration, described by Carslaw and Jaeger (1959) for linear heat flow in infinite regions, provides a flexible, fairly accurate, and computationally-simple alternative to Fourier summations. In order to calculate geotherms using any analytical mathematical technique, it is necessary to find solutions to the second-order differential equation for the diffusion of heat in a solid, given by:

$$\frac{\delta^2 T}{\delta x^2} = \frac{1}{\kappa}\frac{\delta T}{\delta t} \qquad (2.1)$$

where T(x,t)=temperature function
κ= thermal diffusivity, assumed constant

Solutions of the heat flow equation are of the form:

$$T = T_m x/l + (2T_m/\pi)\Sigma(1/n)\sin(n\pi x/l)\, e^{-n^2\pi^2\kappa t/l^2}$$

where l=lithospheric thickness
T_m=constant temperature base of lithosphere
T=temperature at time t and depth x

The size of the exponential expression for a given time obviously governs the number of terms needed in the summation and introduces a complication in the Fourier technique: not until the exponential part of each term under the summation sign has a value less than about 0.01 can many of the terms be dropped. By replacing partial derivatives with arithmetic expressions, the finite difference method avoids solving the heat flow equation, making direct computation of T possible for a set interval in x and t space. Finite difference iteration is perhaps most easily understood by examining the derivatives of a function $y = f(x)$. If $y_1 = f(x_1)$ is one point on the curve, then another point is given by $y_2 = y_1 + \Delta y = f(x_1 + \Delta x)$. Subtracting the two yields:

$$\Delta y_1 = f(x_1 + \Delta x) - f(x_1) = y_2 - y_1$$

and this Δy_1 becomes the first forward difference. By analogy, the forward

difference Δy_n is given by $\Delta y_n = y_{n+1} - y_n$ if all intervals up to $n+1$ are regularly spaced. In a similar manner, the second forward difference of a function $\Delta^2 y_n$ is calculated as follows:

$$\Delta^2 y_1 = \Delta\Delta y_1 = \Delta y_2 - \Delta y_1 \tag{2.2}$$

given: $\Delta y_2 = y_3 - y_2$ and
$\Delta y_1 = y_2 - y_1$

$$\Delta^2 y_1 = y_3 - 2y_2 + y_1$$

and, in general,

$$\Delta^2 y_n = y_{n+2} - 2y_{n+1} + y_n$$

Note that the forward differences given are for y as a function of only one variable, although the original heat flow equation requires a solution for T as a function of both spatial and temporal variables. This difficulty is easily avoided, however, by evaluating T at a point $x = m\epsilon$, where ϵ is the size of an interval and m is one in a set of consecutive integers. This step effectively reduces T(x,t) to T(t), and the original heat flow equation can be rewritten, replacing the result in Equation (2.2) by the corresponding second forward difference:

$$\epsilon/\kappa^2[\delta T/\delta t] = T_{m+1}(t) - 2T_m(t) + T_{m-1}(t) \tag{2.3}$$

This equation does not yet provide a completely numerical formula for calculating T since the partial time derivative remains. Applying the reasoning about evenly-spaced intervals to the time derivative and writing $t = n\tau$ where τ = time interval and n is a set of consecutive integers, Equation (2.3) can be rewritten:

$$T_m/t = [T_{m,n+1} - T_{m,n}]/\tau$$

or:

$$T_{m,n+1} = (\kappa\tau/\epsilon^2)[T_{m+1,n} + T_{m-1,n}] - (2\kappa\tau/\epsilon^2 - 1)\, T_{m,n} \tag{2.4}$$

This expression provides a completely numerical method for calculating equally-spaced solutions to the heat flow equation. Although second forward differences are neglected in writing out the differential equation in numerical form, these terms are generally small and can be dropped without losing much of the accuracy of the approximation. The reliability of the method is, in fact, much more sensitive to the size of the constant or modulus $M = \kappa\tau/\epsilon^2$ than to dropping higher order differences. As the modulus value changes in response to variations in τ and ϵ, the stability and convergence conditions must be met. Using simple error propagation techniques, Carslaw and Jaeger (1959) show that finite difference equation given above is stable -- errors do not increase when the technique is repeatedly applied -- when the modulus M meets the condition:

$$M = \kappa\tau/\epsilon^2 <= 0.5$$

Table 2-I shows the calculated values for M using a set value of 0.008 cm^2/sec (or 3.344 W/m-K) for thermal diffusivity and various values of ϵ. In this application, ϵ represents the size of the depth increment to be used in dividing up the lithospheric slab, and τ is a time increment to be used in repeated calculation of geothermal relaxation out to several million years. Though M=0.167 is the optimal value for the minimization of errors, the technique used must also be computationally-efficient, able to be completed quickly on a high-speed computer. For the purposes of this study, it was found that setting $\tau = 0.1$ my and $\epsilon = 2.5$ km (corresponding to M=0.4125) provided both a fast and fairly accurate method for the relaxation of geotherms over long time periods.

An important characteristic of the finite difference technique is the necessity of specifying the boundary conditions for the linear relaxation problem. In practice, however, the entire initial geotherm (for time t=0.0 my) must be given as a "seed" for the first iteration. Finite difference techniques use values from the immediately

ϵ	M=0.167 τ	M=0.5 τ
1.0 km	0.007 my	0.012 my
2.5 km	0.041 my	0.124 my
5.0 km	0.165 my	0.495 my
10.0 km	0.660 my	1.980 my
15.0 km	1.485 my	4.450 my
20.0 km	2.640 my	7.920 my

Table 2-I: Table showing the relative values of τ and ϵ necessary to maintain the value of the modulus M: $0.167 < M < 0.5$

preceding time interval to generate figures for the next interval. It is therefore not sufficient to specify only the boundary conditions -- the temperatures at the base and top of the lithosphere -- unless the geotherm is linear between the upper and lower boundaries. In order for the finite difference technique to be applied accurately and repeatedly, it is also necessary that the grid-spacing (i.e. the size of ϵ, the spatial interval, and τ, the time interval) remain constant and that the boundary condition temperatures either change not at all or only slowly relative to τ.

2.2 Applicability to Real Geologic Problems

In practice, any mathematical technique used to describe the behavior of real physical systems serves, at best, as an approximation to the actual state of the system. Forward-modelling of geotherm relaxation in various tectonic settings relies heavily on the assumption of ideal behavior of a closed system and the use of the small amount of physical data available. Surface heat flow data, for example, serves to establish a working model for the near-surface thermal gradient, and parameters like the conductivity of the lithosphere can probably be safely assumed. More difficult to pinpoint are the rate of movement on fault surfaces, the precise

nature of the compressional or extensional event that produced the original temperature perturbation, radioactive heat production at various crustal levels, and the thermal thickness of continental lithosphere.

The primary importance of an iterative technique in physical applications is the use of previous geotherms in calculating those in the next time interval. The thermal state in the lithosphere at any given time is obviously dependent on the prior temperature distribution, a fact that makes the finite difference method conceptually simple. In Fourier analysis of geotherm relaxation, the temperature structure is completely recalculated at each time interval, and there is no clear relationship between the geotherms at two different times. Finite difference techniques also provide a rough approximation of one-dimensional heat flow. Figure 2-1 shows the qualitative relationship between the temperature at depth $x=m\epsilon$ at times $n\tau$ and $(n+1)\tau$. Note that, in a gross sense, the process of calculating the geotherm at $(n+1)\tau$ requires the heat from elements above and below depth $x=m\epsilon$ at time $t=n\tau$ to effect changes in the temperature at the same depth in the next time interval ($t=(n+1)\tau$). This yields an intuitively simple model for understanding the linear heat flow problem in one-dimension. Finally, perhaps the most important advantage of numerical analysis in examining changing temperature structures is its flexibility. Unlike the Fourier technique, finite difference modelling is applicable even in problems in which parts of the lithosphere are displaced along discrete normal fault zones.

The full two-dimensional heat flow problem requires more calculations than the one-dimensional description, but proper application of the one-dimensional solution provides a good description of two-dimensional heat transfer. In order to use this approximation technique to follow the temperature changes experienced by a set of particles, the one-dimensional problem must be solved simultaneously for

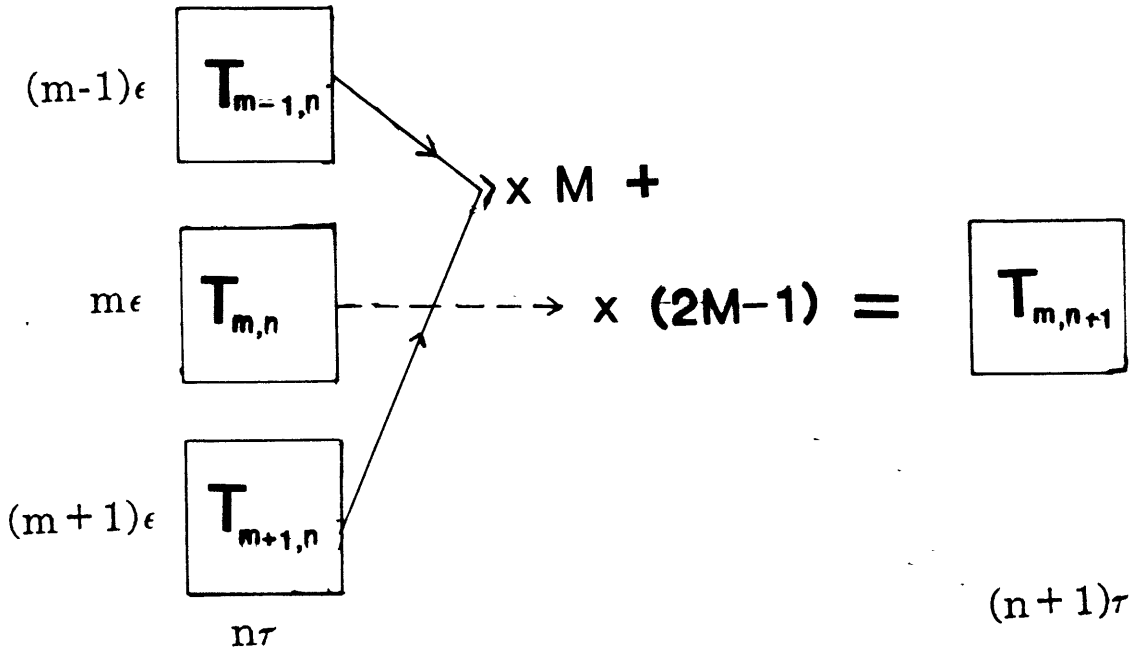

Figure 2-1: The qualitative relationship between the values calculated at time $t=n\tau$ and at time $t=(n+1)\tau$.

several columns. Simple linear extrapolation between the one-dimensional solutions then provides a reasonable description of the two-dimensional part of the problem. This approximation of two-dimensional heat flow assumes that the principal direction of heat transfer within the lithosphere is vertical and that horizontal heat flow can be ignored. The cooling effects of displacing the hanging wall of a normal fault will cause the greatest temperature changes in the vertical direction, and neglecting horizontal heat flow provides a simplified and realistic approximation for the transfer of heat in the lithosphere.

Like Fourier analysis, finite difference modelling examines temperature

changes in an immobile column of the lithosphere. In the terminology of continuum mechanics, the method yields a Eulerian description of the system's behavior, one in which the observer remains fixed at a point and watches the changes that occur in a one-dimensional line of sight. This concept is of special importance in the sort of forward modelling problems that have been examined in this study: When the footwall of a normal fault moves upward from beneath the dipping fault surface, the particles in the lower plate obviously move together. In a Lagrangian description of the problem, the observer attaches himself to the particles in the footwall and moves with them, noting temperature changes that occur in the same set of particles throughout their entire history. His frame-of-reference moves with the footwall, allowing him to observe the complete time and position changes of one set of particles. The Lagrangian description, then, is of obvious importance in modelling the depth-temperature-time paths of individual rock particles, but requires a two-dimensional coordinate system in the place of the one-dimensional column of data generated by the finite difference method.

A finite difference technique based on the linear heat flow equation can be seen as providing a Eulerian description of the system in the simplest case of calculating geotherms at a set position in the lithosphere, but the repeated application of one-dimensional techniques can, as described above, lead to a Lagrangian description. Only through the application of the method to several one-dimensional columns at a given time period can a complete description of the geological problem be given. The ability of the finite difference technique to provide both Eulerian and Lagrangian descriptions makes it especially useful in forward-modelling. It provides the geotherms needed for understanding the effect of tectonic events on temperature regimes, and the pressure-temperature paths used for predicting theoretical metamorphic assemblages and theoretical cooling paths.

2.3 Assumptions Inherent in Analytical Techniques

An important problem in modelling geologic systems is balancing the assumptions of ideality with complicated descriptions of real physical systems. Simplifying assumptions are necessary to satisfy the constraints of the mathematical techniques and to make the particular models tested applicable to a wide range of geologic problems. Theoretically, it is possible to vary almost all problem parameters, to introduce inhomogeneities in the lithosphere, and to model non-linear relaxation of geotherm perturbations. These complications, although possibly rendering a particular model more realistic, serve to obscure the qualitative response of a generalized lithosphere. As the number of dynamic parameters increases, it becomes more difficult to trace anomalies in relaxation patterns to a particular lithospheric property, and the usefulness of the technique is radically reduced.

The most fundamental assumption made in all models developed for this study is that of ideal lithospheric behavior. Not only is it assumed that the lithosphere can be modelled as a homogeneous solid of constant thickness, density, and thermal conductivity, but the lithosphere is also assumed to display perfectly isotropic behavior during pure shear extension and perfectly brittle behavior during normal-faulting episodes. Homogeneity of the lithosphere is undoubtedly the poorest assumption made in this study and also the one that poses the greatest conceptual difficulty. Extension of the lithosphere through the normal-faulting mechanism requires the presence of a detachment surface that, in real geologic settings, often serves as both a structural and compositional boundary between the hanging wall and footwall. By imposing the constraint of lithospheric homogeneity but retaining the normal fault mechanism, the models tested here imply that a detachment surface serves only as a structural boundary and that the rocks below

the detachment can somehow be metamorphosed while adjacent hanging wall rocks with the same bulk compositions and same gross properties remain unmetamorphosed. In real geologic situations, sedimentary rocks typically occur above the detachment level while crystalline basement or plutonic rocks form the footwall. To a first order, this compositional contrast across the detachment represents a discontinuity in density and thermal conductivity across the fault surface.

The most fundamental modification to the computer program used in this study would involve the thermal diffusivity parameter because only this value is involved in every finite difference calculation. Thermal diffusivity κ is defined as:

$$\kappa = k/\rho c$$

where k= thermal conductivity
ρ= density
c = specific heat

Thermal conductivity, density, and specific heat are all properties that are primarily dependent on the nature of the medium they describe. As a function of these properties, thermal diffusivity (κ) must theoretically be changed each time the composition of the system is altered. Because the models developed here aim only to provide a crude approximation of the theoretical pressure-temperature-time paths of metamorphic rocks, variations in κ only complicate the analysis and will not be considered here.

The techniques used in this study require no quantification of the lithosphere's elastic properties, but several assumptions are inherent in the modelling of tectonic processes. As discussed in Section 3.2, the mathematics of the problem of pure shear extension of the crust is taken from the model of Royden et al. (1983), which assumes that a long stretching event may be broken up into a number of instantaneous stretching episodes. Throughout this pure shear

process, the area of a unit element is preserved, an indication that isotropy is an inherent assumption of this technique. Although the idealized homogeneous lithosphere does not necessarily have to deform isotropically, nonisotropic behavior is difficult to model because complicated numerical techniques are required to evaluate the integrals involved in the continuum mechanics description of the system. Nonisotropic behavior of the lithosphere is therefore not considered in this study.

The mathematics of the normal-faulting routines, on the other hand, is premised on the assumption of perfectly brittle behavior of the lithosphere. In real geologic settings, brecciation, mylonitization, shear heating, and ductile attenuation in the hanging wall are often associated with movement of material along a normal fault. Although important, these effects are difficult to quantify and must be ignored in idealized models of perfectly brittle responses to deformation. The normal fault routines, working on the simple premise that a particle must maintain a constant spatial relationship with every other particle in the same wall of the normal fault, are able to mimic brittle behavior in a homogeneous lithosphere.

Related to the problem of parameterizing the elastic and thermal properties of the lithosphere is the difficulty introduced by the presence of hot asthenospheric material at the base of the lithosphere. In the Earth, the asthenosphere acts as a heat source, introducing heat into the lithosphere from below and causing the lowermost lithosphere to undergo partial melting, a decrease in density, and deformation that is more complicated than the simplified pure shear and brittle failure normal-faulting models used here. This assumption of closed system behavior for a cooling slab renders the problem much less realistic, but, on the small scale of the sort of normal faulting effects studied here (typically less than 200 km in lateral extent), the closed system approximation is convenient, practical, and not too inaccurate.

Besides ignoring the transfer of heat from the asthenosphere to the lower lithosphere, the models developed for this study hold the rate of radioactive heat production constant over the duration of each program loop. In order to test the validity of this assumption, it is necessary to examine the decay rates of the most common isotopes of uranium, thorium, and potassium, the elements that produce most of the Earth's radioactively-derived heat. The decay schemes of the four most abundant isotopes of these elements -- ^{238}U, ^{235}U, ^{232}Th, ^{40}K -- have half-lives of 4.47 Ga, 0.74 Ga, 14.0 Ga, and 1.25 Ga respectively. Only in the case of ^{235}U is the half-life even of the same order of magnitude as the longest possible program run (100 my), the half-lives of the other three isotopes being considerably greater than 100 my. Though the rate of heat release is an order of magnitude greater for ^{235}U than for the other abundant radioactive isotopes, its half-life is still long enough to make the assumption of constant heat production from radioactive decay plausible over periods of 100 my or shorter.

Chapter 3

Computer Forward-Modelling in Thermal Problems

Regardless of the mathematical technique chosen, forward-modelling of geothermal relaxation over long periods of time necessarily involves thousands of computations, and it is only practical to approach these calculation-intensive problems with high-speed computers capable of handling very large arrays. For the purpose of this study, a lengthy FORTRAN 77 program was written for execution on DEC VAX 11/750 macroprocessors running under the Berkeley UNIX 4.3 operating system. Though FORTRAN 77 suffers from a lack of elegant recursion algorithms, poor output and string-handling capabilities, and the troublesome requirements of array space allocation prior to running a program, it remains the primary computer language in geophysics, is among the most portable between different systems, and, most importantly, is a fairly efficient language for long programs that require repeated evaluation of arithmetic expressions while avoiding complicated algorithms. FORTRAN's efficiency in handling repetitive calculations was complemented in this study by the use of the high-speed VAX 11/750 computers. The forward-modelling of geotherm evolution over a period of one thousand time intervals may involve up to one million evaluations of arithmetic expressions. A VAX running the FORTRAN program written for this study usually completes the forward-model in under five minutes.

Appendix 1 contains the FORTRAN source-code for the principal programs used in this study. The main program **formodel.f** contains all of the routines necessary for the actual computation of forward-modelled geotherms and is linked, via the **penplot** library capability available at MIT, to the plotting subroutines

subplot.f and **subpath.f**. The first of these subroutines produces a plot of temperature as a function of depth at several time intervals, while the latter reads data from a file created by **formodel.f**, plotting the temperature-depth-time path of a chosen rock particle. Appendix 1 also contains the source code for several auxiliary programs, including **fourier.f**, which calculates geotherms using the traditional Fourier summation technique, and **indplot.f** and **indpath.f**, plotting routines that are not directly linked to the main program. Subroutine **marker.f** is a subprogram that is linked to the plotting routines to produce labels on tic marks in the graphs. Another subprogram **splining.f** fits the temperature-depth and temperature-time output paths of **formodel.f** using FORTRAN cubic spline subroutines available in the **NAG** (Numerical Algorithms Group) library, generating the slope values at each data point and providing a quantitative way to compare curves.

The program written for this study is built around the finite difference calculation routine, and it is important to note that only this part of the program is fundamental in <u>all</u> problem applications. By structuring the routines that calculate the effects of tectonic processes, radioactive heat production, and linear transfer of heat around the kernel of the finite difference expression, it was possible to attain a program with maximal flexibility: In the most elementary case, the program simply models the re-equilibration of a perturbed geotherm prescribed by the user. Figures 1-1, 1-2, and 1-3 give clear examples of this sort of straightforward linear relaxation in which the initial geotherm (at time t=0.0 Ma) adjusts toward the steady-state without the addition of heat production terms. More complicated models can by analyzed through the introduction of radioactive heat sources at various levels in the lithosphere or the repeated application of the relaxation routines at several places in the lithosphere in order to approximate two-

dimensional heat flow. Finally, the attributes of these simpler scenarios can be combined with the actual movement of parts of the lithosphere to provide the most sophisticated and geologically-realistic models for use in thermal studies. The program is designed to analyze not only the effects of diachronous pure shear thinning or movement of material along a normal fault, but also the result of simultaneously extending the lithosphere using both the pure shear and normal fault models.

3.1 Program Input Parameters

Table 3-I gives the basic problem parameters that must be prescribed by the user, and the physical interpretaion of these parameters is shown in Figure 3-1. Of all the variables provided by the user, the most fundamental is the lithospheric thickness x, generally taken between 100 and 125 km for the continents (Sclater et al., 1980). Though it is widely admitted that the continents and ocean floor differ greatly in their heat flow characteristics, geophysicists often use the simplifying assumptions applied to oceanic lithosphere when analyzing the behavior of continental lithosphere and assign the calculated oceanic lithospheric thickness of 125 km (Parsons and Sclater, 1977) to the continents as well. Elevated heat flow and the extreme attenuation of the crust in continental settings such as the Basin and Range Province of the western United States imply that the lithosphere is considerably thinned beneath a large part of the Province and that 125 km is probably a gross overestimate of the present-day lithospheric thickness in this area. It is important to note, however, that this thinned lithosphere is an effect of Cenozoic extensional processes, and that the pre-Cenozoic lithosphere can probably be safely assumed to have been at least 100 to 125 km thick.

Two other parameters of extreme importance in setting up the initial

Variable	Meaning
imbric	number of imbricate fault structures
col	number of lithospheric columns
x	thickness of lithosphere (km)
dx	size of thickness increment (km)
time	total time to run problem (my)
dt	time increment (my)
lat	array of distances bet. adj. columns (km)
mbegin	time at which mvt. on fault begins (my)
mend	time at which mvt. on fault ends (my)
disp	amt. of horizontal displacement on fault (km)
decoll	decollement depth in each column
upxten	% pure shear extension above detachment
loxten	% pure shear extension below detachment
tinit	time at which pure shear begins (my)
tend	time at which pure shear ends (my)
	Geotherm initialization routine
tbase	temp. at base of lithosphere (C)
pnum	number of thermal pulses in the lithosphere
pdept	depths of thermal pulses
ptemp	initial temp. at depth of thermal pulse
disc	number of discontinuities in initial geotherm
tabov	initial temp. at discontinuity
tat	initial temp. one interval below discontiniuity
	Initialization of radioactivity distribution
pts	number of points in radioactive array
dept	depth of points in radioactive array (km)
rad	radioactive heat production of single point source
deep	depth of single point source
radio	radioactivity values (10^{-13} cal/cm^3-s)

Table 3-I: Problem parameters that must be input by the user and their physical interpretation. Variable names correspond to those used in program **formodel.f** listed in Appendix 1.

characteristics of the problem are the time increment, represented by τ in the discussion in Chapter 2 and by *dt* in the program, and the depth increment, denoted by ϵ in Equation (2.4) and by *dx* in the program. These variables prescribe the mesh-size of the finite difference grid and are bounded by the accuracy constraint $0.167 < M < 0.5$ placed on the modulus. As discussed in Chapter 2, most of the program runs done in course of this study used a τ value of 0.1 my and an ϵ value

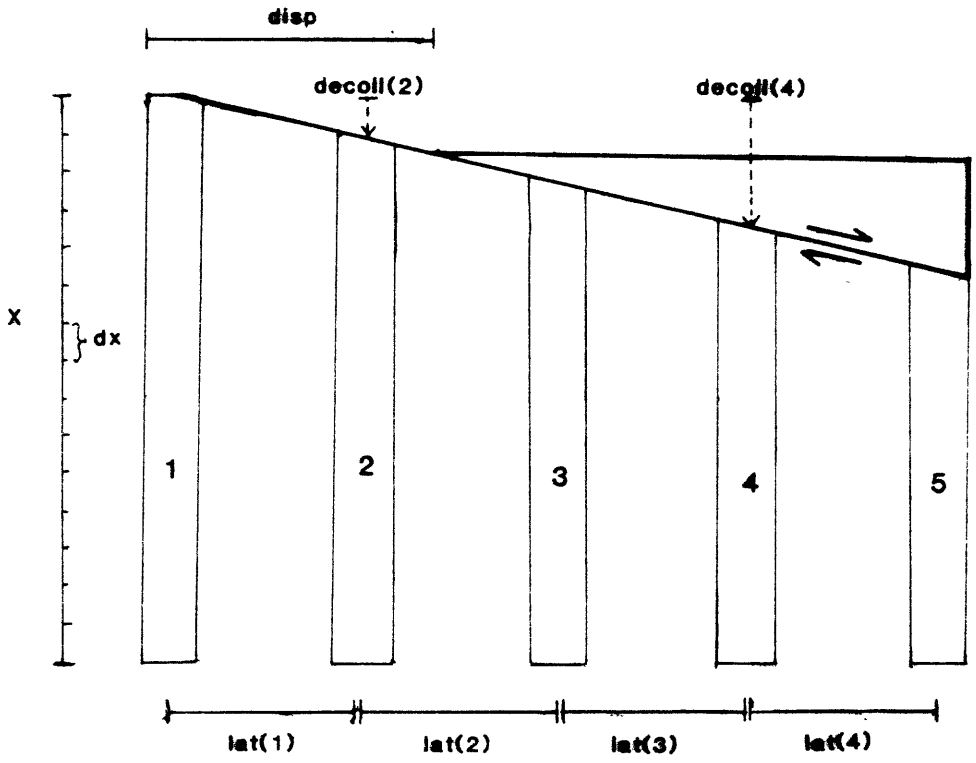

Figure 3-1: Graphical representation of the physical meaning of input problem parameters. Variable names are elaborated in Table 2-I.

of 2.5 km, corresponding to a modulus value of M=0.4125. Though this modulus value is far from the more optimal M=0.167, it does meet the basic accuracy constraint, and its adoption has several advantages. The speed of the program is obviously a major concern for the user; with $\tau = 0.1$ my the program retains its speed since only ten, and not twenty ($\tau = 0.05$ my), time increments are necessary for each million year period. In addition, it is desirable to keep the arrays small enough that the program can be run without loading data onto a hard disk during its execution, a necessity when the program's main temperature array has more than about one thousand elements in its time dimension. For the particular

computer system used in this study, the array size was also limited by the amount of core space available on the VAX. The constraints on array size limit the relaxation time to $t=100$ Ma when $\tau=0.1$ my and to only $t=50$ Ma when $\tau=0.05$ my. A τ value of 0.1 my is probably a wiser choice for long-term geotherm re-equilibration studies and, as discussed in Section 2.3, the accuracy improvement derived from using $\tau=0.1$ my instead of $\tau=0.05$ my will be negligible in most cases.

The choice of the depth increment ϵ is much less dependent on factors of array size and program speed, being subject only to constraints placed on the modulus and the value assigned to the thickness of the lithosphere. The temperature grid established by a finite difference method must include both the surface of the lithosphere and the asthenosphere-lithosphere interface in order to describe completely the characteristics of the cooling slab and to meet the boundary condition constraints discussed in Chapter 2. Not only is it most convenient from the user's standpoint to divide the lithosphere into an integral number of small depth increments, but the finite difference method essentially requires that the lithospheric thickness be evenly divisible by the ϵ value since the validity of replacing the partial derivatives in the heat flow equation with forward differences is dependent on equal spacing of T values in both space and time. With $x=124$ km, for example, the use of $\epsilon=2.5$ km would produce 55 evenly-spaced depth nodes in the finite difference grid from $x=0$ km to $x=122.5$ km, leaving a 1.5 km thin slab adjacent to the lithosphere-asthenosphere interface to be either completely ignored or added to a 1.0 km piece of the asthenosphere to make one last 2.5 km depth increment. Neither of these solutions is acceptable since the first excludes the boundary condition temperature at the asthenosphere interface and the second essentially causes a slab of hotter asthenosphere material to be plated onto the

bottom of the lithosphere. For most of the program runs done for this study, the initial lithospheric thickness x was taken as 125 km or some other multiple of 5 km. A ϵ value of 2.5 km divides the lithosphere into an integral number of thin slabs and allows τ to vary between $\tau = 0.04$ my and $\tau = 0.12$ my while maintaining the modulus value within the acceptable range. One disadvantage of a depth increment as large as 2.5 km, however, is obvious in some of the models discussed in Chapter 4. In order to set up a problem in which the lithosphere is thinned either through pure shear or mass movement along a normal fault surface, it is necessary to specify detachment levels within the crust. Even with a grid as fine-meshed as 2.5 km by 0.05 or 0.1 my, very fine structures in which the decollement occurs at a depth that is not a multiple of 2.5 km can not be easily analyzed. In principle, linear extrapolation between the spatial mesh points would make possible the analysis of problems in which the detachment occurs at 4 km depth, for example, and linear extrapolation is indeed used to follow the upward movement of the decollement surface as the crust is thinned by pure shear extension. It is important to realize, however, that all geological models used in this study are gross approximations of much more complicated structures and that, at most, the decollement level can be half of a depth increment or 1.25 km from its actual position, an inaccuracy that is fundamentally insignificant when compared to other simplifications made in the analyses.

An important effect of crustal extension by either the pure shear or normal fault mechanisms is the lateral movement of lithospheric material. In a lithosphere being thinned by a pure shear mechanism, particles move both vertically and horizontally as the lithosphere is stretched (Figure 3-2a). The normal-fault case is more complicated, with rocks in the footwall moving upward and obliquely relative to fixed particles in the hanging wall (Figure 3-2b). The linear heat flow equation

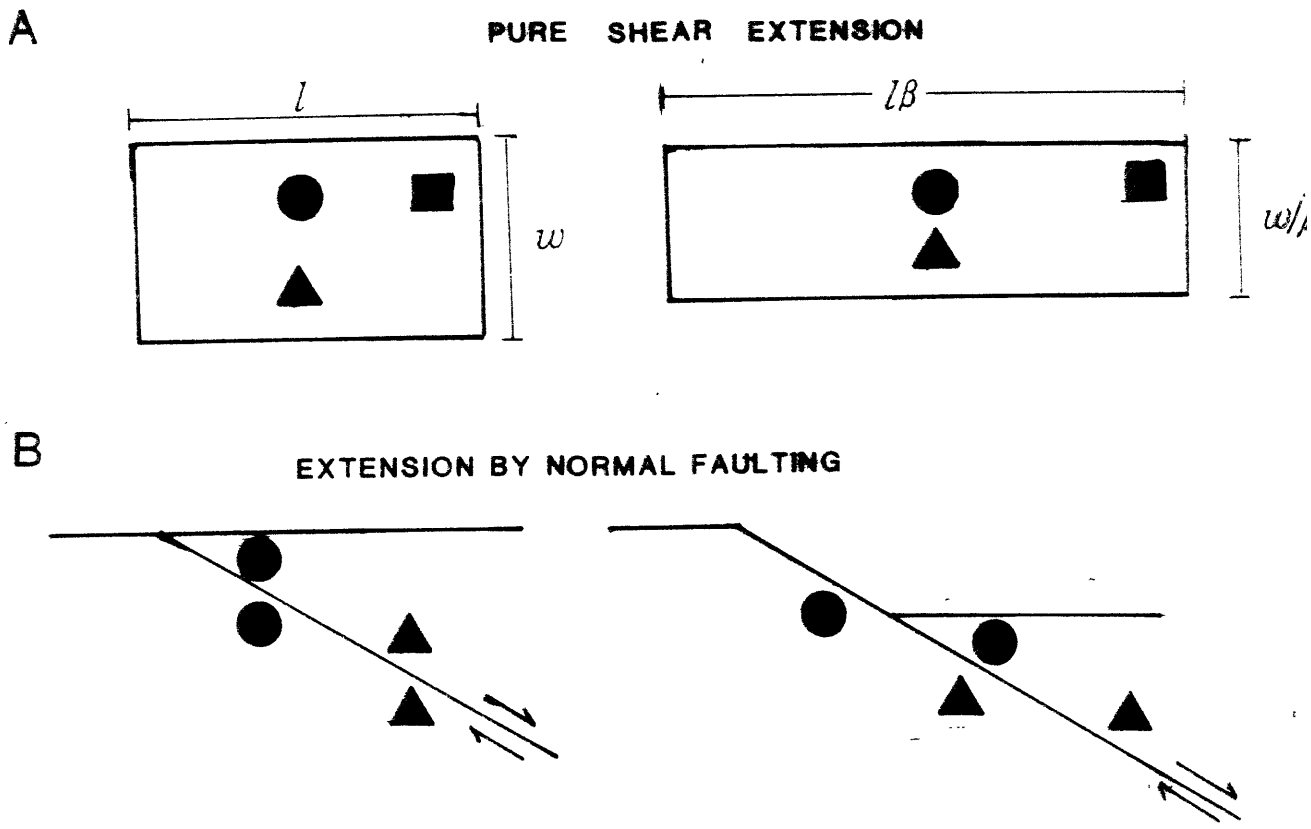

Figure 3-2: The lateral movement of specific rock particles during a) pure shear extension and b) normal faulting.

expresses temperature T as a function of time and a single spatial variable x and has no provision for the simultaneous vertical (in x) and lateral (in y) conduction of heat that occurs in a thinning lithosphere. The two-dimensional heat flow equation is given by:

$$\frac{\delta^2 x}{\delta t^2} + \frac{\delta^2 y}{\delta t^2} = 0 \qquad (3.1)$$

also known as Laplace's equation in two variables. Using the sort of reasoning outlined in Chapter 2 for the one-dimensional heat flow equation, it is possible to replace the partial derivatives in Equation (3.1) by forward differences, thus reducing Laplace's equation to an arithmetic expression similar to Equation (2.4). For the purposes of this study, however, a method based on extrapolating between several parallel one-dimensional geothermal relaxation problems was judged more

straightforward, less calculation-intensive, and fairly accurate in approximating the effects of two-dimensional heat transfer. The generalized lithosphere can be pictured as an horizontally-infinite slab of thickness x with an x-y coordinate system centered at x=0.0 km (the surface) and y=0.0 km, an arbitrarily chosen horizontal position within the slab. At time t=0.0 my, a geotherm is specified for this first one-dimensional column at y=0.0 km and for several other columns of the lithosphere at various distances from the first. Since the finite difference calculation is applied to each column independently, the many one-dimensional problems being solved provide a good, but sketchy, description of the geothermal regime over a large part of the lithosphere. Linear extrapolation between the columns of data completes the two-dimensional description of the temperature distribution within the lithosphere, but does not solve the problem of two-dimensional heat flow. As approached in this study, two-dimensional heat flow necessarily requires mass transport: some of the particles from column 2, for example, must move horizontally as a result of stretching or normal-faulting in some part of the lithosphere. For the purposes of the finite difference calculations, rock particles are viewed in a Lagrangian sense, having a certain temperature and position attached to them at any given time during their movement. Assuming for a moment that particles move only horizontally, instead of both horizontally and vertically, a particle that moves out of column 2 must be replaced by another particle that moves into the same place in the column. In all two-dimensional movements of lithospheric material, then, every depth interval m_ϵ always has a temperature associated with it, and no particle is ever "lost" except by being transported beyond the last column in a problem. At any time interval, the position and temperature of the particle that is about to move into a particular place in a column can be calculated through simple linear extrapolation in both x and y space

given the rate of movement along the fault or stretching. After the column has been filled with the incoming set of particles and the calculated temperatures, the normal finite difference iteration is carried out on the new geotherm and the process of moving particles is then repeated. An approximation of two-dimensional heat flow is developed by first moving new temperatures into a lithospheric column and then using this new geotherm as the seed for the next finite difference calculation, a process that would be impossible with the Fourier technique.

An approximation of two-dimensional heat flow is of fundamental importance in models that involve the movement of pieces of the lithosphere, and the parameters that describe all aspects of this movement are the most variable within the framework of the forward-modelling program. The user must provide values that describe how many lithospheric columns to use (up to five are permitted), the spacing of these columns, the total amount of time (in my) to run the problem, the temperature at the base of the lithosphere, and the parameters that describe the rate of fault movement, the γ and β values for pure shear stretching, and the distribution of radioactive sources in the lithosphere. As the program is set up, problems must be run with at least two lithospheric columns, even if no fault movement (displacement *disp*=0.0 km) and no stretching (upward and lower extensional parameters, *upxten* and *loxten* are 0.0) occur. All problems that are modelled with more than one lithospheric column necessarily require the user to specify the depth of the detachment horizon in each column. In normal-fault problems, the detachment serves to physically separate rocks in the footwall from rocks in the hanging wall, but, in the case of pure shear extension, the detachment zone is only an artificial boundary between pieces of the lithosphere that are stretched at different rates. The breakaway zone -- where the dipping detachment intersects the surface at x=0.0 km -- always occurs in column 1 which can be seen

as consisting entirely of footwall material. The detachment horizons in other columns must be specified to describe a constantly-dipping surface that intersects the columns at depths equal to integral multiples of ϵ . For example, if the intercolumnar spacing of five lithospheric columns is input as 15 km and a low-angle detachment surface is required, then the values 0.0 km, 2.5 km, ..., 10.0 km would be specified for the depth of the decollement in each of the five columns, assuming an ϵ value of 2.5 km. For the simplification of problem geometry and mathematics, only detachments with constant dips were considered in this study.

3.2 Program Flow

Figure 3-3 provides a graphical illustration of the flow of logic in program **formodel.f**. The program initially queries the user for the values of the problem parameters listed in Table 2-I. Control then passes completely to the internal calculation schemes until after all intermediate computations and finite difference iterations have been completed. The first program module that follows the input queries uses the problem variables to calculate various indices related to the number of iterations in time and space and the duration of pre-tectonic, syntectonic, and post-tectonic phases in each model. The main temperature array *temp* is initialized, according to the specifications given by the user, with a steady-state linear geotherm, a discontinuous geotherm similar to those in Figures 1-1 and 1-2, an exponentially increasing geotherm, or a linear geotherm with one or several thermal pulses that die out exponentially with time. Typically, a lithosphere-asthenosphere interface temperature of 1300°C is assumed for a 125 km thick lithosphere, making the steady-state geothermal gradient 10.4°C/km.

As initialized by this program, discontinuous geotherms present a conceptual difficulty for the user. A geotherm produced by instantaneous thrusting, for

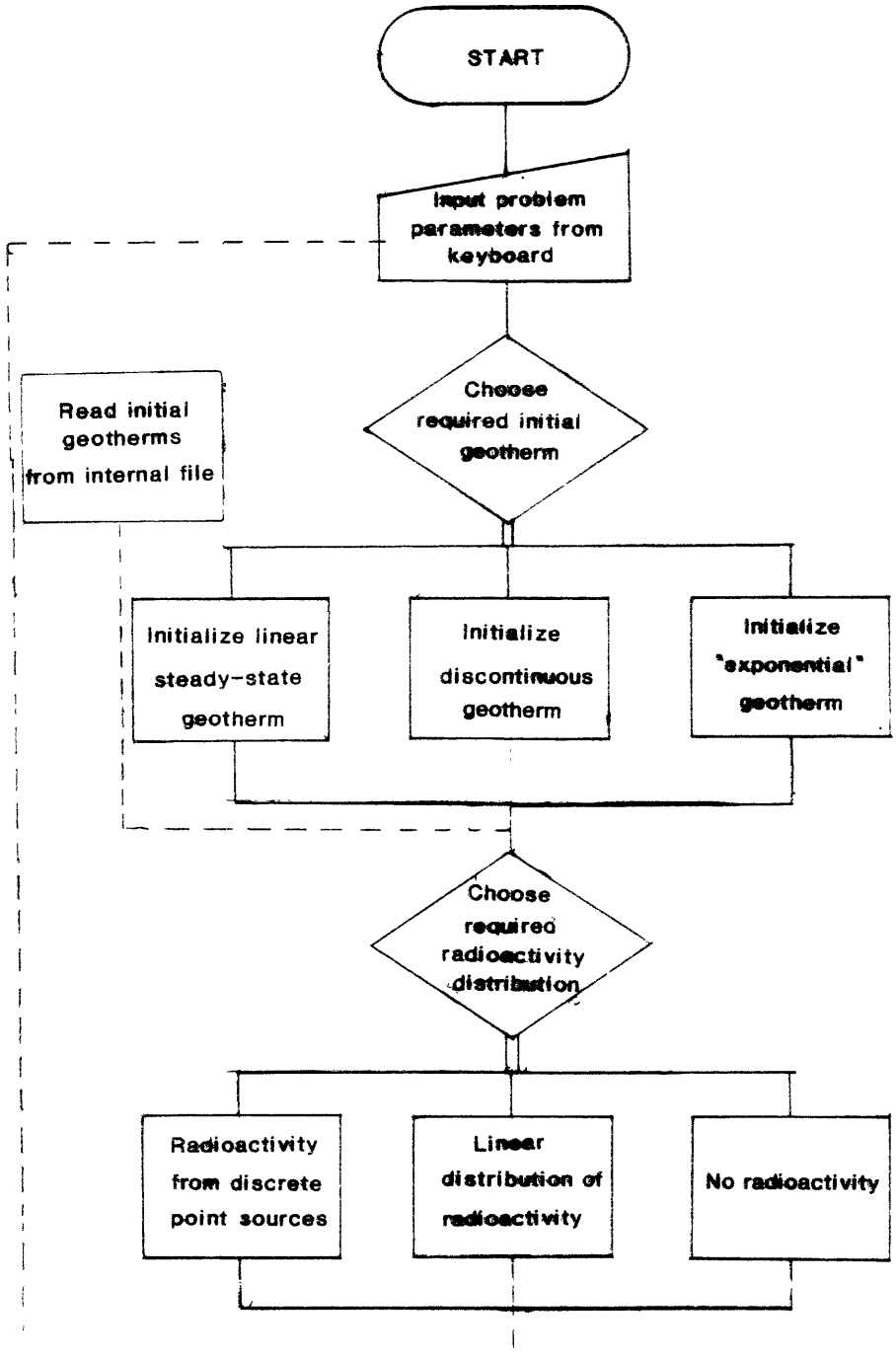

Figure 3-3: Flowchart showing the logic of routine sequence in program **formodel.f**. Diagram continues on next page.

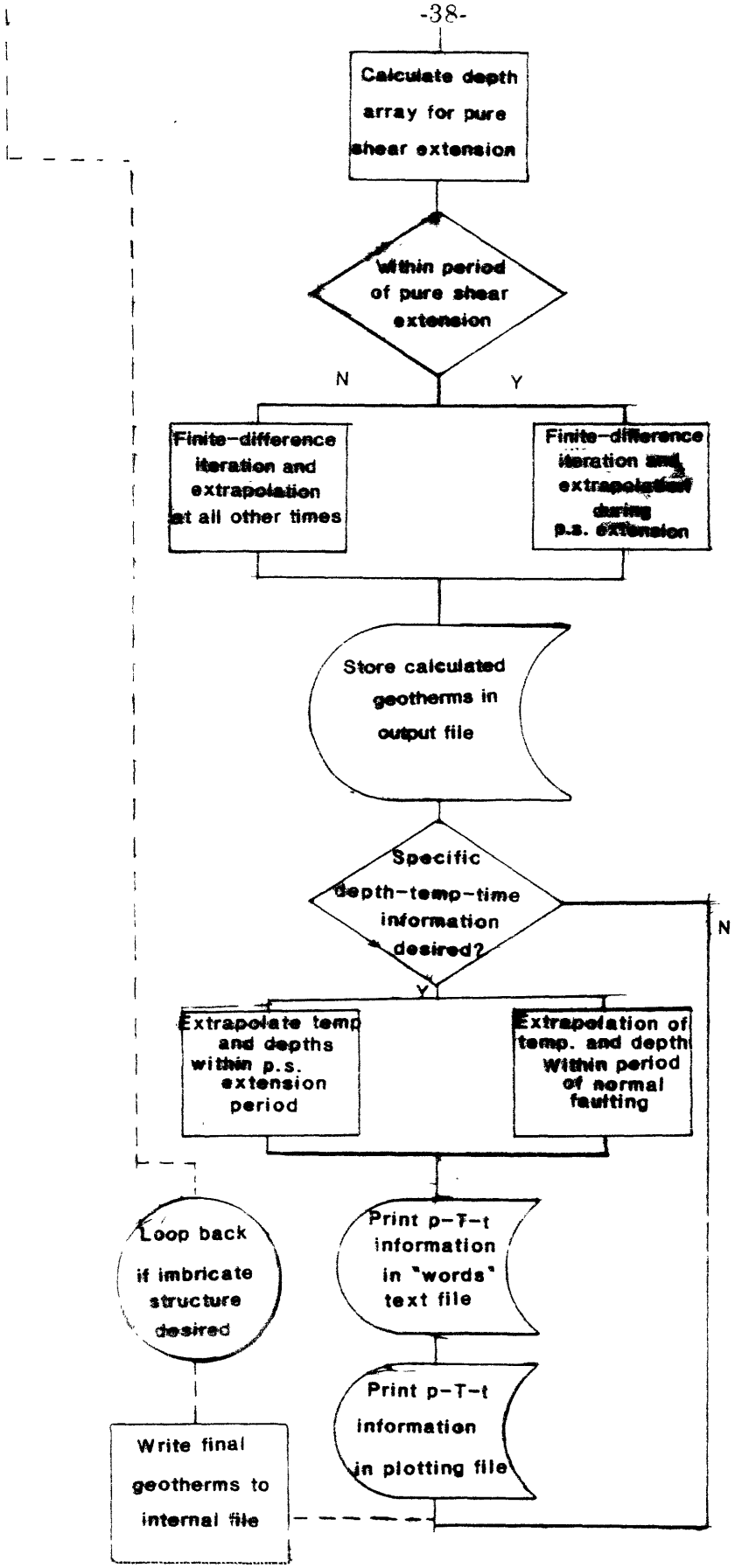
Calculate depth array for pure shear extension
Within period of pure shear extension
N
Y
Finite-difference iteration and extrapolation at all other times
Finite-difference iteration and extrapolation during p.s. extension
Store calculated geotherms in output file
Specific depth-temp-time information desired?
N
Y
Extrapolate temp and depths within p.s. extension period
Extrapolation of temp. and depth within period of normal faulting
Loop back if imbricate structure desired
Print p-T-t information in "words" text file
Print p-T-t information in plotting file
Write final geotherms to internal file

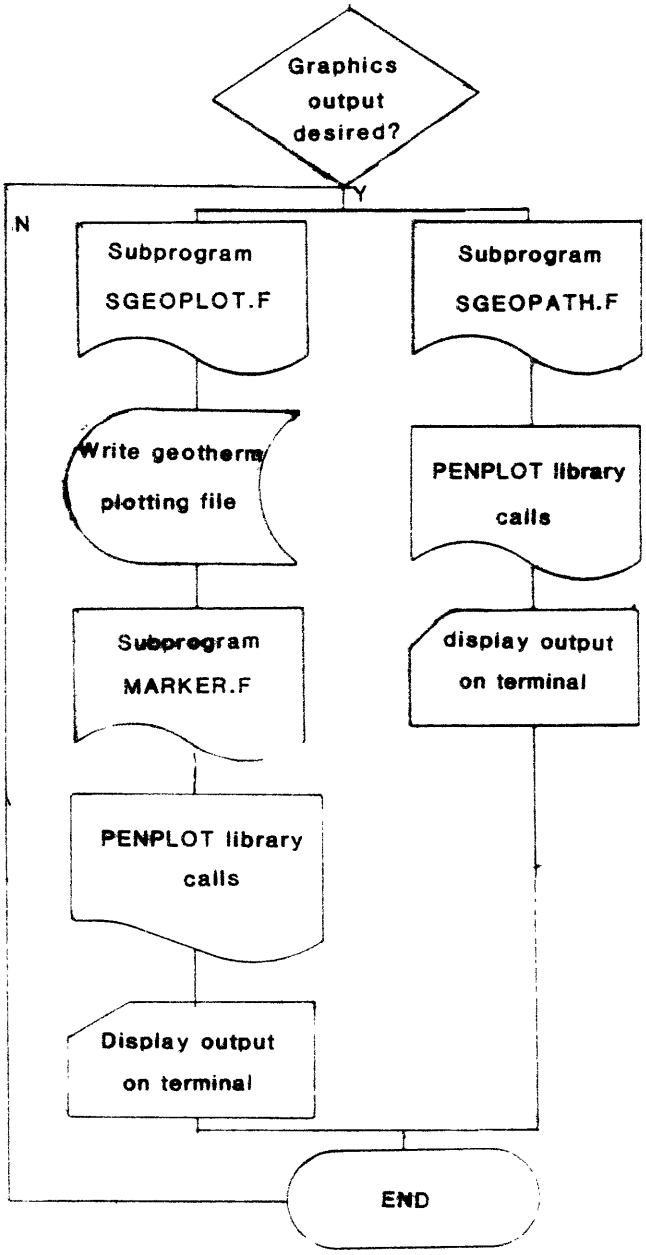
Graphics output desired?
Y
N
Subprogram SGEOPLOT.F
Subprogram SGEOPATH.F
Write geotherm plotting file
PENPLOT library calls
Subprogram MARKER.F
display output on terminal
PENPLOT library calls
Display output on terminal
END

example, is usually modelled by assigning two temperatures to one crustal level. In Figure 1-1 , this would correspond to giving the temperature at 62.5 km as both 1300°C and 52°C, obviously an impossibility for the program, which can handle only one temperature value in each array cell. To overcome this difficulty, it is necessary to assign the array element at 62.5 km a temperature of 1300°C and place the 52°C value in the cell at 55 km depth, effectively spreading the discontinuity out over a 2.5 km thick zone. Another possible discontinuous geotherm has one or more thermal pulses at various depths in the lithospheric columns. The user describes the position and temperature of the thermal pulses that may be viewed as representing the intrusion and subsequent cooling of plutonic material. The program calculates the difference in temperature between the pulse and the background steady-state geotherm, multiplies by an exponential factor $e^{-n\tau/t}$ (the first term in the Fourier expansion where t=total time), and adds the result, the new temperature difference, to the background steady-state geotherm in the next time increment. Since the temperature difference becomes smaller and smaller as the exponential term goes to its limit of e^{-1}, the value of the temperature difference term being added to the background temperature in each time interval approaches 0°C.

One of the greatest advantages afforded by the program's flexibility is the recycling of final geotherms calculated in the first model structure as the initial geotherms in the next model structure, modelling the effects of imbricate faulting in the lithosphere. After the first run of the program, final geotherms for each column that will be included in the next problem are written into an internal file. If the user decides to analyze three consecutive fault structures, then, after the first initialization of the geotherm as steady-state, discontinuous, or exponentially dependent on depth, all geotherm initialization will be handled internally by the

program, which will pass final geotherms from the first fault structure into the array that specifies the initial geotherm for the second structure. This capability renders the program exceedingly useful in the analysis of imbricate faults in the hanging wall of a major detachment and also serves to make the models more realistic since the geothermal perturbations caused by the movement on one fault will continue to affect temperature relaxation as movement on the next fault begins.

After temperature initialization has been completed, control passes to the radioactivity routine. The program models radioactive heat production in the lithosphere either as a set of point sources at various levels in the slab or as a linear function of depth between known values of heat production provided by the user for specific horizons. The heat flow Equation (2.1) can be modified to include a heat production term:

$$\frac{\delta^2 T}{\delta x^2} = \frac{1}{\kappa}\frac{\delta T}{\delta t} + \frac{A}{K}$$

The temperature increase caused by a source producing heat at the constant rate of A $\mu W/m^3$ is given by:

$$\Delta T = A\kappa\, dt/k \quad ,$$

where κ=thermal diffusivity (m^2/s)
k=thermal conductivity ($W/m^{\circ}K$)

For a problem in which no mass transport occurs, ΔT is simply added directly to the temperature value at the depth of the source in each iteration. In geologic settings, it is often possible to specify the heat production rate at several depths within the lithosphere. Instead of assuming that these are the only heat sources within the lithosphere, it is probably more realistic to regard these values as those that happen to be known and to use a linear extrapolation routine to assign heat production rates to depth levels that do not coincide with the known points. For

very generalized models for which a grossly-quantitative solution is required or no radioactive heat production rates are known, the radioactivity routine can be bypassed.

The pure shear extension routine, though not strictly necessary in many problem applications, is executed each time the program is run. Among the required input parameters are *upxten* and *loxten*, the variables that describe the percentage by which the lithosphere is stretched through pure shear deformation, and these are simply set to 0.0 when it is desirable to avoid pure shear altogether. Geophysicists typically use the factors like β and γ in mathematical modelling of the effects of pure shear extension. β and γ can be physically interpretated as ratios: With 75% extension in the upper part of the lithosphere (*upxten*=0.75), a unit element of pre-tectonic lithosphere will be $\gamma = 1.0 + upxten = 1.75$ as long and 1.75^{-1} as thick in its post-tectonic state. It is important to note that, in the ideal case, the pure shear mechanism preserves area through correlated horizontal and vertical transport of mass elements.

Continuing the example above, in order to reach a net γ factor of 1.75 over a period of ten time increments, it is necessary to develop a relation for instantaneous stretching in the lithosphere at the beginning of each time interval. Simply dividing the γ factor or the *upxten* value by the number of time intervals to obtain 0.175 and 0.075 for $\dot{\gamma}/dt$ and *upxten/dt* respectively will not produce the final desired 75% extension rate. With a lithosphere 100 km thick and using the *upxten/dt* value of 0.075, the lithospheric thickness after each of the few time increments is:

n = 1	100.0	- (100.0) (0.075)	=	92.50 km
2	92.50	- (92.50) (0.075)	=	85.56 km
3	85.56	- (85.56) (0.075)	=	79.14 km
4	79.14	- (79.14) (0.075)	=	73.20 km
5	73.20	- (73.20) (0.075)	=	67.71 km
6	67.71	- (67.71) (0.075)	=	62.63 km
7	62.63	- (62.63) (0.075)	=	57.93 km
8	57.93	- (57.93) (0.075)	=	53.59 km
.	.	.		.
.	.	.		.

By the time the eighth instantaneous stretching event is completed, this faulty method produces a lithosphere thinner than the final desired thickness of 100 km/1.75 = 57.14 km. What is required, then, is a technique that divides up the instantaneous stretching events among the ten time increments in such a way that the desired final thickness is achieved in the correct number of iterations. Royden et al. (1983) outline a method that requires the recalculation of a $d\gamma$ value for each time period in a pure shear episode but produces the desired results. The relation:

$$d\gamma = \{ [(\gamma - 1.0)] / [t + (n - 1)] \} + 1.0$$

gives the value of $d\gamma$ for time interval $n\tau$. In this expression, t is the total amount of time over which pure shear extension occurs, and n is an integral value ranging, in the case above, from 1 to 10. Assuming that the extension takes place over 1.0 my, corresponding to a τ value of 0.1 my for each of ten increments, the lithospheric thickness after each instantaneous stretching episode is now:

n = 1	= 1.075	100.00 / 1.075	=	93.02 km
2	= 1.070	93.02 / 1.070	=	86.95 km
3	= 1.065	86.95 / 1.065	=	81.63 km
4	= 1.061	81.63 / 1.061	=	76.94 km
5	= 1.058	76.94 / 1.058	=	72.74 km
6	= 1.055	72.74 / 1.055	=	68.94 km
7	= 1.052	68.94 / 1.052	=	65.54 km
8	= 1.049	65.54 / 1.049	=	62.48 km
9	= 1.047	62.48 / 1.047	=	59.67 km
10	= 1.045	59.67 / 1.045	=	57.10 km

The variation between this final lithospheric thickness of 57.10 km and the value of 57.14 km obtained above by simply dividing the pre-tectonic thickness by the γ value is merely an artifact of having retained only three significant figures in $d\gamma$ and two in lithospheric thicknesses in the hand calculations. Using the method of Royden et al. (1983), it is possible to stretch pieces of lithosphere above and below the chosen detachment level simultaneously and by different amounts. This capability is particularly valuable if a detachment level is introduced at a depth corresponding to the upper-lower crust interface or the crustal-lower lithosphere boundary. Though the elastic properties of the slabs above and below the arbitrary detachment level can not be changed, extending the two parts of the lithosphere by different amounts permits the upper plate to stretch relatively more quickly or more slowly than the lower plate and provides a rough model for the response of an isotropic solid being deformed inhomogeneously.

After arrays have been filled with the thicknesses of the upper and lower plates following each instantaneous extensional event, the program enters the main incrementation routine that lies at the core of all problems. Theoretically, the one-line finite difference expression should be the only necessary element in this part of the program, but, in practice, several complicated two-dimensional linear extrapolation routines are required to determine the temperatures at the depth intervals $m\epsilon$ as particles move in x and y space. In the pure shear events of the sort discussed above, particles move both vertically and horizontally at a progressively slower and slower rate. Thinning of the lithosphere by the relative movement of the hanging wall and footwall of a normal fault, however, is much more easily modelled since mass tranfer takes place at a constant rate over a period of time. If the total displacement along the fault measured in the horizontal plane is 10 km over a period of 10 my, the program assumes that horizontal displacement

occurs at the rate of 1 km/my or 1 mm/yr. If a column of the lithosphere at y = 10 km and with a detachment surface at 5 km (angle of dip is 45°) is subsequently introduced, it is seen that a particle moves 1 km/my in the horizontal dimension and 0.5 km/my in the vertical dimension for a total displacement of 1.25 km/my parallel to the dipping fault surface. In practice, the program holds the surface steady as a datum level and models movement along the normal fault as the downslope displacement of the hanging wall. In real geologic settings, though, the hanging wall typically consists of sedimentary rocks and poorly-consolidated fill, and it is the footwall that moves upward, causing the break-up of the hanging wall rocks. The problem is entirely one of relativity, however, since modelling the thermal response to the downward movement of the hanging wall is mathematically equivalent to modelling the temperature changes resulting from upward movement of the footwall.

Following the last finite difference iteration for a problem, control passes to a number of user-interface routines that write specific information in files. The first of these routines provides a two-dimensional description of the temperature structure by creating the file **twodee** that lists the geotherms for each column at fourteen time intervals chosen by the user. An internal file **nxt.st** containing the final geotherms of each column necessary for the next problem application is also created at this time. The routine that follows is the most important and most complicated of the entire program and is solely responsible for providing the Lagrangian description of particle motion. The program queries the user for the original position of the particle whose time-temperature-depth path is desired, and then, through a series of complicated and inelegant "if" statements, determines whether, at a given time, the tectonic regime is one of pure shear extension, normal fault movement, or no activity. The file **words** contains a header that gives all

problem parameters, a graphical representation of the distances involved in the calculations, and the time-temperature-depth and lateral position information for the particles chosen. It is this information that is the most useful in making the leap from theoretical forward-modelling to metamorphic petrology. The temperature-depth points are also recorded in a plotting file named by the user and can later be used as the input for both the plotting routines **indpath.f** and for an RPL data analysis system (**RS/1**) available at MIT.

As discussed in Chapter 3, an important consequence of the program's flexibility is its ability to loop back to the input parameter queries and proceed with the analysis of a new fault structure using initial geotherms generated by the analysis of a previous fault structure. Figure 3-4 shows a two-stage extension process in which movement along two low-angle normal faults produces net thinning of the crust. Using five lithospheric columns spaced at $y = 0.0$ km, 15 km, ..., 60 km and with the detachment levels as $x = 0.0$ km, 2.5 km, ..., 10.0 km respectively, the hanging wall of the first fault moves until the breakaway is at $y = 15$ km, effectively thinning the lithosphere by 2.5 km. If the second fault has the same dip and a breakaway zone at the position of the original column 3, the computer is told to retain the last three of the original columns for the next analysis. The original column 3 is shifted over to the column 1 position within the program's arrays, and final geotherms from the first run are copied into the initial temperature array for the second run such that:

```
original column 3 -----> new column 1
original column 4 -----> new column 2
original column 5 -----> new column 3
```

Since no data are available for the new columns 4 and 5, it is assumed that the lithosphere at these positions has the same temperature regime as the new column 3. Now, with the temperature array initialized and given the new

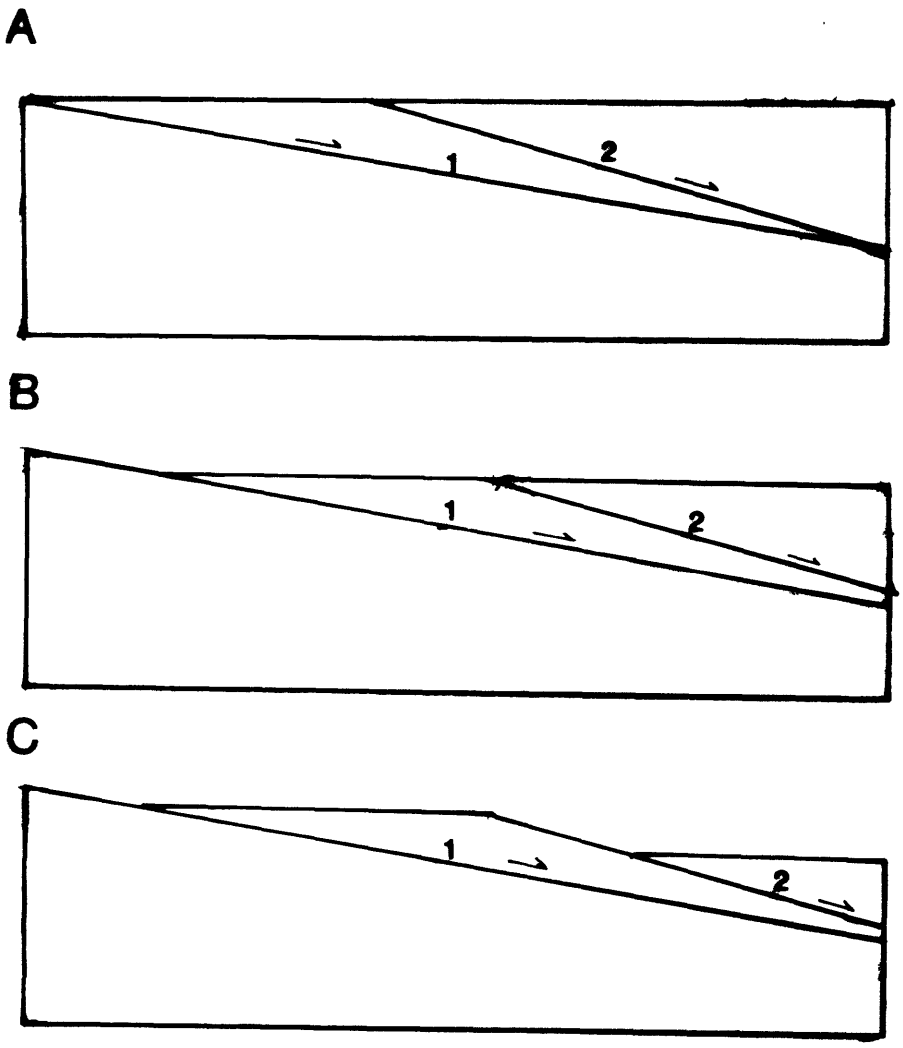

Figure 3-4: A two-stage extension process: Consecutive movement on faults 1 and 2 causes thinning of the crust. Geotherms calculated during movement along first fault serve as the initial geotherms for the stage two faulting.

lithospheric thickness of 122.5 km, the program proceeds to carry on the second stage of normal fault movement. Theoretically, an infinite number of imbricate fault structures could be run. The program requires, however, that a great deal of information be provided at the onset of each new faulting episode, and running the program for more than three or four fault structures can become tedious, especially since a failure to use properly formatted input will cause the termination of the program and the loss of generated data.

After movement along the last fault has been completed, control finally passes out of the loop that encompasses most of the program and into a short sequence that permits direct connection with plotting routines. At this point, the user needs to determine only whether a plot of geotherms or the time-temperature-depth path of a specific particle is desired. In either case, it should be noted that the files read by the plotting routines will contain only the data generated by movement on the final fault. Once finished with the program, however, it is possible to use plotting files generated during the run to provide x-y pairs for graphs using **indpath.f** or **RS/1** (some knowledge of linking FORTRAN ASCII files into RPL required) or to read from the plotting files and fit cubic splines to the data using **splining.f**.

3.3 Systematic Errors

Approximating the analytic Fourier solution for the geothermal relaxation problem through the application of a finite difference method is expected to cause discrepencies in the results of the two techniques. Since the Fourier solution is analytic and can theoretically be reached exactly by summing over an infinite number of terms, error analysis is best undertaken by comparing the results of several finite difference calculations with the Fourier solution. Using the simple program **fourier.f** listed in Appendix 1, analytic solutions were found for the relaxation of the geotherm in which the surface temperature is 0°C while the rest of the lithosphere is assigned the asthenosphere temperature of 1300°C. The program calculates and sums the first twenty Fourier terms at a time t Ma given by the user and prints these values in an internal file. Though the discrepancy between temperature values calculated with the Fourier model and the finite difference method using both $\tau = 0.1$ my and $\tau = 0.05$ my may be be as great as 15°C at

smaller t, this represents less than a 1.5% difference between the Fourier and finite difference calculated values at these depths. By $t=20$ Ma, the Fourier and finite difference geotherms differ by less than 0.5% for $\tau=0.05$ my and 1.0% for $\tau=0.1$ my, a range of errors well within the tolerance limits for this study. Of particular importance is that fact that decreasing the τ value to 0.05 my ($M=\kappa\tau/\epsilon^2$) from 0.10 my ($M=0.4125$) places the modulus value more acceptably within the limits of the constraint $0.25 < M < 0.5$ and should presumably give a considerably more stable solution, but the accuracy improves by only one-half of one percent, not enough to merit the additional time required to run the program with a smaller τ increment.

Chapter 4

Forward Models of Depth-Temperature-Time Paths

The primary purpose of this study is the development of quantitative relationships between the pressure-temperature-time paths of rocks in extensional terrains and parameters that describe how the lithosphere thins. Theoretically, any change in the problem parameters listed in Table 2-I will produce a variation in the path of a particle, but, for the purposes of this study, it is most important to determine the effect of changing the most basic of the parameters, namely the dip of the normal fault and the rate of movement along discrete fault zones in the crust.

Input Parameters for Models Tested

lithospheric thickness	125 km	
thickness increment (ϵ)	2.5 km	
total time to run problem	99.9 my	
time increment (τ)	0.1 my	
distance bet. adjacent columns	25 km	
% pure shear extension	0%	(γ=β=1.0)
radioactive heat production	5 $\mu W/m^3$	
thickness of radioactive layer	20 km	
temperature at lithosphere base	1300°C	
normal fault mvt. begins	0.1 my	

Table 4-I: The set of input problem parameters for each of the models tested.

Table 4-I lists the full set of problem parameters used in testing the models. In order to simplify the comparison of p-T-t curves, only five models were tested, and in all cases the upper plate was moved until five kilometers of material remained above the decollement at a distance of 100 km from the origin. The initial geotherm

for these runs was developed by superimposing radioactive heat production of 5 $\mu W/m^3$ in the upper 20 km on a linear steady-state background geotherm until thermal effects had raised the temperature of the particle at 40 km to 600°C. This geotherm, shown in Figure 4-0, then became the initial temperature structure for each run, and radioactive heat production was allowed to continue at the same rate in the upper 20 km of lithosphere during the course of the run. For the models tested here, the thermal boundary layer, corresponding to the thickness of the lithosphere for the purposes of this study, was taken at a depth of 125 km and a temperature of 1300°C in accordance with the values determined by Parsons and Sclater (1977) for the oceanic case.

4.1 Effects of Fault Dip on Particle Paths

The first group of models was designed to test the effects of fault dip on the temperature-time uplift path of particles. The parameters for the three models tested are given in Table 4-I and illustrated in Figure 4-1. In each of the models, the hanging wall was moved at a rate of 5 mm/yr (measured along the horizontal) above the detachment surface as the paths of particles at various depths within the lithosphere were monitored. Since the amount of cover being removed varies from column to column, comparison of the depth-temperature paths for these models shows only the primary effect of particles originally at the same depth in each column ending up at different depths and yields little information about the overall relationship between fault dip and thermal changes related to varying only this parameter.

The primary difference in geometry among models in which the dip angle has been varied is the depth to the detachment surface in each of the stationary columns. In the 6° case, for example, the depth to the decollement in column 2 is

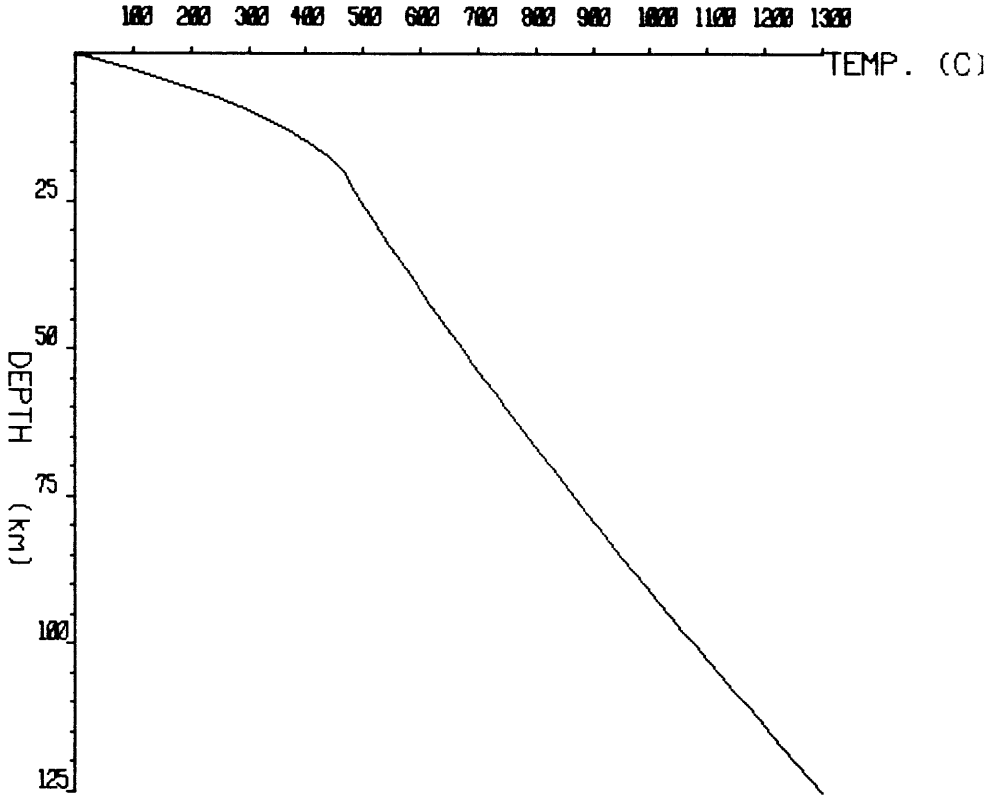

Figure 4-0: The initial geotherm used for each of the models run. This temperature structure was generated by introducing a 20 km thick layer with radioactive heat production of $5\mu W/m^3$ at the top of the lithosphere and allowing the geotherm to develop for about 96 my, until a temperature of 600°C was reached at a depth of 40 km.

2.5 km whereas for the 17° model, the detachment lies at 7.5 km below the surface. Obviously, an increase in fault dip angle will result in cool upper plate rocks being placed on deeper particles in the lithosphere.

The direct effect of varying the angle of fault dip is evident in Figure 4-2 where time is plotted against the normalized temperature of particles that begin at 2.5 km below the decollement at a horizontal distance of 25 km from the breakaway. In the 17° dip model, this particle undergoes a very rapid temperature

Dip angle	Depth to detachment					Horizontal displacement	Duration of displacement	Horiz. disp. rate
	col. 1	2	3	4	5			
6°	0	2.5	5.0	7.5	10	50.0 km	10 my	5 mm/yr
9°	0		7.5		15	66.7 km	13.4 my	5 mm/yr
11°	0	5.0	10.	15.	20	75.0 km	15 my	5 mm/yr
17°	0	7.5	15.	22.5	30	83.3 km	16.7 my	5 mm/yr

Table 4-II: Input parameters used for testing the effects of fault dip variation on the depth-temperature-time paths of rocks.

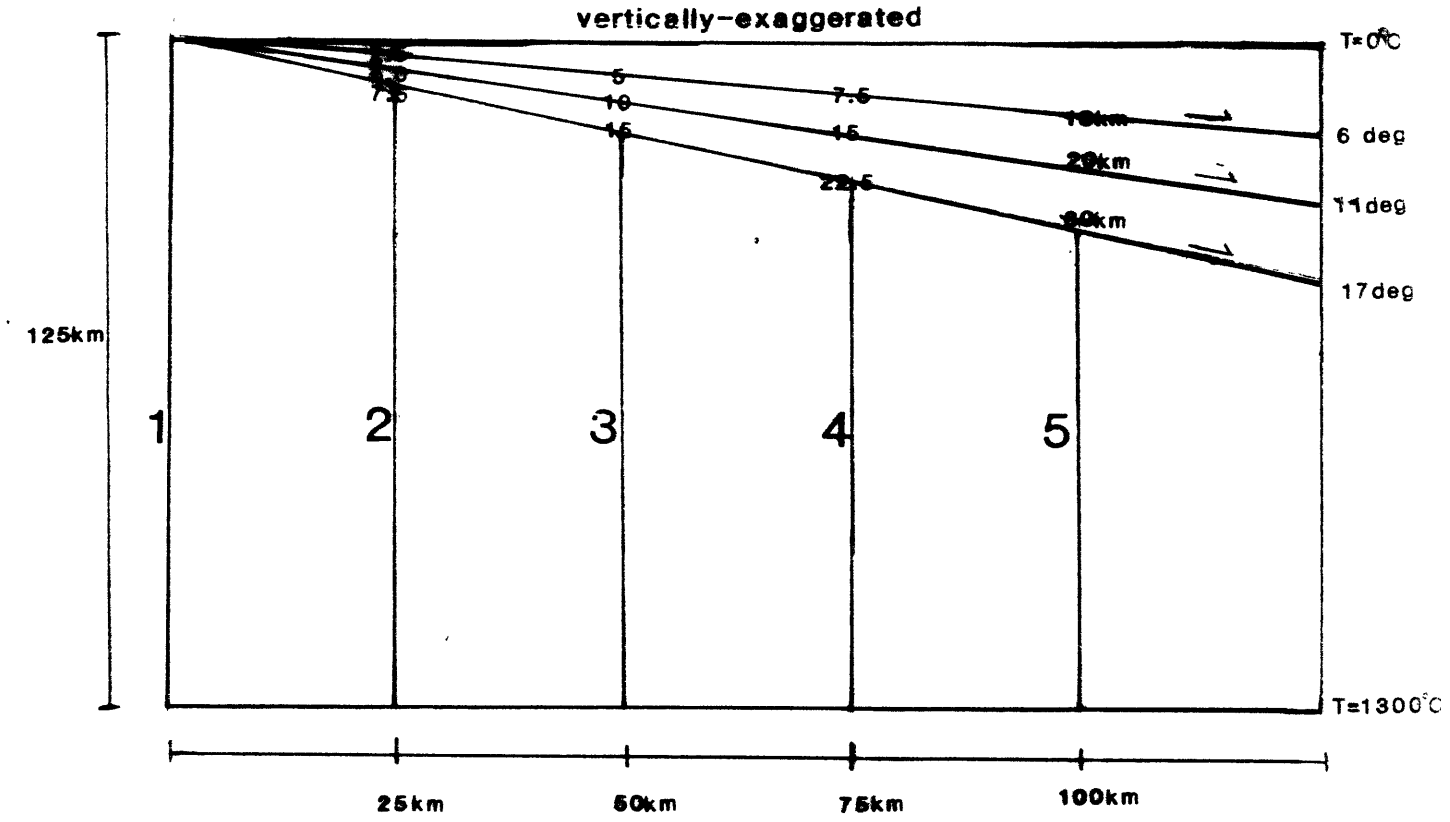

Figure 4-1: An illustration of the geometry in the three models used to test the variation of rock path with changes in fault dip angle.

decrease as the cool and thin upper plate is first moved over and then completely off

the top of column 2. The particle at the same structural level in the 6° model, however, undergoes equally rapid but less pronounced initial cooling and remains at a temperature slightly greater than half its initial temperature for the remaining 85 my of the run. (In all of the plots that follow in this chapter, the end of the period of displacement along the normal fault is marked by a square on the time-temperature curves.) This analysis is particularly important as it provides a first-order comparison of the effect of dip angle changes on the temperature of rocks at the same structural level as opposed to the same absolute depth within the lithospheric column. (For the purposes of this study, "structural" level refers to the depth of a particle relative to the detachment.) Unfortunately, however, the differences in T-t and d-T paths are merely the result of cooler rocks being carried over deeper structural levels as the fault dip is increased for each model. Rocks that begin nearer the surface have a lower initial temperature and do not undergo as much cooling in response to tectonic denudation as rocks farther below the surface but at the same structural level relative to the detachment. Although these rocks begin and end at the same structural level then, they do not provide a good basis for direct comparison.

Comparison of the t-T and d-T paths of rocks originally at the same absolute level within a single lithospheric column also suffers from the difficulty outlined above. Figure 4-3 shows the time-temperature and depth-temperature paths of rock particles that begin at a depth of 25 km in the same lithospheric column for each of the tested dip angles. In this case, though the rocks begin at the same temperature, their final depths and therefore pressures are different. For a dip of 6°, the particle that begins at a depth of 25 km is uplifted to 22.5 km, and its temperature therefore re-equilibrates to the expected steady-state background temperature at its new crustal level. A particle originally at 25 km below a detachment dipping at

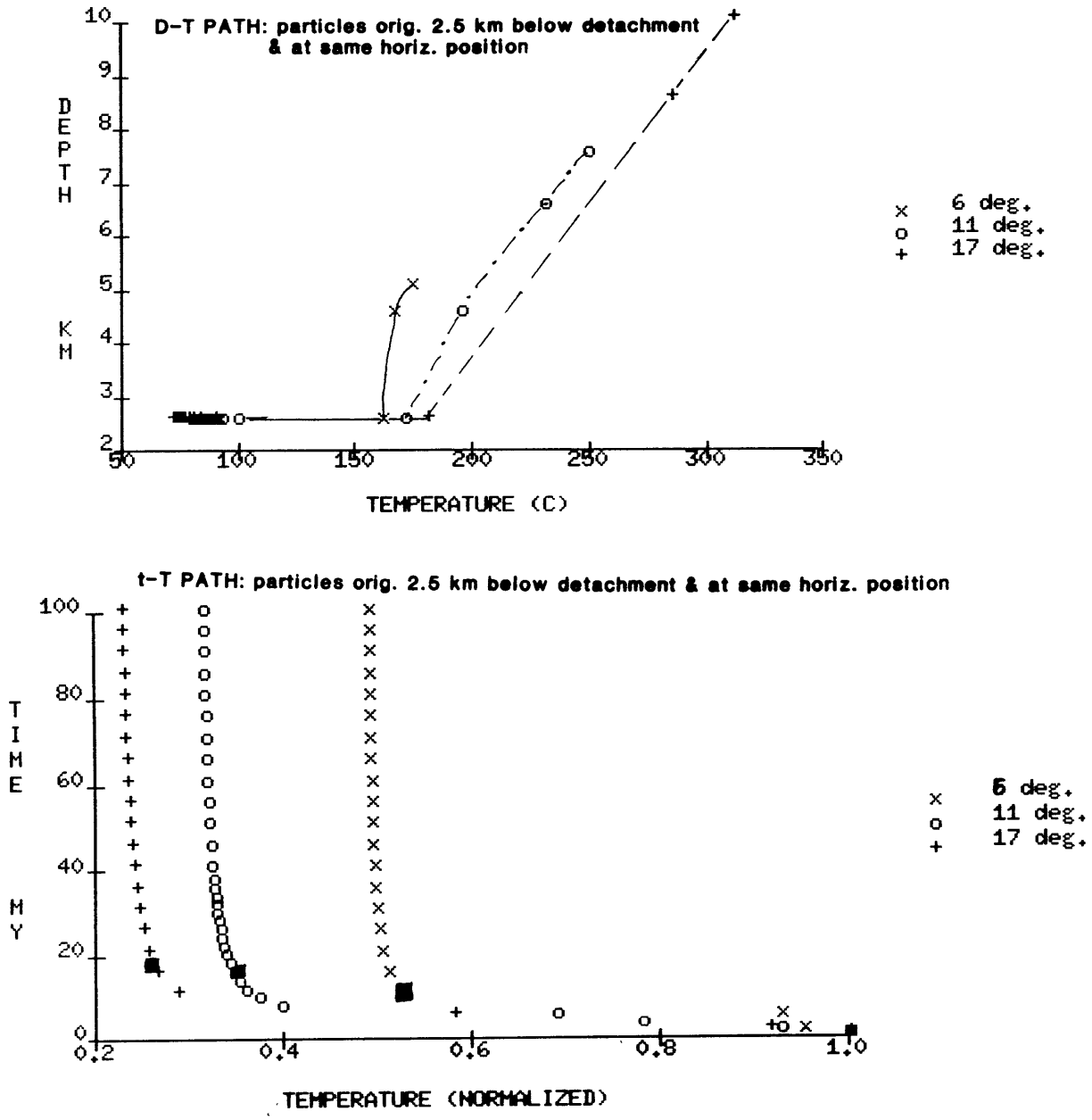

Figure 4-2: Depth-temperature and temperature-time paths of particles 2.5 km below the decollement for each of the dip angles. Note relative cooling rates for the different dip angles.

17°, however, reaches a post-tectonic level of 17.5 km and re-equilibrates to the lower steady-state temperature at this crustal horizon. The greater drop in temperature observed for the particle originally at the 25 km level below a fault interface dipping at 17° is seen merely as result of its ending up nearer the surface.

A direct comparison of t-T and d-T paths of rocks is only possible, then, when particles begin at both the same structural and initial depths within the lithosphere. As discussed in Chapter 3, the computer program written for this study sets up a system of two to five lithospheric columns for which the user specifies the detachment levels and lateral spacing. By choosing rocks originally at 10 km depth and 2.5 km below the detachment horizon from different columns, the effect of varying fault dip angle can be studied independently of other parameters. The original positions of particles whose depth-temperature-time paths were monitored are shown in Figure 4-4, and the depth-temperature and time-temperature paths are plotted in Figure 4-5. Note that a different intermediate dip angle was used for these analyses in order to simplify the geometry. From Figure 4-5a, it is obvious that there is no significant variation in the depth-temperature paths of rocks that begin at the same structural level in the footwall of normal faults with displacements of 5 mm/yr, even when the fault angle varies between 6° and 17°. The particles below the fault surfaces dipping at these two angles arrive at their final depth of 2.5 km with only a 25°C difference in temperature, a change in temperature that would not be detectable in the rocks' compositions or textures. These rocks then quickly equilibrate isobarically, reaching the same temperature by 20 Ma.

The time-temperature plots in Figure 4-5b also show little variation for different dip angles, the only notable difference being that the particle monitored for the 6° dip case does not reach the isothermal part of the t-T path until about

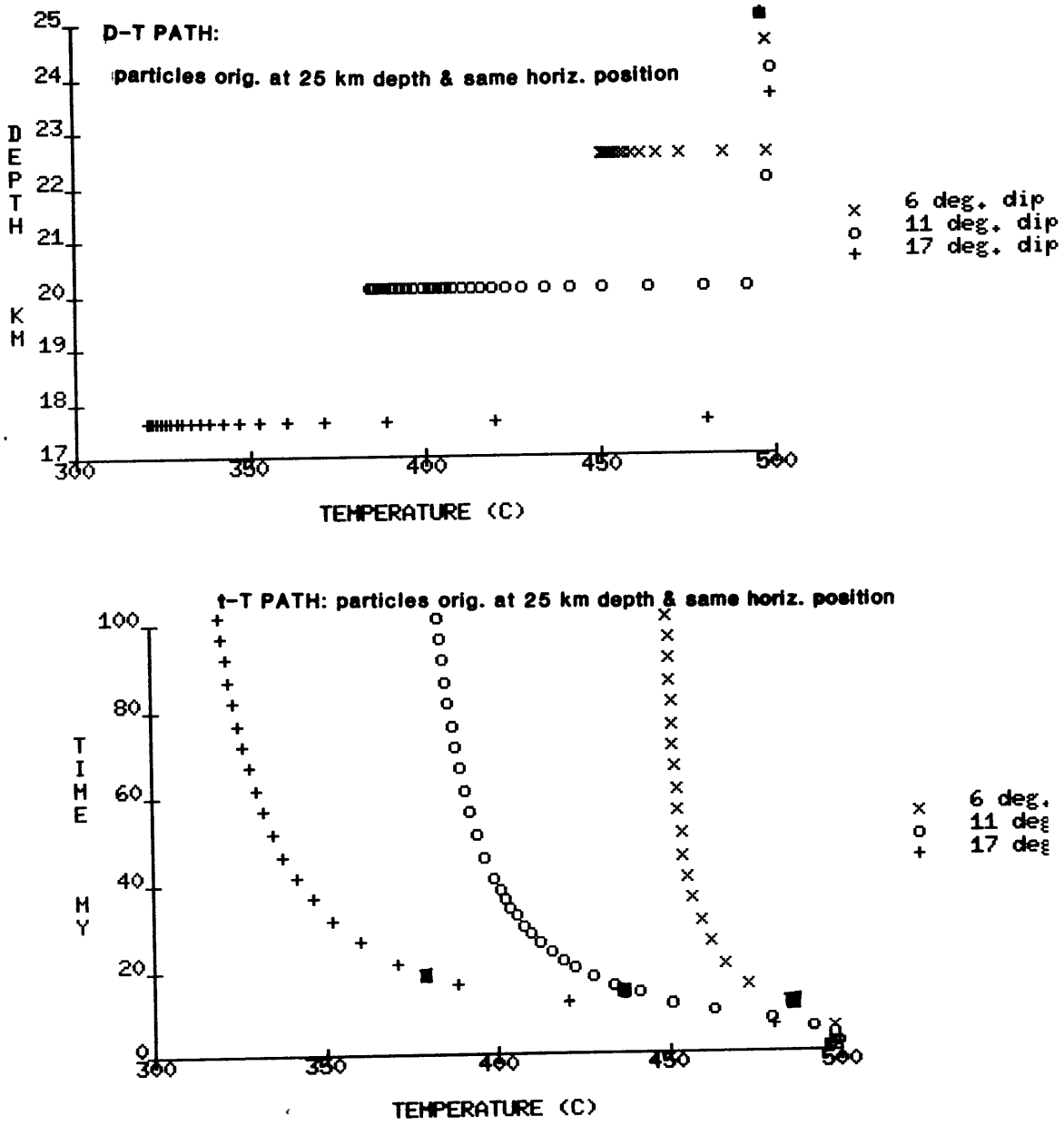

Figure 4-3: Depth-temperature and time-temperature paths of particles originally at the depth of 25 km is shown for different dip angles. The variations seen here are primarily an effect of differences in the particles' positions relative to the decollement and their final depths relative to the surface.

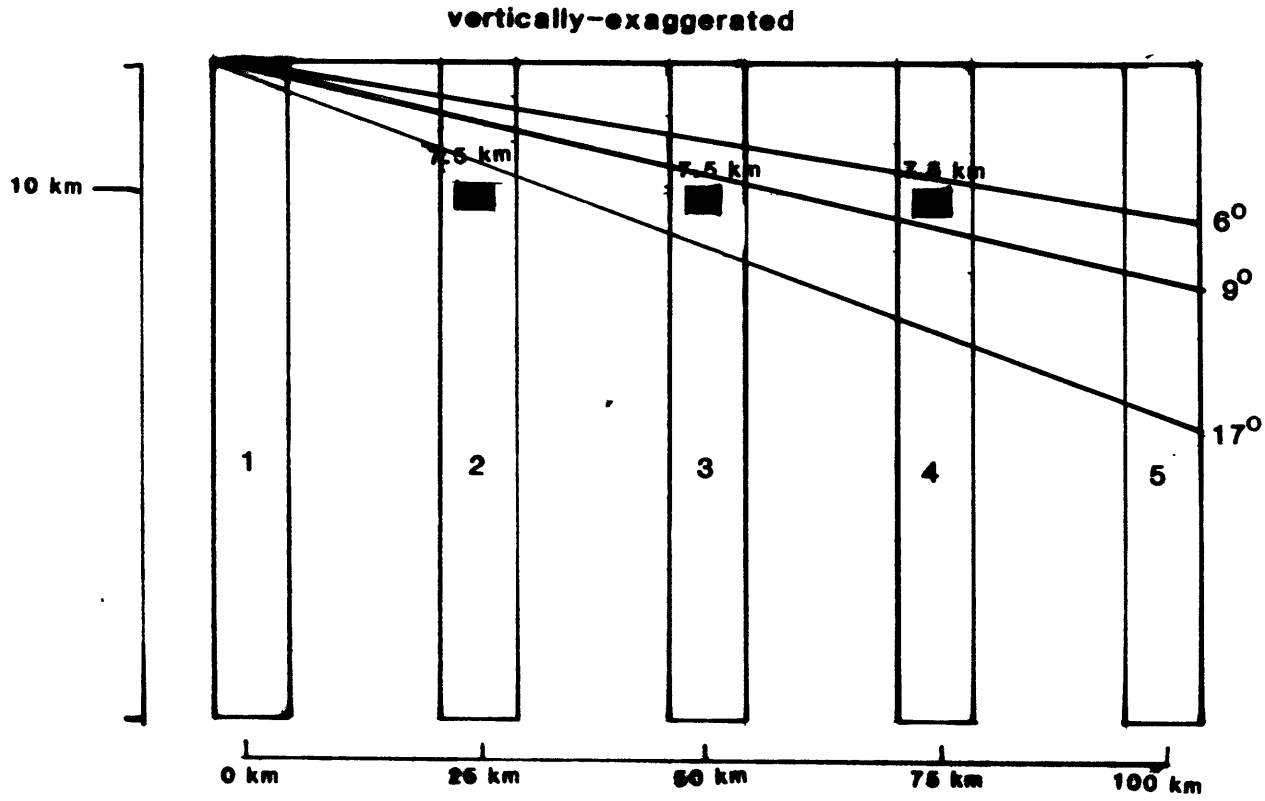

Figure 4-4: Original positions of the particles whose depth-temperature-time paths were monitored in order to directly compare the effects of dip angle.

5 my after the other two particles. This effect is clearly a result of the original horizontal position of the monitored particle. For the 6° case, the monitored particle occurs at a distance of 75 km from the breakaway, the place where the detachment zone intersects the surface. In contrast, for the 17° case where the monitored particle is 75 km from the breakaway, unroofing is not completed until several million years later, after unroofing of particles nearer the breakaway zone has ended, and cooling to the isothermal part of the path is therefore delayed. Once again, however, this time-temperature difference is not significant, and it can be concluded that there is nearly no variation in the depth-temperature-time paths of particles that begin at the same structural and absolute depths and are exposed by

constant lateral displacement of the hanging wall, even when these particles occur below faults that dip at different angles.

The discussion above dealt with the effects of varying dip angle while holding the rate of lateral displacement constant. The vertical displacement rate on a fault can be related to the lateral movement rate by the expression:

vert. disp. rate = horiz. disp. rate x tan(θ of fault dip)

Although the horizontal displacement rate is held constant as the dip angle varies, in each case outlined above, material is being unroofed at a different rate. In the 17°C case, for example, the lower plate is being unroofed at a rate of 1.5 mm/yr while for the 6° case the unroofing takes place at a rate of only 0.5 mm/yr. It is important, then, to study the effects of varying the dip angle while holding the unroofing rate constant. The depth-time-temperature paths of the same particles chosen for study above were monitored for the 6° and 17° cases, and plots of this information are given in Figure 4-6. Whereas the curves differed in minor ways for constant rates of lateral displacement (different rates of unroofing), the depth-temperature and time-temperature paths are <u>exactly</u> the same when the unroofing rate is held constant. These results have important implications in terms of understanding the histories of geologic samples since they show that varying two of the three parameters of fault dip, rate of lateral displacement, and unroofing rate while holding the other one constant will have no significant effect on the depth-time-temperature paths of particles.

A

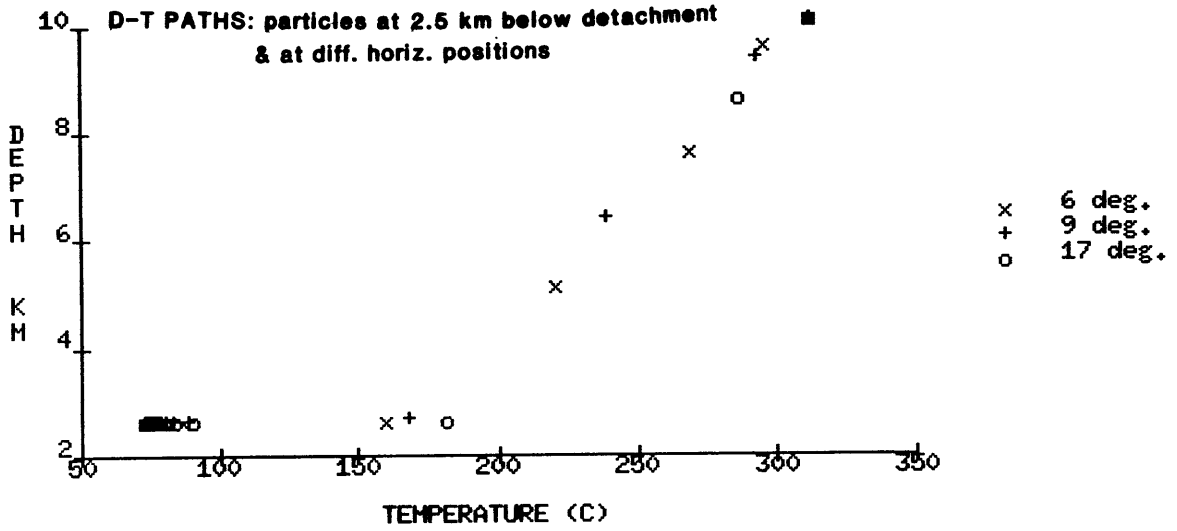

B

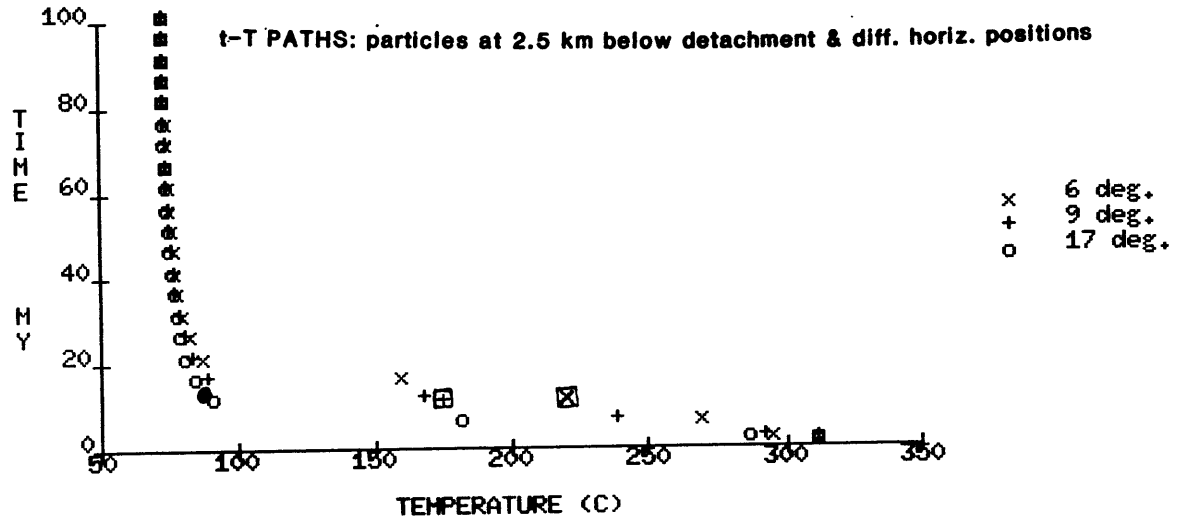

Figure 4-5: The depth-temperature and time-temperature paths of rocks that begin at the same structural and initial depths below fault surfaces with different dips. The original positions of the particles is shown in Figure 4-4.

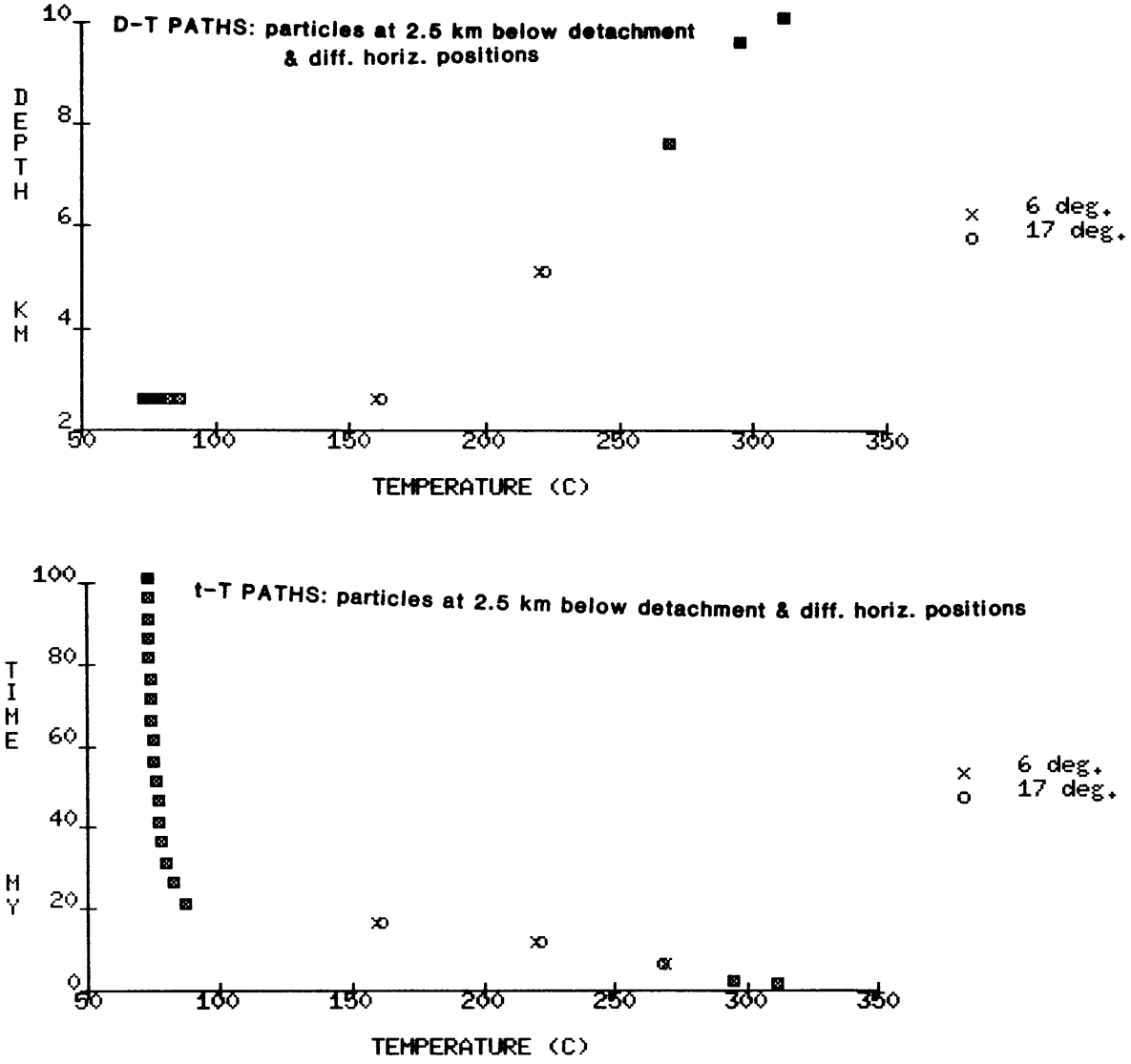

Figure 4-6: The depth-temperature and time-temperature paths of rocks that begin at the same structural and absolute depths below fault surfaces with different dips. In this case, the unroofing rate is held constant while the lateral displacement rate is allowed to vary.

UNROOFING RATE CONSTANT

4.2 Effects of Varying Rate of Lateral Movement

Variations in the rate of movement along the normal fault should theoretically have a notable effect on the predicted depth-temperature-time paths of rock particles. In order to isolate the effects of varying the rate of movement, runs were done for a fault surface dipping at 11° for movement at the rate of 2, 5, and 7.5 mm/yr. The input parameters for these runs are the same as those given in Table 4-I, and values specific to these particular runs are listed in Table 4-III. Since the fault dip is held constant for each of these cases, rocks that have the same initial depth with respect to the surface and begin at the same horizontal positions are also at the same structural depths and always end up at the same depth relative to the surface regardless of how the rate of lateral displacement is varied. For these runs, then, it is possible to compare directly the depth-temperature-time paths of rocks that begin at the same depth in the same column for different rates of fault displacement, eliminating the problems associated with comparing the paths of particles that are at different horizontal distances from the breakaway.

Dip angle	Depth to detachment					Horizontal displacement	Duration of displacement	Horiz. disp. rate
col.	1	2	3	4	5			
11°	0	5	10	15	20	75 km	37.5 my	2 mm/yr
11°	0	5	10	15	20	75 km	15 my	5 mm/yr
11°	0	5	10	15	20	75 km	10 my	7.5 mm/yr

Table 4-III: Input parameters used for testing the effects of variation in the rate of lateral displacement on the depth-temperature-time paths of footwall rocks.

Figures 4-7 and 4-9 show the cooling paths of particles initially at the same absolute depth in two different columns and for two different rates of displacement

of the hanging wall. For the fast rate of 7.5 mm/yr, particles initially at the same depth in the two columns cool primarily during the period of displacement and the ten million years immediately following the end of movement along the normal fault, but reach the isothermal parts of their temperature paths earlier than for the 2 mm/yr rate. As expected, particles that start closer to the detachment level experience a greater change in temperature. At the slower rate of displacement for the particle in column 5, geotherms re-equilibrate nearly as quickly as they are perturbed by the movement of cool upper plate material over the deeper footwall rocks, producing a nearly linear time-temperature path for this rock during the period of displacement along the normal fault. The particle in column 2, being farther from the detachment level, does not experience a significant change in temperature until it has already reached its final depth and the temperature drop near the surface has had time to effect changes at greater depths.

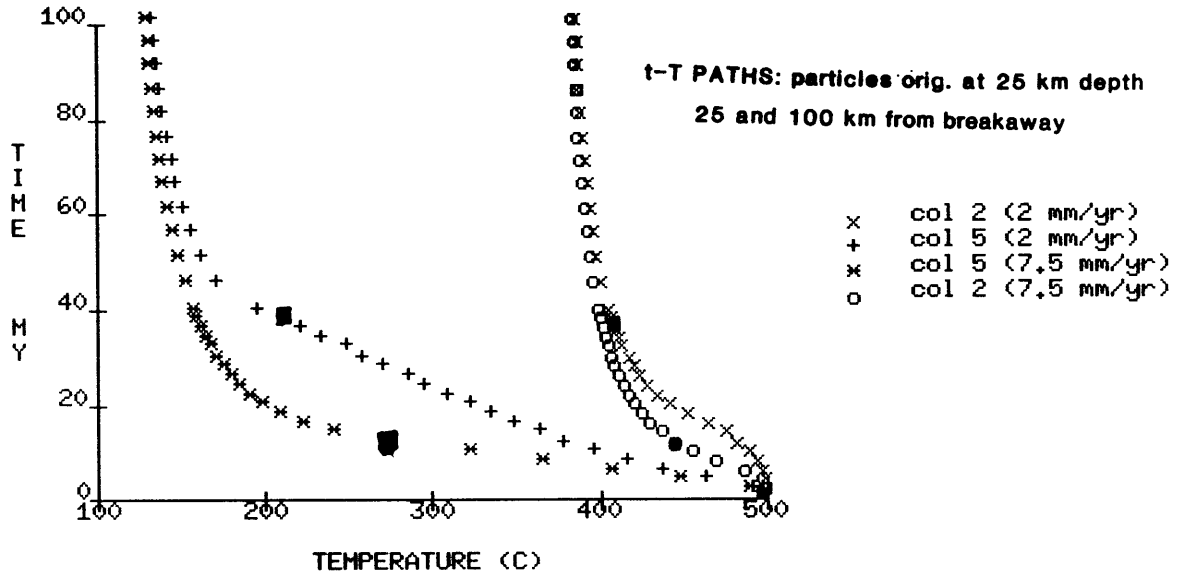

A

Figure 4-7: The T-t paths of particles at 25 km depth for a dip of 11° and displacement rates of 7.5 and 2 mm/yr. Columns 2 and 5 are at distances of 25 km and 100 km from the breakaway, respectively. The particles initially at 25 km are 20 km and 5 km below the detachment surface in columns 2 and 5 respectively.

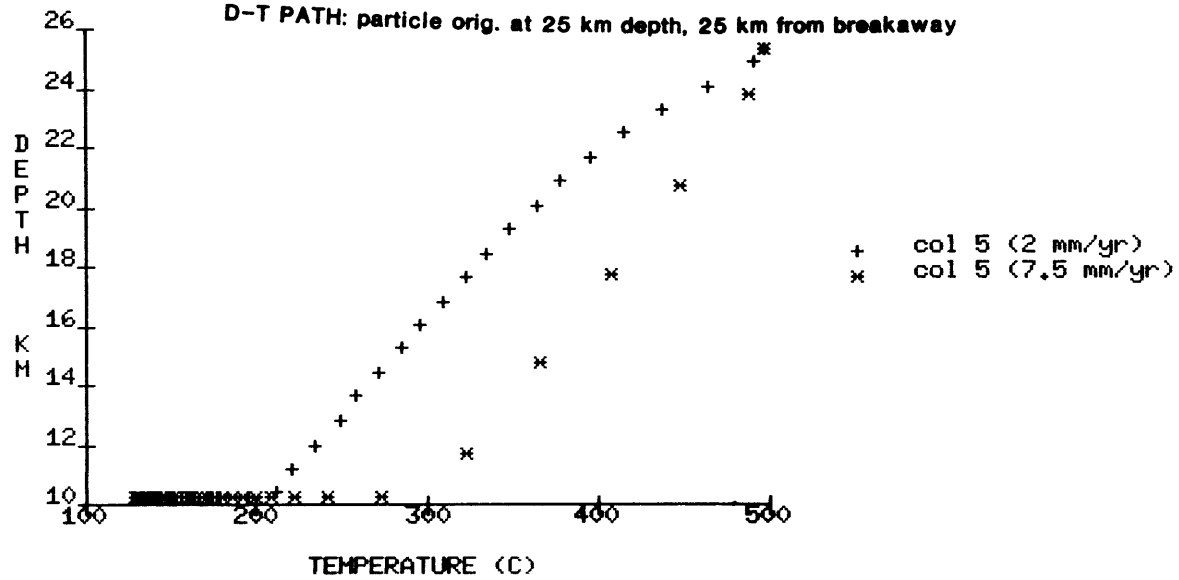

Figure 4-7: The depth-temperature paths of particles originally at 25 km depth in column 2.

B

Figure 4-10 shows the time-temperature and depth-temperature paths of a

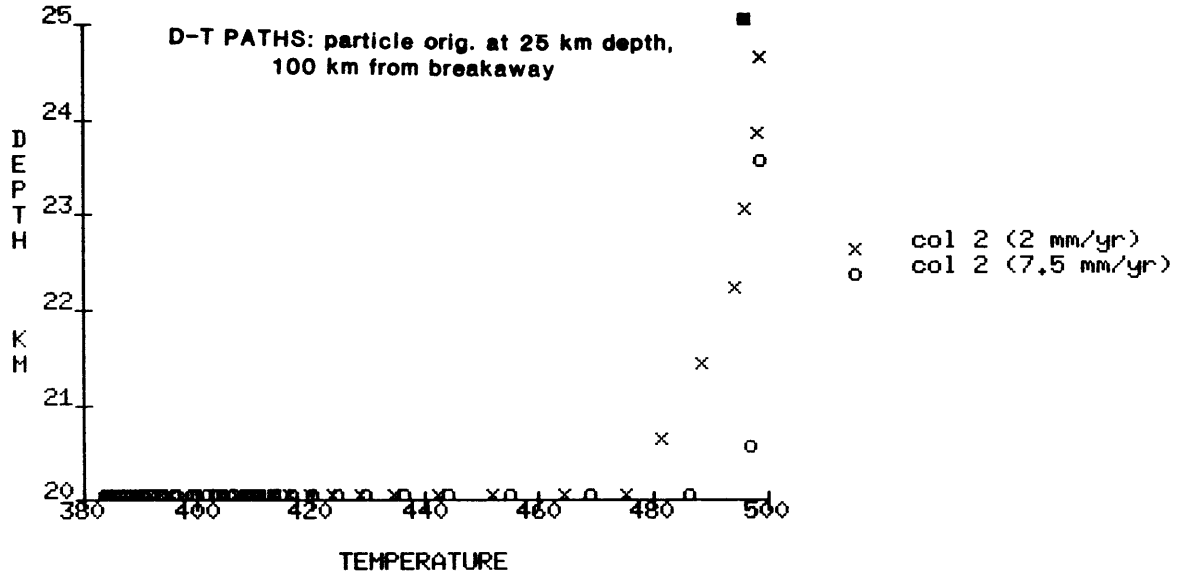

Figure 4-9 : The depth-temperature paths of particles originally at 25 km depth in column 5.

particle that begins at a depth of 17.5 km in column 4 (75 km from the breakaway). Varying the rate of lateral displacement has little effect on the depth-temperature paths of rocks that begin at this level, and the temperature and depth conditions of the particles show only minor differences after 40 Ma. A particle originally at a depth of 25 km (Figure 4-11) at the same distance from the breakaway has distinctly different temperature-depth paths for the two rates of movement however. For a lateral displacement rate of 2 mm/yr, the particle reaches its final depth 50°C cooler than for the faster displacement rate, and depth versus temperature changes occur at a constant rate of approximately 15°C/km. At this slower rate of displacement, some sort of steady-state is reached between relaxation of the geotherms and the downward penetration of cooling effects of unroofing to greater depths. Based on the plots in Figures 4-10 and 4-11, it can be tentatively concluded

that the depth-temperature paths of rocks near the detachment level are not significantly affected by varying the rate of lateral displacement along the normal fault. The time-temperature paths are somewhat more perturbed, however, and differences between the curves are significant enough that dating methods would probably be able to distinguish between the two cases. In contrast to the rock at a depth of 2.5 km below the detachment, particles that begin at greater depths relative to the decollement have depth-temperature paths that show significant differences as the movement rate is changed.

Although the depth-temperature paths (Figure 4-10a) of particles originally at 17.5 km depth are not very different for the two rates of lateral displacement along the fault, the time-temperature curves (Figure 4-10b) for the same particle show that, at a faster rate of displacement, the near-equilibrium temperature is reached much more quickly. At a distance of 75 km from the breakaway, significant changes in temperature continue throughout the duration of movement along the normal fault since unroofing is not completed until late in the period of hanging wall displacement. The isothermal part of the time-temperature path is therefore reached after only about 20 my for lateral displacement at a rate of 7.5 mm/yr while the particle takes 40 my to reach the same temperature when rocks are displaced at only 2 mm/yr. This result has potentially important implications for predicting metamorphic textures and assemblages since, for the faster rate of displacement, it is unlikely that a rock would remain at certain pressure-temperature conditions long enough to begin equilibrating. In addition, Figure 4-10a suggests that it may be possible to determine the rate of lateral displacement along a normal fault zone by dating of metamorphic rocks.

In Figure 4-10 it will be noted that small discontinuities occur in the depth-temperature and time-temperature plots for the slow rates of fault displacement.

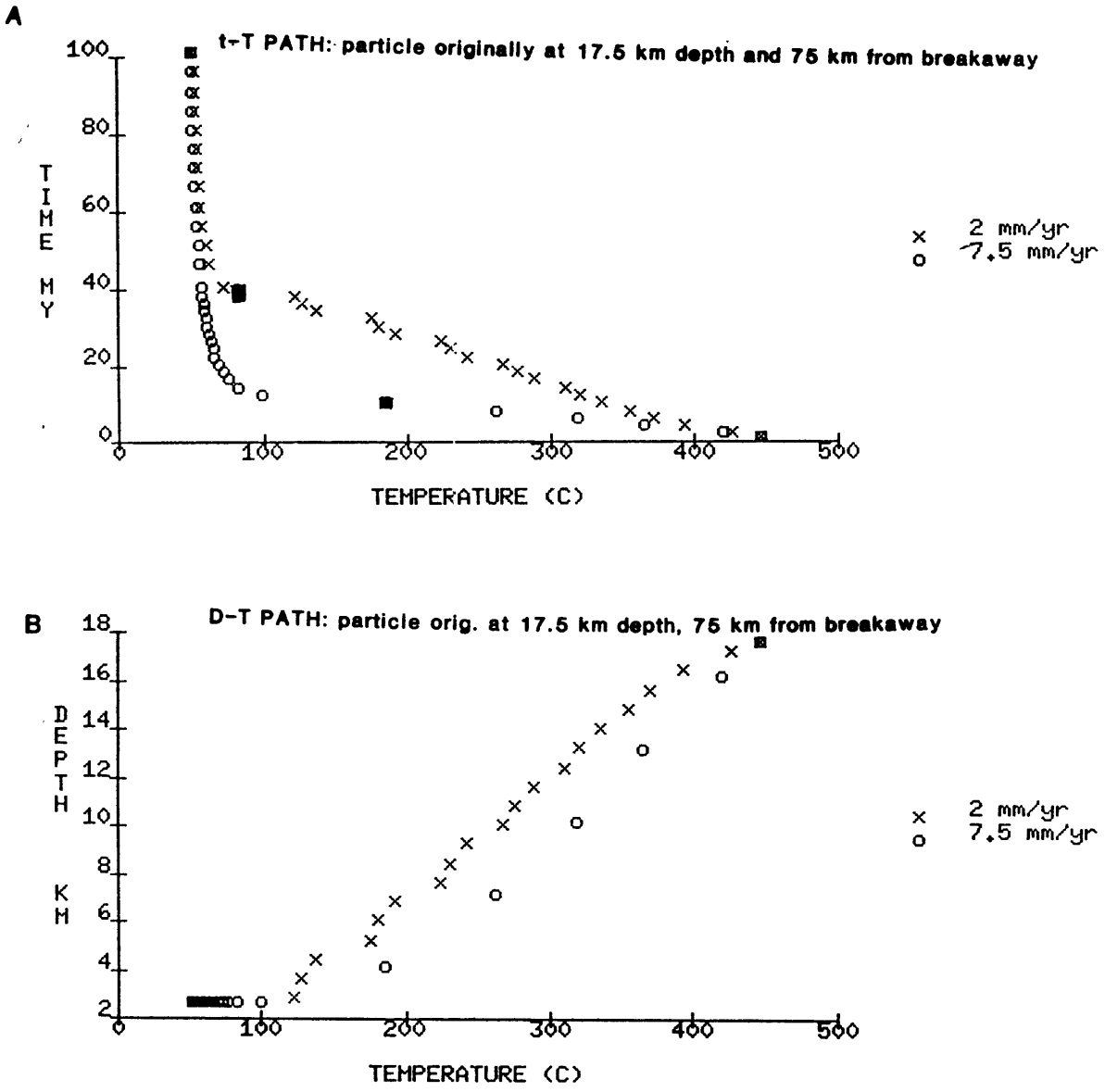

Figure 4-10: The time-temperature and depth-temperature paths of particles originally at 17.5 km depth at 75 km from the breakaway for two rates of lateral displacement along the normal fault. These rocks are 2.5 km below the detachment surface.

These discontinuities are an artifact of problems encountered in applying the finite difference technique to problems in which unroofing is occurring at a rate of less than about 1 mm/yr. The discontinuities do not present a serious difficulty and can probably be eliminated by decreasing the size of the finite difference grid. The best approximation of depth-temperature-time paths at slow rates of displacement can be obtained by smoothing out the discontinuous curves across the temperature jumps.

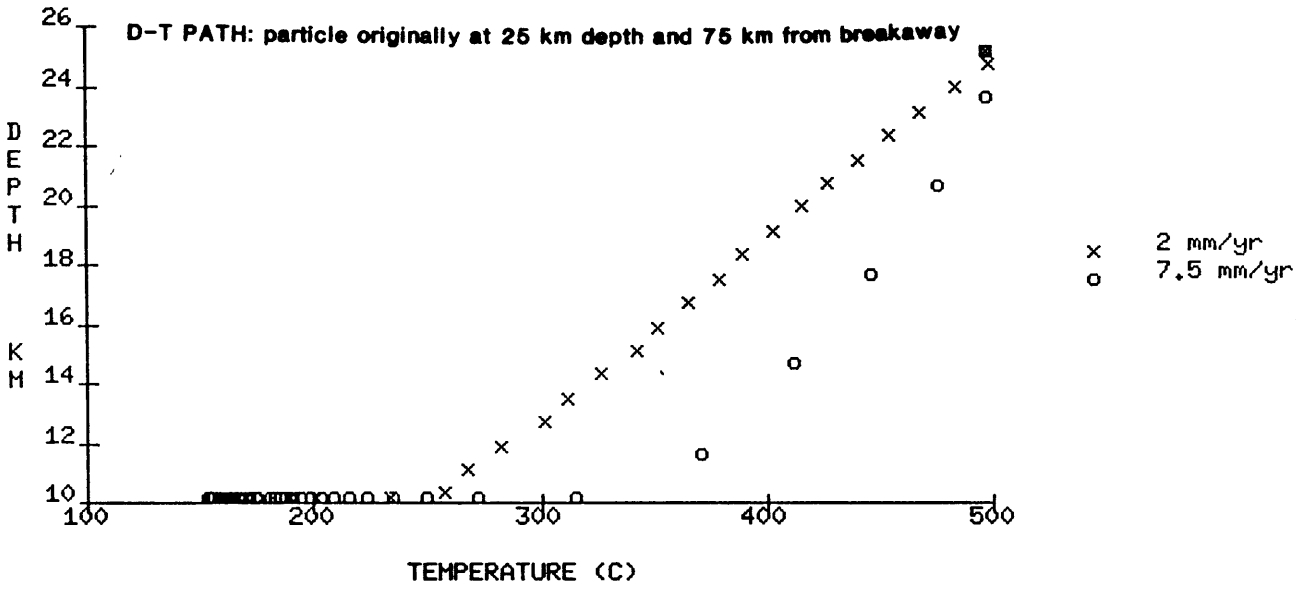

Figure 4-11: The depth-temperature paths of particles originally at 25 km depth at 75 km from the breakaway for two rates of lateral displacement along the fault. These rocks are 2.5 km below the detachment surface. Note the differences between the depth-temperature paths in this figure and those in Figure 4-10.

The final set of depth-temperature and time-temperature plots, shown in Figures 4-12 and 4-13, provide a basis for comparing the combined effects of particle depth and rate of displacement on the cooling paths of rocks at the same horizontal distance from the breakaway zone. Figures 4-12 and 4-13 show the

depth-temperature and time-temperature plots of particles that are originally at depths of 25 and 50 km in a column 100 km from the breakaway. The particles occur at 5 and 30 km below the detachment surface respectively. For a displacement rate of 2 mm/yr, the particle originally at 25 km (Figures 4-12a and 4-13a) follows a path that is slightly concave toward the depth axis as it is uplifted and cooled. At a displacement rate of 7.5 mm/yr, however, the depth-temperature path for this particle is slightly convex during the period of uplift, and the rock reaches its final depth 75°C hotter than for the slower displacement rate. From the time-temperature plot for this particle (Figure 4-13a), it is seen that, regardless of the rate of lateral displacement, the particles cool to the nearly the same temperature by 100 Ma. Cooling of the particles occurs more quickly for the 7.5 mm/yr displacement rate, but, following the period of uplift, the particles must undergo an isobaric change in temperature greater than that for the 2.5 mm/yr case.

The time-temperature and depth-temperature paths for the particle that begins at a depth of 50 km also at a distance of 100 km from the breakaway are shown in Figures 4-12b and 4-13b. The very different shapes of these curves as compared to those in the 25 km case demonstrate the effect of particle depth on the depth-time-temperature path of a metamorphic rock. At the slow 2 mm/yr displacement rate, the initial p-T path is one of isothermal uplift, but, by about 5 my after the onset of faulting (as seen on the time plot in Figure 4-12b), the effects of moving cool upper plate rocks over a decollement set at 20 km have penetrated to the depth of the particles originally at 50 km, and cooling of these rocks begins. The linear portion of the depth-temperature plot has a slope of approximately 8°C/km and represents a level in the column where the effects of emplacing the cool upper plate rocks is almost exactly balanced by the relaxation of

the geotherm. The change in temperature along the isobaric cooling path of the 50 km particles is much greater than for the corresponding part of the 25 km plot, indicating that the geotherm continues to relax significantly at great depths long after the active displacement has ended. For rapid rates of displacement, the particle originally at 50 km is unroofed nearly isothermally during the period of tectonic denudation and then cools isobarically following the completion of movement along the fault. The isothermal part of this path is an effect of the cooler near-surface temperatures not having had time to penetrate to the mid-lithospheric levels before the period of displacement has ended. Once the rock has reached its final depth, however, it must undergo over 200°C of cooling before reaching equilibrium.

The time-temperature plot for the particle originally at a depth of 50 km has two important features. Most significant is the fact that the time-temperature curves have the same shape and that there is at most a 10 my time difference between when rocks unroofed at the two displacement rates reach the same temperature. Some dating methods may be refined enough to distinguish between points on these time-temperature curves. Secondly, at 100 Ma, the temperature of the rapidly unroofed particle varies from that of the more slowly unroofed particle by less than 10°C, a completely insignificant amount in terms of the pressure-temperature conditions that will be recorded in the rock at this time interval. For the particle originally at 50 km then, distinguishing between the metamorphic effects of different rates of lateral displacement is probably nearly impossible unless the early uplift path of the rock can be determined to be either nearly isothermal or spread out over a measureable change in temperature.

Figure 4-12: Depth-temperature plots for particles originally at 25 km and at 50 km at a distance of 100 km from the breakaway for two rates of movement.

A

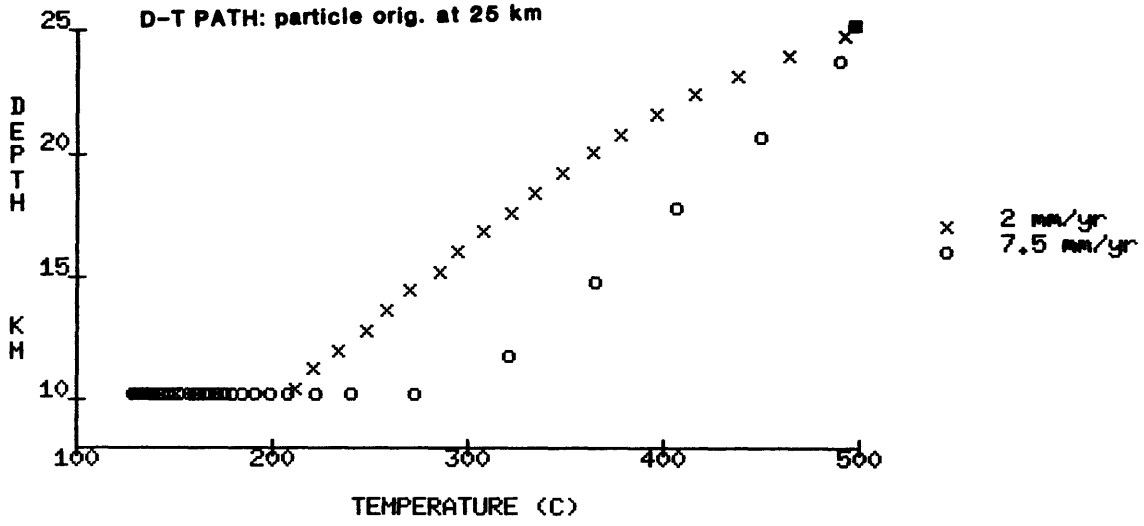

B

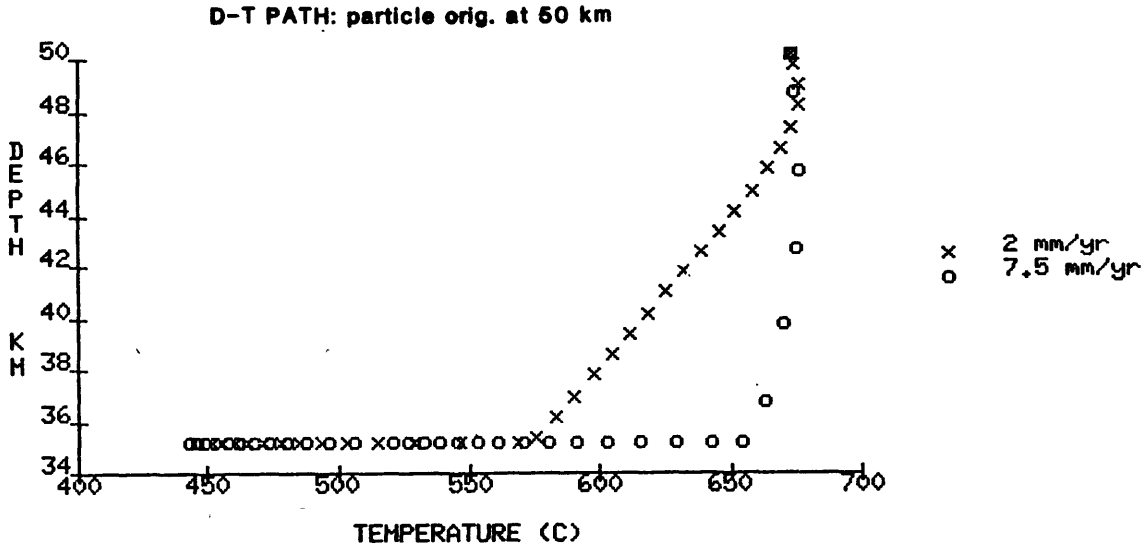

A

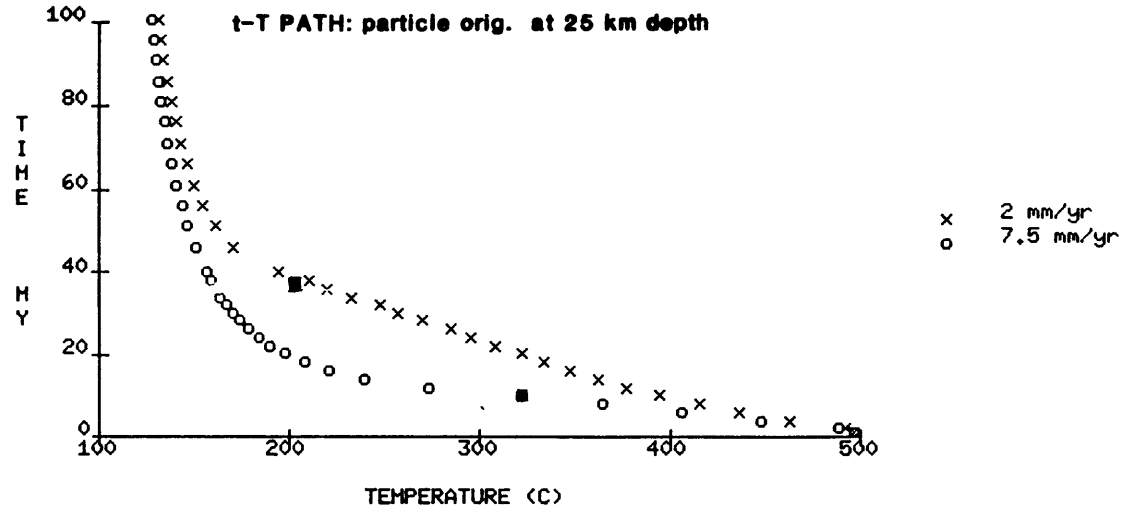

B

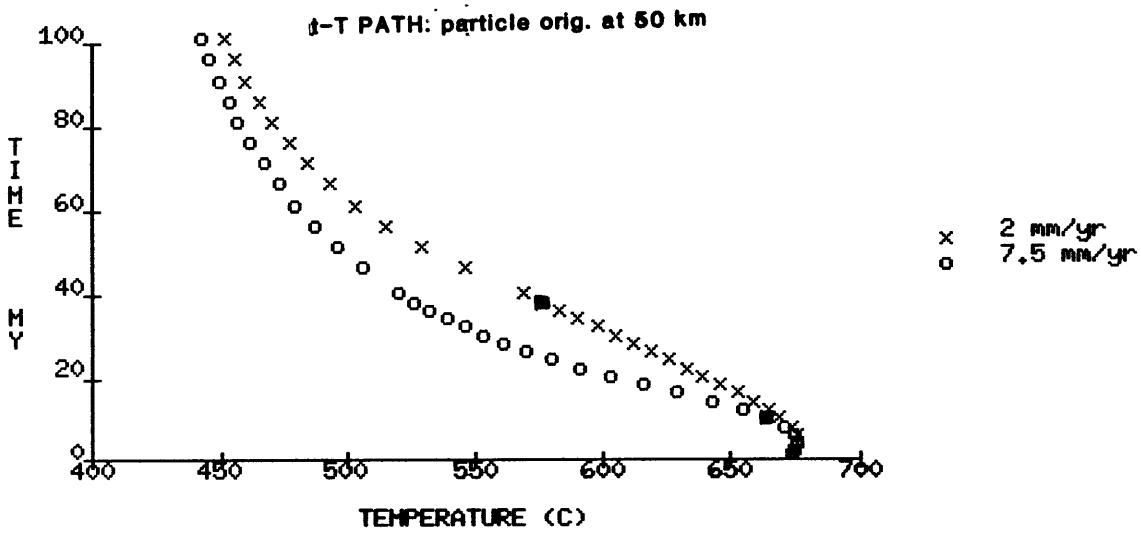

Figure 4-13: Time-temperature plots for particles originally at 25 km and at 50 km at a distance of 100 km from the breakaway for two rates of displacement along the normal fault.

4.3 Effects of Pure Shear Extension vs. Extension by Normal Faulting

As discussed in Chapter 1, two processes have been proposed to explain how the lithosphere is thinned. The pure shear mechanism involves simultaneously thinning and lengthening a lithospheric element while preserving its overall area whereas the normal faulting thins the lithosphere by causing the displacement of near-surface particles relative to footwall rocks. An important question is whether it is possible to distinguish between the two mechanisms by studying the metamorphic paths of rocks in extensional terrains. A forward modelling computer program like the one developed for this study provides a basis for straightforward comparison of the theoretical depth-temperature-time paths of rocks in a lithosphere undergoing either pure shear extension or thinning as a result of normal faulting.

Two models were chosen to compare the effects of pure shear and brittle extension of the lithosphere. The initial geotherm used for these analyses was linear and steady-state between 0°C at the surface and 1300°C at the base of a 125 km lithospheric plate. Radioactive heat production was set at 0 $\mu W/m^3$ for each run, and the period of active thinning of the lithosphere lasted 25 my. For the case of normal faulting, a dip angle of 11° was used, and the hanging wall was moved down the fault surface until the lithosphere had been thinned by 5 km to a thickness of 120 km. The depth-temperature-time changes of a particle 50 km from the breakaway and 5 km below the decollement (at an original depth of 15 km) were monitored as the particle was unroofed to the depth of 10 km.

For the pure shear case, there were two ways to set up the problem for direct comparison with the normal faulting scenario. As discussed above, the normal fault model was designed to yield a post-displacement lithospheric thickness of

120 km, and it would be possible to thin the entire lithosphere by 5 km with a pure shear mechanism by setting $\beta = \gamma = 1.04$. Although this model is theoretically the most valid in terms of directly comparing the effects of pure shear and normal faulting processes that thin the lithosphere by the same amount, the discussion in the previous sections has focussed on the comparison of the depth-temperature-time paths of particles that begin at the same depth and have the same post-uplift depths as well. In order for a particle originally at 15 km to be uplifted to the 10 km depth through a pure shear process, the lithosphere must be thinned by 66% ($\beta = \gamma = 1.66$). Since thinning by this amount provides a basis for directly comparing the effecs of pure shear and normal faulting for a specific rock particle, this $\beta = \gamma = 1.66$ value was deemed most appropriate, and the problem was set up to monitor the depth-temperature-time changes of the particle originally at 15 km.

Figure 4-14 shows the depth-temperature and time-temperature plots of the particle originally at 15 km in the two extensional models. For the pure shear model, the syntectonic path is one of isothermal uplift followed by isobaric cooling after extension has been completed. In the normal faulting case, however, the rock cools primarily during the period of active displacement along the fault and for approximately 20 my years after movement ends, and follows a nearly isothermal path after 40 Ma. The change in temperature for the isobaric cooling path of the rock in the normal fault model is smaller than that for the particle in the pure shear case by only 17°C, it is expected that for particles originally at greater crustal depths, the ΔT along the isobaric part of the cooling path would be considerably larger for the pure shear model. The time-temperature paths also show an interesting effect at 100 Ma; although 75 my have passed since the end of the pure shear episode, the temperatures at a depth of 10 km for this model have not relaxed completely to the background steady-state temperature of 104°C.

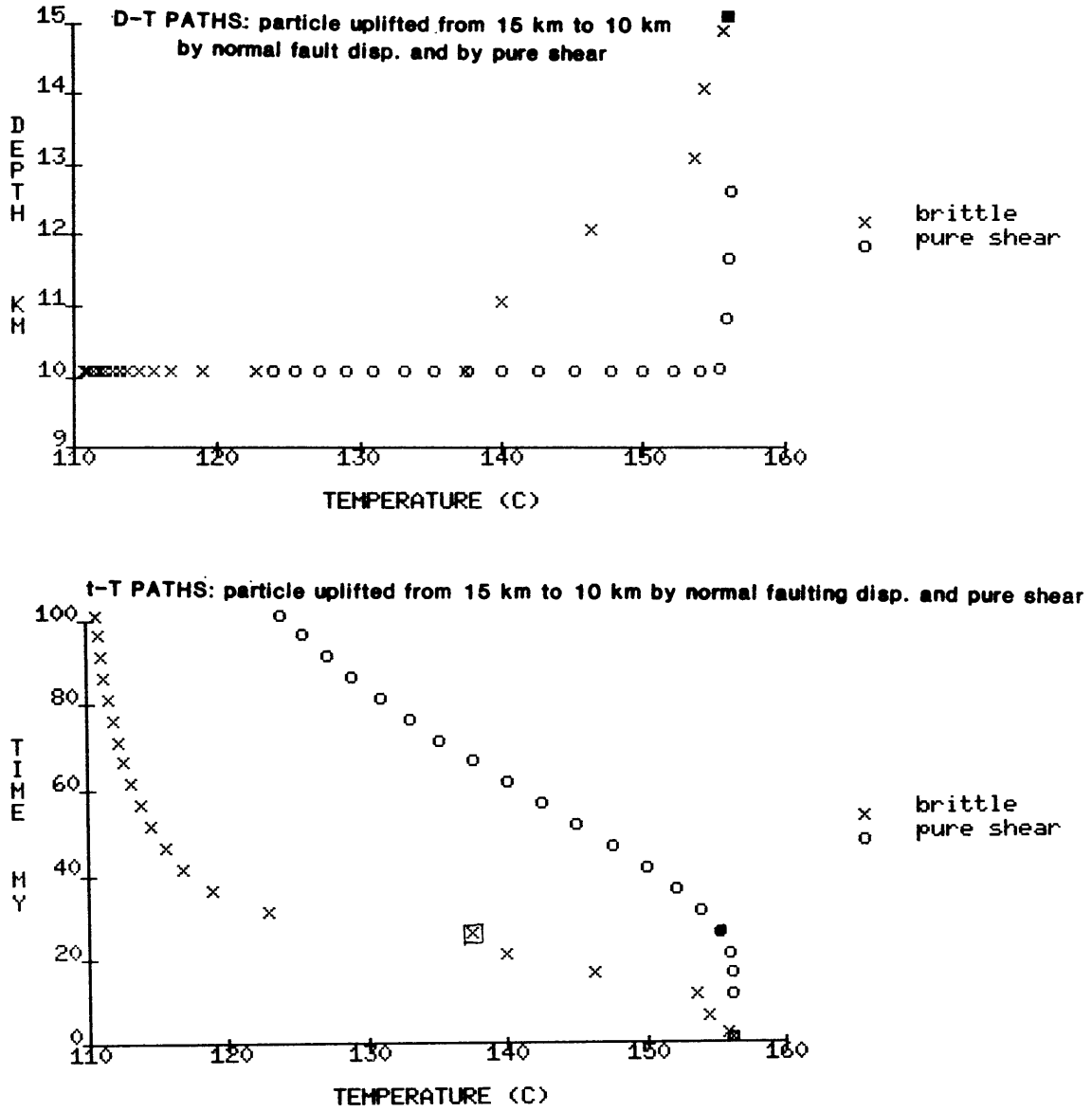

Figure 4-14: The depth-temperature and time-temperature paths of rocks uplifted from 15 km to 10 km depth through thinning of the lithosphere by pure shear and normal faulting processes. For both mechanisms, thinning occurs during the first 25 my period plotted on the time-temperature curve. For the normal faulting case, the monitored particle is at a depth of 5 km below the decollement.

This comparison of the effects of thinning by pure shear versus normal faulting provides only a preliminary basis for understanding how these two extensional processes affect the depth-temperature-time paths of rocks, but the qualitative differences are important. Theoretically, it may be possible to distinguish between rocks uplifted primarily through a pure shear or normal fault mechanisms if the overall depth-temperature-time relationship can be determined. For rocks that begin at deeper lithospheric levels, it is expected that the difference between the temperatures at the same time would be greater than those observed in the time-temperature plot in Figure 4-14. In that case, dating methods might be useful in distinguishing between the two modes of extension. Without dating methods, it might still be possible to distinguish between pure shear and normal faulting if it were known that the early depth-temperature path was one of isothermal uplift as opposed to gradual cooling as the rocks approached their final depths.

Chapter 5

Conclusions and Suggestions for Further Study

One of the primary aims of this study was to establish a realistic framework for understanding the metamorphic conditions associated with extensional tectonics. On the basis of the models presented in Chapter 4, it is obvious that extension through simple shear along discrete normal fault zones produces a wide variety of depth-temperature-time paths. The shape of these paths depends on the initial depth of the particle relative to the surface and to the detachment, the rate of displacement along the fault zone, the angle of dip of the normal fault surface, the horizontal distance between a particle and the breakaway, and the rate of unroofing of the footwall.

This study shows that varying the dip of a fault has little effect on the depth-temperature-time paths of particles that are initially at the same depth below the surface and at the same depth relative to the detachment. Regardless of the angle of dip of the fault, unroofing rocks at the same rate will produce exactly the same depth-temperature-time relationships for rocks initially at the same depths below the detachment and the surface. Holding the angle of dip constant while increasing the rate of movement along the normal fault causes footwall rocks to experience a smaller drop in temperature during the period of faulting and unroofing. After reaching their final depths, these rocks cool isobarically through a greater interval than those below a hanging wall displaced at slower rates.

The depth of a particle below the detachment is an important factor in distinguishing between the depth-temperature curves of rocks unroofed at different rates. Particles near the detachment horizon yield depth-temperature paths that

are very similar despite the variation in displacement rate. However, rocks that begin 20 km or more below the decollement level have depth-temperature paths that vary significantly with displacement rate, and these variations might be important in the analysis of data from metamorphic terrains.

A preliminary comparison of the effects of uplifting a particle from 15 km to 10 km depth through pure shear extension and through thinning the lithosphere by movement along a normal fault revealed important differences in the pressure-temperature-time paths. Whereas the rock in the normal fault model underwent cooling throughout the duration of tectonic activity and for approximately 20 my following the end of movement along the fault zone, there is no syntectonic cooling for a particle that begins and ends at this same level in the pure shear mode. For the pure shear case, the particle is uplifted isothermally and begins cooling only after it has reached its final depth. The change in temperature is therefore much larger for the isobaric part of the cooling path for the particle in the pure shear model than for the rock in the normal fault model.

The computer program developed in this study can be used to generate forward models of the thermal structure in a variety of extensional terrains. The flexibility of the program makes it applicable to many tectonic settings and renders it especially useful in studying the changes in the depth-temperature-time paths of rocks in response to varying a single problem parameter. Further work is necessary to solve specific problems with the present version of the forward modelling program. As discussed in Chapter 4, a modification is necessary to eliminate the temperature discontinuities that occur in the depth-temperature and time-temperature paths of rocks being unroofed at very slow rates. Reducing the size of the depth increment ϵ may solve this problem, but it will probably be necessary to rewrite substantial portions of the program to make possible the use of the larger

temperature arrays required for finer grid spacing. Other changes are necessary to simulate simultaneous pure shear thinning and displacement of the hanging wall of the normal fault, and several extrapolation routines must be modified to permit the tracking of depths and temperatures of particles near the surface (within the upper 7.5 km) in the hanging wall. At present, however, the program yields useful information about the depth-temperature-time paths of rocks in the footwall of normal faults and, for the preliminary work presented here, provides forward models that establish a good basis for the direct comparison of metamorphic rocks that have been uplifted by tectonic denudation.

A final goal of this study will be to predict the theoretical depth-temperature-time paths of metamorphic rocks in extensional terrains. By assuming an initial bulk composition for a rock at a particular structural level (particular depth below the detachment), and modelling its theoretical depth-temperature path, the forward models developed for this study can be extended to predict the mineralogy and textural changes that would be expected in certain extensional settings. In the future, work should concentrate on establishing a complete set of forward models that test the effects of varying not only lateral displacement rate and fault dip angle, but also the initial radioactive heat distribution, the initial geotherm, and the number of imbricate faults used to thin the lithosphere. After this complete set of models is developed, it will be possible to decide which of the differences in the depth-temperature and time-temperature paths will be sufficiently large to produce noticeable variation in a standard metamorphic assemblage. In particular, future work should focus on analyzing the depth-temperature-time changes experienced by rocks that begin and end at the same depths relative to the detachment and to the surface because information about the horizontal distance between a particle and the breakaway zone is almost never available.

Much work is still needed in order to transfer the theoretical information produced by this study to the domain of practical applications. Eventually, it may be possible to use a technique like that outlined for thrust terrains by Royden and Hodges (1984) to determine the complete pressure-temperature path of a metamorphic rock in an extensional setting. In the final analysis, only this sort of inverse modelling will provide a completely valid basis for comparison with the theoretical forward models. If the pressure-temperature information from metamorphic rocks in extensional terrains can be inverted, it should be possible to use the forward models to determine the values between which physical parameters can vary while still producing pressure-temperature paths similar to those inferred from field data. Defining the possible ranges in variation of the physical parameters may help to characterize the extensional processes primarily responsible for the uplift of a particular metamorphic sample. The comparison of the forward models with the reconstructed pressure-temperature paths of rocks from metamorphic terrains should provide an understanding of the relative importance of pure shear extension in uplifting rocks from intermediate or deep crustal depths.

References

Carslaw, H.S., and Jaeger, J.C., 1972, Conduction of Heat in Solids, 496 pp., Clarendon, Oxford.

Coney, P.J., 1979, Tertiary evolution of Cordilleran metamorphic core complexes. In Armentrout, J.M., Cole, M.R., and Terbest, H. ed., Cenozoic Paleogeography of the Western United States SEPM, 15-28.

Coney, P.J., 1980, Overview and introduction. In Crittenden, M., Coney, P.J., and Davis, G., ed., Cordilleran Metamorphic Complexes, GSA Memoir 153, 3-26.

Davis, G.H., 1980, Structural characteristics of metamorphic core complexes, southern Arizona. GSA Abstracts with programs 7(5), 602.

Davis, G.H. and Coney, P.J., 1979, Geologic development of the Cordilleran metamorphic core complexes. Geology 7, 120-124.

Eskola, P., 1948, The problem of mantled gneiss domes. Geological Society of London Quarterly Journal 104. 461-476.

Furlong, K.P., and Londe, M.D., in press, GSA Special Paper, ed. Larry Mayer.

Hamilton, W., and Myers, W.B., 1966, Cenozoic tectonics of the western United States. Reviews of Geophys. 5, 509-549.

Oxburgh, E.R. and Turcotte, D.L., 1974, Thermal gradients and regional metamorphism in overthrust terrains with special reference to the Eastern Alps. Schweiz. miner. petrogr. Mitt. 54, 641-662.

Parsons, B., and Sclater, J. G., 1977, An analysis of ocean floor bathymetry and heat flow with age, J. Geophys. Res. 82, 802-825.

Royden, L., Horvath, F., Nagymarosy, A., and Stegena, L., 1983, Evolution of the Pannonian Basin system 2. Subsidence and thermal history. Tectonics 2, 91-137.

Royden, L.H., and Hodges, K.V., 1984, A technique for analyzing the thermal and uplift histories of eroding orogenic belts: a Scandinavian example, J. Geophys. Res. 89, 7091-7106.

Sclater, J.G., Jaupart, C., and Galson, O. ,1980, The heat flow through oceanic and continental crust and the heat loss of the earth, Rev. Geophys. Space Physics 18(1), 269-311.

Stewart, J.H., 1971, Basin and Range structure--a system of horsts and grabens produced by deep-seated extension. Geol. Soc. America Bull. 82, 1019-1044.

Wernicke, B., 1981, Low angle normal faults in the Basin and Range Province: nappe tectonics in an extending orogen. Nature 291, 645.

Wernicke, B., 1985, Uniform-sense normal simple shear of the continental lithosphere. Can. J. Earth Sci. 22, 108-125.

Appendix A
FORTRAN Source-Code

A.1 Formodel.f

FORTRAN source-code for the main thermal modelling program. This program uses formatted input, and great care should be taken in entering numbers according to the indicated format code. In the future, some of the sections in this program will be broken out as subroutines, but, at this time, a working model has highest priority, and the code was left in inelegant form when necessary. This version contains several modifications necessary to run the models tested for this study.

```
C       PROGRAM TO DO THERMAL MODELLING USING A FINITE DIFFERENCE METHOD

C       by C.D. Ruppel, 1985-86
C       Copyright (C) 1986 Massachusetts Institute of Technology
C       Thesis Supervisor:  Prof. Leigh Royden

C       This program models the thermal structure of a lithosphere
C               undergoing extension either through a pure shear
C               mechanism or as a result of movement along normal
C               fault surfaces.

C       The user of the program must input the following problem
C       parameters:
C               number of consecutive fault movements to be studied
C               how many columns of lithosphere to examine
C               thickness of lithosphere
C               depth increment (x part of mesh-spacing for calculations)
C               total time to run the problem
C               time increment (t part of mesh-spacing for calculations)
C               what sort of initial geotherm to use
C               temperature at the base of the lithosphere
C               distance between lithospheric columns
C               amount of movement on fault
C               time period of fault movement
C               depth of decollement in each column
C               percent pure shear extension above and below decollement
C               time during which pure shear extension occurs
C               radioactive heat production


C       This program uses formatted input.  The format codes are given
C               in parentheses after each query.  Use a decimal point for
C               all real input; never use a decimal in integer input.
C               Failure to input numbers properly will cause the program
C               to crash.
```

```
C       Be certain to calculate ahead of time thickness of the lithosphere
C             after the faults have removed the upper part of the crust.
C       The program can be run for a maximum of 100 my if 0.1 my increments
C             are used.  For 0.05 my incrementation, then, the maximum is
C             50 my.  Pure shear extension may last up to 200 time
C             increments.

      character*10 string
      character*7 name
      character*1 dum(5)
      integer answ,tincr,increm,pts,i,j,yorn,j1,j2,sum,sum1,sum2
      integer k1,p1,w,l,ia,ib,diff,n1,n2,s,a,g,p,imbric,resp,disc
      integer tpts,npts,n4,c,col,c1,rcol,n6,ic,id,div,c2,cont,break
      integer pnum,pulse,v,v1,count
      integer i3(25),n3(25),i5(14),d(5),i2(5),h(5),c3(10),idept(5)
      real base(5),baset(5),baseb(5),horiz(203,121,5),add(203)
      real x,dx,dt,k,f,dtsec,time,m2,tinit,tend,strtch,upthin
      real cond,thin,disp,ddisp,val,mend,mbegin,extra
      real power,tbase,sumgam,sumbet,sumh,suma,tmax,dmax
      real deltat,beta,gamma,upxten,loxten,vert,vert1,vertic
      real rad(5),deep(5),lthick(5),parcel(25),radio(52,5)
      real dbeta(200),dgamma(200),ctime(14),ddepth(5),decoll(5)
      real m(121,5),b(121,5),m1(121,5),b1(121,5),number(52,5)
      real ptemp(5),pdept(5)
      real radio1(52,5),radio2(52,5),slope(25,5),dept(52,5)
      real depth(121,5),depth2(201,121,5),r(55,5),r1(55,5),q1(55,5)
      real z(25,25),y(25,25),lat(5),angle(5),sumlat(5),q(55,5)
      real tprint(25),xprint(25,55),dprint(25,55),dprint2(25,55)
      real temp(1001,121,5),temp2(201,55,5),temp3(201,55,5)
      real temp5(52,5),temp6(201,52,5),temp7(25,55,5)
      real temp4(25,55,5),tabov(5),tat(5),ddisc(5)

C       Variable list:

C         imbric = number of fault structures
C            col = number of lithospheric columns
C           cont = number of columns whose final geotherms are to be saved
C                        for next fault structure
C              x = thickness of lithosphere in km
C             dx = size of thickness increment in km
C           time = total time to run problem in my
C             dt = time increment in my
C          break = at what column breakaway will be in next run
C            lat = array of distances between adjacent columns
C         mbegin = time at which fault movement begins (my)
C           mend = time at which fault movement ends (my)
C           disp = amount of horizontal displacement on fault (km)
C         decoll = array of decollement depths in each column
C         upxten = % pure shear extension above the decollement
C         loxten = % pure shear extension below the decollement
C          tinit = time at which pure shear begins (my)
C           tend = time at which pure shear ends (my)
C          tbase = temperature at base of lithosphere (C)
C           pnum = number of thermal pulses in the lithosphere
C          pdept = depths of thermal pulses
C          ptemp = initial temperature at the depth of the thermal pulse

      open (7,file="words",form="formatted")
      open (11,file="twodee",form="formatted")

C     User inputs how many imbricate structures are to be analyzed

      write(*,120)
120   format('How many faults are there? (input 1 for 1 set data)')
      read(*,121)imbric
121   format(i2)
```

```
C     Input variables of problem to be studied

      write(*,806)
806   format('Input number of lithospheric columns (up to 5) (int)')
        read(*,807)col
807     format(i2)

      if (imbric.eq.1) go to 2

      write(*,895)
895   format('How many columns from this problem are needed in the next
     +problem?')
        read(*,896)cont
896     format(i1)

      break=col-cont+1

2     do 1,l=1,imbric

      write (*,10)
10    format ('Enter thickness of lithosphere, depth increment 2(f5.2)')
        read (*,20)x,dx
20      format (f5.1,f5.2)

      write (*,330)
330   format ('Enter time increment (my) and total time (f4.2,f5.1)')
        read (*,40)dt,time
40      format (f4.2,f5.1)

      if (l.eq.1) go to 883
      write(*,897)cont,(lat(n2),n2=break,break+cont-2)
897   format('Distance between first ',i1,' columns is assumed ',3f7.2,
     +'respectively.')

      do 885,n2=1,cont-1
      lat(n2)=lat(break+n2-1)
885   continue

      write(*,898)col-cont
898   format('Input the last ',i1,' intercolumnar distances (f5.2)')
      read(*,882)(lat(n2),n2=break+cont-2,col-1)
882   format(4(f5.2))
      go to 990

883      write(*,662)col-1
662   format('Distance between adjacent columns:',i3,' values (f6.2)')
        read(*,663)(lat(n2),n2=1,col-1)
663     format(4(f6.2))


990   write(*,664)
664   format('Fault moves between what times? (f4.1)')
        read(*,665)mbegin,mend
665     format(f4.1,f4.1)

      write(*,666)
666   format('Final amount of horizontal displacement on fault (f6.2)')
        read(*,667)disp
667     format(f6.2)

      write(*,801)col
801   format('Input depth to decollement in col. 1 through',i2,'; note:co
     +lumn one must be at breakaway (depth to decollement=0.0 km) f5.2')
        read(*,802)(decoll(n),n=1,col)
802     format(5f5.1)
```

```
894   write(*,803)
803   format('Input % extension (as decimal) above decollement (f4.2)')
        read(*,804)upxten
804     format(f4.2)

      write(*,800)
800   format('Input % extension (as decimal) below decollement (f4.2)')
        read(*,805)loxten
805     format(f4.2)

      write(*,810)
810   format('Extension begins? Extension ends? (my) 2(f4.1)')
        read(*,815)tinit,tend
815     format(f4.1,f4.1)


C     Input parameters for initial geotherms
        if (1.ne.1) go to 134

      write(*,132)
132   format('Temperature at base of lithosphere in degrees C?')
        read(*,133)tbase
133     format(f7.2)

      write(*,130)
130   format('Initial temperature structure is 1)linear 2)discontinuous
     +3)an exponential funtion of depth')
        read(*,131)resp
131     format(i1)

      if (resp.eq.3) go to 134
      if (resp.eq.2) go to 135

        write(*,260)
260     format('Do you want to include a thermal pulse? 1=yes')
        read(*,261)pulse
261     format(i1)
        if (pulse.ne.1) go to 134
        write(*,262)
262     format('At how many depths do thermal pulses occur?')
        read(*,263)pnum
263     format(i1)
        write(*,264)
264     format('Input depth 1, space, temp. at this depth <CR> 2(f6.1):')
        do 267,i=1,pnum
        read(*,265)pdept(i),ptemp(i)
265     format(f6.1,f6.1)
267     continue
        go to 134

135   write(*,138)
138   format('How many discontinuities are there?')
        read(*,139)disc
139     format(i1)

        write(*,170)
170     format('Do the discontinuities occur at the same depth in each
     +column? yes=1')
        read(*,171)answ
171     format(i1)

      write(*,140)
140   format('Input depth of discontinuity, temp. at discontinuity,
     +and temp. below discontinuity.  New line each entry. 3(f6.1)')
        read(*,141)(ddisc(i),tabov(i),tat(i),i=1,disc)
141     format(3(f6.1))
```

```
C     Calculation of basic problem parameters
134   tincr=int(time/dt)
      increm=int(x/dx)
      dtsec=dt*3.15527
      k=0.008
      cond=0.0075
      ic=int(mbegin/dt)+1
      id=int(mend/dt)+1
      ddisp=disp/(id-ic)
      ddisc(disc+1)=x
        do 268,i=1,pnum
        idept(i)=int(pdept(i)/dx)+1
268     continue
      sumlat(1)=0.0
      do 607,c=2,col
      sumlat(c)=sumlat(c-1)+lat(c-1)
607   continue

      do 809, c=1,col
      d(c)=int(decoll(c)/dx)+1
809   continue

      do 8,i=1,5
      dum(i)=''
8     continue


C     Calculate initial thermal gradient
      if (l.gt.1) go to 146


        if (resp.ne.3) go to 1901

        open(3,file='exp',form='formatted',status='old')
        read(3,1850,end=1849)(depth(j,1),temp(1,j,1),j=1,increm+1)
1850    format(2f7.2)
1849    k=0.008
        close(3)

        do 1904,c=1,col
        do 1903,j=1,120
        if (j.le.increm+1) temp(1,j,c)=temp(1,j,1)
        if (j.gt.increm+1) temp(1,j,c)=tbase
        if (j.le.increm+1) depth(j,c)=depth(j,1)
        if (j.gt.increm+1) depth(j,c)=(j-1)*dx
1903    continue
1904    continue
        go to 71

1901  do 49, c=1,col
      do 50, j=1,120
         m2=real(j-1)
         depth(j,c)=m2*dx
         if (resp.eq.1) go to 51

C       ...for discontinuous geotherm
        do 150,i=1,disc
           if (depth(j,c).le.ddisc(1)) f=tabov(1)*(dx/ddisc(1))*m2
           if (depth(j,c).gt.ddisc(disc)) go to 149
           if (depth(j,c).gt.ddisc(i) .and. depth(j,c).le.ddisc(i+1))
     , +f=(tat(i)-tabov(i+1))/(ddisc(i)-ddisc(i+1)+dx)*(depth(j,c)-
     +ddisc(i)-dx)+tat(i)
           go to 148
149        f=(tbase-tat(disc))/(x-ddisc(disc)-dx)
     +*(depth(j,c)-ddisc(disc)-dx)+tat(i)
148     k=0.008
```

```
150     continue
        go to 53

C       ...for linear geotherm
51       f=(m2*tbase*dx)/x
         go to 53

C       ...for exponential geotherm
52       f=tbase*((1-exp(-m2*dx/(k*100.)))/(1-exp(-x/(k*100.))))
53       temp(1,j,c)=f

C       ...temp. at base of lithosphere must be tbase
         if (depth(j,c).gt.x) temp(1,j,c)=tbase
         if (pulse.ne.1) go to 215

C       ...temperature with pulse added
         do 216,i=1,pnum
         if (j.eq.idept(i)) temp(1,j,c)=ptemp(i)
216      continue
215     k=0.008
50    continue

      do 62, i=2,tincr+1
         temp(i,1,c)=temp(1,1,c)
         temp(i,increm+1,c)=temp(1,increm+1,c)
62    continue
49    continue

      go to 71

C       Geotherm initialization routine when analyzing several faults
146    open(9,file='nxt.st',form='formatted',status='old')
       do 480,j=1,increm+1
       read(9,143,end=294)(temp(1,j,c),c=1,cont)
143    format(4(f7.2))
480    continue

294    do 145,c=1,cont
       do 293,j=increm+2,120
       temp(1,j,c)=tbase
293    continue
145    continue
       close(9)

       do 880,c=cont+1,col
        do 881,j=1,120
        temp(1,j,c)=temp(1,j,cont)
881     continue
880    continue

71    write(*,70)
70    format ('Include radioactive heating? 1=pt.source, 2=linear gradie
     +nts, 3=no')
      read (*,65)yorn
65    format(i1)
      if (yorn.eq.1) goto 199
      if (yorn.eq.3) goto 818



C     ,   Radioactive heating routines
C                 linear extrapolation between several point sources

      write(*,72)
72    format('Enter no. of pts at which you will specify radio heating')
      read(*,74)pts
```

```
74     format(i3)
       write(*,76)
76     format('Input radioactive term in units of cal/cc-sec, space, then
      +the depth for which this figure applies.  The first value must be
      +for 0 km (surface) depth, followed by your number of points, then the
      +value for the base of the lithosphere. for columns:')
       write(2,73)
73     format(/'Radioactivity values:')
       do 78, i=1,pts+2
          read(*,79)radio(i,1),dept(i,1)
79        format(f4.1,f5.1)
          write(7,75)radio(i,1),dept(i,1)
75        format(5x,f5.2,' cal/sec cm**3 at ',f5.1,' km')
          number(i,1)=dept(i,1)/dx+1.0
78     continue

         do 1650,c=1,col
          do 1649, i=1,pts+2
          radio(i,c)=radio(i,1)
          dept(i,c)=dept(i,1)
          number(i,c)=number(i,1)
1649     continue
1650     continue

            do 85, i=1,pts+1
            slope(i,1)=(radio(i+1,1)-radio(i,1))/(dept(i+1,1)-
     +dept(i,1))
            b(i,1)=radio(i,1)-slope(i,1)*dept(i,1)
85          continue
            do 86, i=1,pts+1
            j1=int(number(i,1))
            j2=int(number(i+1,1))
               do 95, w=j1,j2-1
               radio(w,1)=slope(i,1)*depth(w,1)+b(i,1)
               radio1(w,1)=radio(w,1)*dtsec*k/cond
95             continue
86          continue
          temp(1,1,1)=0.0
          do 417,c=1,col
          do 100, j=1,increm+1
          radio1(j,c)=radio1(j,1)
          temp(1,j,c)=temp(1,j,c)+radio1(j,c)
100       continue
         write(*,435)(radio1(w,c),w=1,increm+1)
435      format(10(f7.4))
417      continue
       go to 818


C        Radioactive with point sources, no linear gradients between
c         rad = heat production due to point source
c        deep = depth of point source
c       ptsrc = temperature chg. due to point source

199    write(*,395)
395    format('How many columns have a point source for radioactivity')
       read(*,415)rcol
415    format(i2)
       do 416,c=1,rcol
       write(*,200)c
200    format('Input radioactivity & depth of point source for column'
      +,i2)
       read(*,210)rad(c),deep
210    format(f4.2,f5.2)
       write(7,220)deep,rad(c)
220    format('Heating due to pt. source at',f5.2,'km is',f4.2,'
```

```
     +cal/cc-sec')
      i2(c)=int((deep(c)/dx)+1.0)
      radio1(i2(c),c)=rad(c)*dtsec*k/cond
      temp(1,i2(c),c)=temp(1,i2(c),c)+radio1(i2(c),c)
        do 495,j=1,increm+1
        if (j.ne.i2(c)) radio1(j,c)=0.0
495     continue
416   continue

C       Pure shear extension of lithosphere
c        calculate amount of time to extend lithosphere and
c        amount to extend by in each increment of that time in
c        order to get a net extension of "xtend" % over the entire
c        time interval.

C              beta = lower crust extensional parameter
C             gamma = upper crust extensional parameter
c            deltat = (delta-t) time of extension = tend-tinit
c             tinit = input initial time of extension
c              tend = input ending time of extension
c             ia,ib = indices to indicate which array element to read
c            depth2 = storage array for depths to horizons after extension
c              diff = time period of extension
c               sum = indexing variable

818   beta=1.0+loxten
      gamma=1.0+upxten
      deltat=tend-tinit
      ia=int(tinit/dt)+1
      ib=int(tend/dt)+1
      diff=ib-ia
      add(1)=0.0
      do 919,c=1,col
      lthick(c)=x-decoll(c)
      if (c.eq.1) go to 723
      do 722,j=1,120
      horiz(1,j,c)=sumlat(c)
722   continue

723   d(c)=int(decoll(c)/dx)+1
      do 819, sum=0,diff
        dbeta(sum+1)=dt*loxten/(deltat+(sum*dt*loxten))+1.0
        dgamma(sum+1)=dt*upxten/(deltat+(sum*dt*upxten))+1.0
        add(sum+2)=add(sum+1)+(sumlat(2)*(1.0-1.0/dbeta(sum+1)))
        if (d(c).eq.1) go to 884

        do 820,j=1,d(c)
        if (sum.gt.0) go to 816
        depth2(1,j,c)=depth(j,c)/dgamma(sum+1)
        go to 817
816     depth2(1+sum,j,c)=depth2(sum,j,c)/dgamma(sum+1)
817     horiz(sum+2,j,c)=horiz(sum+1,j,c)*dgamma(sum+1)

820     continue

884     lthick(c)=lthick(c)/dbeta(sum+1)
        if (d(c).eq.1) depth2(1+sum,d(c),c)=0.0
        depth2(1+sum,increm+1,c)=lthick(c)+depth2(1+sum,d(c),c)
        ddepth(c)=lthick(c)/(increm+1-d(c))
        sum1=0
        do 821,j=d(c),120
        depth2(1+sum,j,c)=depth2(1+sum,d(c),c)+sum1*ddepth(c)
        horiz(sum+2,j,c)=horiz(sum+1,j,c)*dbeta(sum+1)
        sum1=sum1+1
821     continue
819     continue
```

```
919     continue


c.....iteration/calculation of thermal structure
c          use carslaw and jaeger finite difference equation to
c          determine temperature structure. extend the lithospheric
c          plate, extrapolate between temperature elements to find
c          the new temperatures at the original depth levels. repeat
c          the loop until extension has finished.  then continue iterating
c          to adjust the geotherm to equilibrium value after several
c          hundred million years.

c                    temp2 = storage array for newly calc. temp.
c                    temp3 = temperature array for printout temperatures
c                        m = slope storage array for extrapolating t
c                       b1 = intercept storage array for extrapolating t
c                  n1,n2,n4 = indexing variables
c                  sum,sum1 = do loop lap counters


81     do 957, c=1,col
       sum=0
       vert1=0.0
       sum2=1
       do 80, i=1,tincr+1,1

c      do not execute the following statements if extension has been
c      completed (i.e. the extensional time parameters do not meet the
c      prescribed conditions.)

       if ((i+1).lt.ia .or. (i+1).gt.ib) go to 788

c      extrapolate between temperatures calculated above:  find
c      lines between two adjacent temperature points and solve for
c      the temperature at the printout depths.
         do 910,n1=2,120
          do 905,n=1,increm+1
          if (depth2(1+sum,n1,c).le.depth(n+1,c) .and.
     +depth2(1+sum,n1,c).ge.depth(n,c)) n4=n
905       continue
901        if (n1.le.d(c)) thin=dgamma(sum+1)*depth(n4,c)
          if (n1.gt.d(c)) thin=dbeta(sum+1)*depth(n4,c)+
     +(dgamma(sum+1)-dbeta(sum+1))*depth2(1+sum,d(c),c)
          n6=int(thin/dx+1.0)
          m(n4,c)=(temp(i,n6+1,c)-temp(i,n6,c))/dx
          b(n4,c)=temp(i,n6,c)-m(n4,c)*depth(n6,c)
          temp2(1+sum,n4,c)=m(n4,c)*thin+b(n4,c)
904      if (n1.ne.d(c)) go to 902
         temp2(1+sum,n4,c)=m(n4-1,c)*thin+b(n4-1,c)
902        k=0.008
910        continue

         if (c.eq.1) go to 94

         do 532,n1=1,increm+1
        if (c.ne.2) go to 542
        strtch=horiz(sum+2,n1,2)-add(sum+2)
        go to 543
542     strtch=horiz(sum+2,n1,c)-horiz(sum+2,n1,c-1)
543     m(n1,c)=(temp2(1+sum,n1,c)-temp2(1+sum,n1,c-1))/strtch
        b(n1,c)=temp2(1+sum,n1,c)-m(n1,c)*horiz(sum+2,n1,c)
        if (n1.le.d(c)) go to 537
        temp6(1+sum,n1,c)=m(n1,c)*sumlat(c)/dbeta(sum+1)+b(n1,c)
        go to 531
537     temp6(1+sum,n1,c)=m(n1,c)*sumlat(c)/dgamma(sum+1)+b(n1,c)
531     k=0.008
```

```
532    continue

c     incrementation routine within the times of extension

94      do 90, j=2,119
        if (j.gt.increm) go to 743
        if (c.eq.1) go to 713
        temp(i+1,j,c)=(k*dtsec*1000.0/(dx**2))*(temp6(1+sum,j+1,c)+
     +temp6(1+sum,j-1,c))-((2.0*k*dtsec*1000.0)/(dx**2)-1.0)*
     +(temp6(1+sum,j,c))
        go to 714
713     temp(i+1,j,c)=(k*dtsec*1000.0/(dx**2))*(temp2(1+sum,j+1,c)+
     +temp2(1+sum,j-1,c))-((2.0*k*dtsec*1000.0)/(dx**2)-1.0)*
     +(temp2(1+sum,j,c))
714     temp(i+1,j,c)=temp(i+1,j,c)+radio1(j,c)
        if (i2(c).eq.j) temp(i+1,i2(c),c)=temp(i+1,i2(c),c)+radio1(j,c)
        go to 967
743     temp(i+1,j,c)=tbase
967      k=0.008
90      continue

c      test if overlap of extension and fault movement
       if ((i+1).lt.ic) go to 744


       do 677,n1=2,d(c)+1
       if (temp(i,n1,c).eq.0.0) temp(i+1,n1,c)=0.0
677    continue

c      calculation of temperature at decollement
744     do 222,n1=2,increm+1
           do 223,n=1,increm
           if (depth2(1+sum,n1,c).le.depth(n+1,c) .and.
     +depth2(1+sum,n1,c).ge.depth(n,c)) n4=n
223        continue

        if (n1.ne.d(c)) go to 629
        if (n1.eq.d(c)) base(c)=(temp(i+1,n4,c)-temp(i+1,n4-1,c))/dx
        baseb(c)=temp(i+1,n4,c)-m(n1,c)*depth(n4,c)
        baset(c)=base(c)*depth2(1+sum,d(c),c)+baseb(c)
629     k=0.008
222     continue

        if (c.eq.1) go to 609
        if ((i+1).gt.id) go to 609

c      branch to another extrapolation loop
       go to 787

c     incrementation routine when no extension
788   do 91,j=2,119
      if ((i+1).lt.ib) go to 99
538   temp(i,j,c)=(k*dtsec*1000.0/(dx**2))*(temp(i-1,j+1,c)+
     +temp(i-1,j-1,c))-((2.0*k*dtsec*1000.0)/(dx**2)-1.0)*
     +(temp(i-1,j,c))

      if (j.ge.(increm+1)) temp(i,j,c)=tbase

      go to 97

99    temp(i+1,j,c)=(k*dtsec*1000.0/(dx**2))*(temp(i,j+1,c)+
     +temp(i,j-1,c))-((2.0*k*dtsec*1000.0)/(dx**2)-1.0)*
     +(temp(i,j,c))

        if (j.gt.d(c) .and. j.lt.increm+1) temp(i+1,j,c)=
     +temp(i+1,j,c)+radio1(j,c)
```

```
        do 525,v=1,pnum
        extra=temp(i,j,c)-temp(i+1,j,c)
        if (j.eq.idept(v)) temp(i+1,j,c)=temp(i+1,j,c)+extra*
     +exp(-(i-1)*dt/time)
525     continue

C       Assign temperature at base of lithosphere equal to constant
       if (j.ge.(increm+1)) temp(i+1,j,c)=tbase

97     k=0.008
91     continue

       if (c.eq.1 .and. (i+1).lt.ic) go to 789
       if((i+1).lt.ic) go to 789

       do 676,j=2,d(c)+1
       if ((i+1).lt.ib .and. (temp(i,j,c)).eq.0.0) temp(i+1,j,c)=0.0
       if ((i+1).ge.ib .and. (temp(i-1,j,c)).eq.0.0) temp(i,j,c)=0.0
676    continue

       if ((i+1).ge.id .and. (i+1).lt.ia) go to 789
       if (c.eq.1) go to 789

787     if ((i+1).lt.ia) h(c)=d(c)
        if ((i+1).ge.ia .and. (i+1).lt.ib) h(c)=int(depth2(sum+1,d(c),c)
     +/dx+1.0)
        if ((i+1).ge.ib) h(c)=int(depth2(ib-ia,d(c),c)/dx+1.0)

        do 670,n2=1,h(c)
         go to 1720
         r(n2,c)=(radio1(n2,c)-radio1(n2,c-1))/lat(c-1)
         q(n2,c)=radio1(n2,c)-r(n2,c)*lat(c-1)
         radio2(n2,c)=r(n2,c)*(lat(c-1)-ddisp)+q(n2,c)
1720     m(n2,c)=(temp(i+1,n2,c)-temp(i+1,n2,c-1))/(lat(c-1)+ddisp)
         temp5(n2,c)=temp(i+1,n2,c-1)+m(n2,c)*lat(c-1)
670     continue

        if ((i+1).lt.ia) angle(c)=atan(decoll(c)/sumlat(c))
        if ((i+1).ge.ia .and. (i+1).le.ib) angle(c)=
     +atan(depth2(sum+1,d(c),c)/sumlat(c))
        if ((i+1).gt.ib) angle(c)=atan(depth2(ib-ia,d(c),c)/sumlat(c))
        vert=ddisp*decoll(c)/sumlat(c)
        vert1=vert1+vert
        div=int((vert1+0.025)/dx)+1

        if ((i+1).le.ia .and. vert1.ge.(decoll(c)))
     + div=d(c)
        if ((i+1).gt.ib .and. vert1.gt.(depth2(ib-ia,d(c),c)+0.0001))
     + go to 609
        if ((i+1).lt.ia .or. (i+1).gt.ib) go to 611
        if (vert1.gt.depth2(sum+1,d(c),c)) go to 609
611     do 692,n6=1,div
        temp(i+1,n6,c)=0.0
         radio1(n6,c)=0.0
692     continue
        val=decoll(c)
        if (div.eq.d(c)) go to 609

        do 693,n6=div+1,h(c)
         go to 1710
        r1(n6,c)=(radio2(n6,c)-radio2(n6-1,c))/dx
        q1(n6,c)=radio2(n6,c)-r1(n6,c)*(val+(n6-h(c))*dx)
         radio1(n6,c)=r1(n6,c)*(val-vert+(n6-h(c))*dx)+q1(n6,c)

1710     if (n6.eq.(div+1)) temp(i+1,n6,c)=temp5(n6,c)-(temp5(n6,c)/
     +dx)*vert
```

```
      if (n6.eq.(div+1)) go to 1777
      m1(n6,c)=(temp5(n6,c)-temp5(n6-1,c))/dx
1999  if (yorn.ne.3 .and. x.eq.125.) go to 1700
      if (yorn.ne.3 .and. x.eq.120.) go to 1701
      temp(i+1,n6,c)=temp5(n6,c)-m1(n6,c)*vert
      go to 1777

     temp(i+1,n6,c)=m1(n6,c)*(val-vert+(n6-h(c))*dx)+b1(n6,c)+
    +radio1(n6,c)

1700  if (n6.gt.1 .and. n6.le.9) temp(i+1,n6,c)=temp5(n6,c)-
    +m1(n6,c)*vert+radio1(1,2)
      go to 1777
1701  if (n6.gt.1 .and. n6.le.7) temp(i+1,n6,c)=temp5(n6,c)-
    +m1(n6,c)*vert+radio1(1,2)
1777  k=0.008
693   continue

      sum2=sum2+1

609   if ((i+1).lt.ia .or. (i+1).ge.ib) go to 789
      sum=sum+1
      sum1=sum1+1
789   k=0.008


80    continue
      write(*,499)vert1,(radio1(j,c),j=1,increm+1)
499   format(9f8.5)
957   continue

      if (imbric.eq.1) go to 991
c     routine to print out data for individual columns
      open(9,file='nxt.st',form='formatted')
      k1=int((decoll(2)/lat(1)*disp+0.01)/dx)
      do 475,j=k1+1,increm+1
      write(9,292)(temp(tincr+1,j,c),c=break,col)
292   format(4(f7.2))
475   continue
      close(9)

991   write(*,61)
61    format('Do you want to print out geotherms for columns? 1=yes')
      read(*,67)p
67    format(i2)
      if (p.ne.1) go to 509
      write(*,380)
380   format('input times for which you want thermal data for each colum
    +n (14 times required) --- (7f6.2 on two lines)')
      read(*,381)(ctime(n),n=1,14)
381   format(7f6.2)

      do 391,a=1,14
      i5(a)=int((ctime(a)+0.05)/dt)+1.0
391   continue

      do 398, c=1,col
      write(11,384)c
384   format(//8x,'column',i3,':depth(km) vs time(my) profile of temper
    +ature (c)')
      write(11,425)decoll(c)
425   format(12x,'decollement at ',f5.2,'    km')
      write(11,385)(ctime(n),n=1,7)
385   format(//2x,'time(my)',7(10(1x,f6.1,2x)))

      do 386, j=1,increm+1
```

```
        write(11,387)depth(j,c)
387     format(f6.2,'km')
        write(11,388)(temp(i5(s),j,c),s=1,7)
388     format(9x(7(2x,f7.2)))
386     continue

       write(11,612)(ctime(n),n=8,14)
612    format(////2x,'time(my)',7(10(1x,f6.1,2x)))

          do 613,j=1,increm+1
          write(11,623)depth(j,c)
623       format(f6.2,'km')
          write(11,614)(temp(i5(s),j,c),s=8,14)
614       format(9x(7(2x,f7.2)))
613       continue

398    continue

c      routine to print out extensional parameters, radioactivity etc.
509    write(7,510)x,dt,dx,time,100.0*upxten,gamma,100.0*loxten,beta,
     +tinit,tend,disp,mbegin,mend
510    format(//'Lithospheric thickness: ',f6.2/,'Grid spacing: ',f3.1,
     +'my  by ',f4.1,'km'/,'Total iteration time: ',f6.2,'my'/,'% Extens
     +ion above decollement: ',f5.1,'   (gamma: ',f5.2,')'/,'% Extension
     + below decollement: ',f5.1,'   (beta: ',f5.2,')'/,'Extension betwe
     +en: ',f4.1,' my  and ',f4.1,' my'/,'Total movement on fault (measu
     +red along horizontal): ',f5.1,'km'/,'Movement along fault occurs b
     +etween: ',f4.1,' my and ',f4.1,' my'//)

       write(7,281)(dum(s),s=1,col)
281    format(5(5x,a,'________'))
       do 276, i=1,15
       if (i.eq.5) go to 274
       write(7,275)(dum(s),s=1,col)
275    format(5(5x,a,'¦',6x,'¦'))
       go to 271
274    write(7,277)(decoll(s),s=1,col)
277    format(5(6x,'¦',f6.1,'¦'))
271    k=0.008
276    continue
       write(7,278)(dum(s),s=1,col-1)
278    format(7x,4(a,'-------------->'))
       write(7,279)(sumlat(s),s=1,col)
279    format(6x,f5.1,4(10x,f5.1))


         write(*,1790)
1790     format('Create an intermediate geotherm plotting file? 1=yes')
         read(*,1795)answ
1795     format(i1)
         if (answ.ne.1) go to 1100

         write(*,1800)
1800     format('How many geotherms do you want to plot on one graph?')
         read(*,1810)pl
1810     format(i2)
         write(*,1820)
1820     format('Input column number of the geotherms and times')
         read(*,1830)(c3(i),ctime(i),i=1,pl)
1830     format(10(i2,f5.2))
         do 1840,i=1,pl
         i5(i)=int(ctime(i)/dt)+1
1840     continue


         write(*,1805)
```

```
1805    format('What do you want to call the intermediate temp. file?')
        read(*,1807)name
1807    format(a7)
        open (4,file=name,form='formatted')

        do 8410,j=1,increm+1
        write(4,8400)depth(j,1),(temp(i5(i),j,c3(i)),i=1,p1)
8400    format(11f7.2)
8410    continue
        close(4)

1100   count=1
c      routine to print out temperature, depth, and time path of specific
c      rock parcel
551    write(*,319)
319    format('print out specific t-t-depth information for a rock parcel?
     + 1=yes, 2=no')
       read(*,331)yorn
331    format(i1)
       if (yorn.eq.2) go to 790
409    write(*,332)
332    format('input no. of "parcels" for which you want information:')
       read(*,333)npts
333    format(i2)
       write(*,397)
397    format('input column number of the rock "parcels"')
       read(*,371)c1
371    format(i2)
       write(*,334)
334    format('input original depths of "parcels" (f5.1)')
       read(*,335)(parcel(i),i=1,npts)
335    format(20(f5.1))
       if (count.eq.1) go to 403
       write(*,399)
399    format('Use the same time printout increms. as last time? 1=yes')
       read(*,401)v1
401    format(i1)
       if (v1.eq.1) go to 402
403    write(*,336)
336    format('input no. of time increments for which you want values')
       read(*,337)tpts
337    format(i2)
       write(*,338)
338    format('input the times: 13(f5.1)')
       read(*,339)(tprint(i),i=1,tpts)
339    format(13(f5.1))
402    do 340,i=1,npts
       n3(i)=int(parcel(i)/dx)+1
340    continue
       if (v1.eq.1) go to 404
       do 341,i=1,tpts
       i3(i)=int((tprint(i)+0.05)/dt)+1
341    continue
       count=count+1

404    sum=1
       do 352,i=1,tpts
          n=i3(i)
       if (n.lt.ia .or. n.ge.ib) go to 356
       g=(n-ia+1)

C        Calculate depths and temperatures for times within pure shear
C                extensional period

C                (There are ways to consolidate the following string of
C                        "if" statements.  These will be modified in later
```

```
C                    versions of this program.)

C       Horizontal linear extrapolation of temperatures
        do 702,n1=1,increm+1
        if (c1.eq.1) go to 717
        if (n.ge.ic .and. n.lt.id) go to 421
        if (n1.gt.d(c1)) sumh=horiz(g+1,n1,c1)
        if (n.ge.id) sumh=sumlat(c1)+disp
        if (n.lt.ic) sumh=horiz(g+1,n1,c1)
        if (n.ge.id .and. n1.gt.d(c1)) sumh=horiz(g+1,n1,c1)
        go to 711

421     if (n1.le.d(c1)) sumh=sumlat(c1)+ddisp*(ia-ic)
        if (n1.gt.d(c1)) sumh=sumlat(c1)

423     do 422,j=1,g
        if (n1.le.d(c1)) sumh=sumh*dgamma(j)
        if (n1.gt.d(c1)) sumh=sumh*dbeta(j)
422     continue
        if (n1.le.d(c1) .and. n.lt.id) sumh=sumh+ddisp*(n-ia+1)

        go to 711
717     if (n.ge.ic .and. n.lt.id) sumh=add(g+1)+ddisp
        if (n.ge.id) sumh=add(g+1)+disp
        if (n.lt.ic) sumh=add(g+1)
        if (n1.gt.d(c1)) sumh=add(g+1)

711        do 772,c2=1,col
        if (sumh.ge.sumlat(c2) .and. sumh.le.sumlat(c2+1)) a=c2
        if (sumh.ge.sumlat(col)) a=col-1
772     continue

        if (a.eq.1) m(n1,a)=(temp(n,n1,2)-temp(n,n1,1))/lat(1)
        if (a.eq.1) go to 703
718     m(n1,a)=(temp(n,n1,a+1)-temp(n,n1,a))/lat(a)
703     b(n1,a)=temp(n,n1,a)
        temp3(sum,n1,a)=m(n1,a)*(sumh-sumlat(a))+b(n1,a)
        xprint(i,n1)=sumh
        if (n1.lt.d(a)) go to 755
        if (xprint(i,n1).ne.xprint(i,d(c1))) temp4(sum,n1,c1)=
     +m(n1,a)*(xprint(i,d(c1))-sumlat(a))+b(n1,a)
755     k=0.008
702     continue

C       Vertical linear extrapolation of temperatures
        do 933,n1=2,increm+1
         if (n.lt.ic) sumgam=decoll(c1)/sumlat(c1)*xprint(i,n1)
         if (n.ge.ic .and. n.lt.id) sumgam=decoll(c1)/sumlat(c1)*
     +ddisp*(n-ic+1)
        if (n.ge.id) sumgam=decoll(c1)/sumlat(c1)*disp
        sumbet=depth(n1,c1)-decoll(c1)/sumlat(c1)*xprint(i,n1)
        upthin=decoll(c1)/sumlat(c1)*xprint(i,n1)-sumgam

       do 280,j=1,g
       sumbet=sumbet/dbeta(j)
       upthin=upthin/dgamma(j)
280    continue

       do 937,n2=2,increm+1
       if (n.ge.ic) go to 730
       go to 731
730    if (n1.gt.d(c1)) dprint(i,n1)=depth2(g,n1,c1)
       if (n1.le.d(c1)) dprint(i,n1)=depth2(g,n1,c1)
       if (n1.gt.d(c1)) dprint2(i,n1)=depth2(g,n1,c1)-(decoll(c1)
     +-upthin)
       if (n1.le.d(c1)) dprint2(i,n1)=depth2(g,n1,c1)+sumgam
```

```
731     if (dprint2(i,n1).lt.depth(n2,1) .and.
     +dprint2(i,n1).ge.depth(n2-1,1)) n4=n2
937     continue
936     m(n1,c1)=(temp3(sum,n4,c1)-temp3(sum,n4-1,c1))/dx
        b1(n1,c1)=temp3(sum,n4,c1)-m(n1,c1)*depth(n4,c1)
        temp7(sum,n1,c1)=m(n1,c1)*(dprint2(i,n1))+b1(n1,c1)
        if (dprint2(i,n1).ge.decoll(a) .and. n1.le.d(a)) go to 21
        go to 32
31      if (n4.eq.(d(c1)+1)) go to 29
        m(n1,c1)=(temp4(sum,n4,c1)-temp4(sum,n4-1,c1))/dx
        go to 27
29      m(n1,c1)=(temp4(sum,n4,c1)-temp3(sum,n4-1,c1))/dx
27      b1(n1,c1)=temp4(sum,n4,c1)-m(n1,c1)*depth(n4,1)
        temp7(sum,n1,c1)=dprint2(i,n1)*m(n1,c1)+b1(n1,c1)
32      k=0.008

933     continue
        go to 682


C       Calculate depths and temperatures for times not within period of
C               pure shear extension


C       Lateral linear extrapolation of temperatures
356      do 502,n1=1,increm+1
         if (n.ge.ic .and. n.lt.id) go to 521
         if (n.ge.id) go to 3020
         if (n.lt.ic) sumh=sumlat(c1)
         suma=sumh
         go to 511
3020     if (n.ge.id) sumh=sumlat(c1)+disp
         suma=sumlat(c1)+disp
         if (n.ge.id .and. n1.gt.d(c1)) sumh=sumlat(c1)
         go to 511
521      if (n1.le.d(c1)) sumh=sumlat(c1)+ddisp*(n-ic+1)
         suma=sumlat(c1)+ddisp*(n-ic+1)
         if (n1.gt.d(c1)) sumh=sumlat(c1)

511      if (n1.le.d(c1) .and. c1.ne.1) go to 582
         if (n.ge.ib .and. n1.gt.d(c1)) sumh=beta*sumh
         if (n.ge.ib .and. c1.eq.1) sumh=add(ib-ia+1)+sumh
         go to 581

582      if (n.ge.ib) sumh=gamma*sumh
         if (n.ge.ib .and. ib.le.id) sumh=gamma*(sumlat(c1)+ddisp
     +*(ia-ic))+ddisp*(n-ia+1)

581       do 514,c2=1,col
         if (suma.ge.sumlat(c2) .and. suma.le.sumlat(c2+1)) a=c2
         if (suma.ge.sumlat(col)) a=col-1
514      continue

         if (a.eq.1) m(n1,a)=(temp(n,n1,2)-temp(n,n1,1))/lat(1)
         if (a.eq.1) go to 503
513      m(n1,a)=(temp(n,n1,a+1)-temp(n,n1,a))/lat(a)
503      b(n1,a)=temp(n,n1,a)
         temp3(sum,n1,c1)=m(n1,a)*(suma-sumlat(a))+b(n1,a)
         xprint(i,n1)=sumh
         if (n1.lt.d(a)) go to 555
         if (xprint(i,n1).ne.xprint(i,d(c1))) temp4(sum,n1,c1)=
     +m(n1,a)*(xprint(i,d(c1))-sumlat(a))+b(n1,a)
555      k=0.008
502      continue

        do 644,n1=2,increm+1
```

```
      do 14, c2=1,col
      if (suma.ge.sumlat(c2) .and. suma.le.sumlat(c2+1)) a=c2
      if (suma.ge.sumlat(col)) a=col
14    continue

C     Vertical linear extrapolation of temperatures

C     If pure shear extension has not been completed, execute this
C           sequence then exit to end of DO loop
      do 641,n2=2,increm+1
      if (c1.eq.1) vert=0.0
      if (c1.eq.1) go to 833
      if (n.ge.ic) go to 830
      go to 833
830   if (n.lt.id) vert=(decoll(c1)/sumlat(c1))*ddisp*(n-ic+1)
      if (n.ge.id) vert=(decoll(c1)/sumlat(c1))*disp
      if (vert.gt.decoll(c1) .and. n1.gt.d(c1)) vert=decoll(c1)
      if (vert.gt.decoll(c1) .and. n1.le.d(c1)) vert=vert
      if (n.lt.ic) vert=0.0
833   if (n.ge.ib) go to 832
      vertic=vert
      if (n.lt.ic) vert=0.0
      if (n1.gt.d(c1)) dprint(i,n1)=depth(n1,c1)-vert
      if (n1.le.d(c1)) dprint(i,n1)=depth(n1,c1)
      if (n1.gt.d(c1)) dprint2(i,n1)=depth(n1,c1)
      if (n1.le.d(c1)) dprint2(i,n1)=depth(n1,c1)+vert
836   if (dprint2(i,n1).lt.depth(n2,1) .and.
     +dprint2(i,n1).ge.depth(n2-1,1)) n4=n2

      go to 831

C     If pure shear extension has been completed, execute this sequence
C           to calculate new depths
832   if (n.lt.ic) sumgam=0.0
      if (n.ge.ic .and. n.lt.id) sumgam=decoll(c1)/sumlat(c1)*
     +ddisp*(n-ic+1)
      if (n.ge.id) sumgam=decoll(c1)/sumlat(c1)*disp
      sumbet=depth(n1,c1)-decoll(c1)/sumlat(c1)*xprint(i,n1)
      upthin=decoll(c1)/sumlat(c1)*xprint(i,n1)-sumgam
      if (upthin.lt.0.0) upthin=0.0

      if (n1.gt.d(c1)) dprint(i,n1)=depth2(ib-ia,n1,c1)
      if (n1.le.d(c1)) dprint(i,n1)=depth2(ib-ia,n1,c1)
      if (n1.gt.d(c1)) dprint2(i,n1)=depth2(ib-ia,n1,c1)
      if (n1.le.d(c1)) dprint2(i,n1)=depth2(ib-ia,n1,c1)
      if (dprint2(i,n1).lt.depth(n2,a) .and.
     +dprint2(i,n1).ge.depth(n2-1,a)) n4=n2

831   k=0.008
641   continue

      if (n1.le.d(c1)) go to 19
      if (n.ge.ib) go to 19
      temp7(sum,n1,c1)=temp(n,n1,c1)
      go to 834
19    m(n1,c1)=(temp3(sum,n4,c1)-temp3(sum,n4-1,c1))/dx
      b1(n1,c1)=temp3(sum,n4,c1)-m(n1,c1)*depth(n4,1)
      temp7(sum,n1,c1)=m(n1,c1)*dprint2(i,n1)+b1(n1,c1)
      go to 834
      if (dprint2(i,n1).ge.decoll(a) .and. n1.le.d(a)) go to 21
      go to 834
      if (n4.eq.(d(c1)+1)) go to 21
      go to 834
      m(n1,c1)=(temp4(sum,n4,c1)-temp4(sum,n4-1,c1))/dx
     go to 834
21    m(n1,c1)=(temp4(sum,n4,c1)-temp3(sum,n4-1,c1))/dx
```

```
22      b1(n1,c1)=temp4(sum,n4,c1)-m(n1,c1)*depth(n4,1)
        temp7(sum,n1,c1)=dprint2(i,n1)*m(n1,c1)+b1(n1,c1)

834     k=0.008
644     continue
682     sum=sum+1
352     continue


C       Print calculated depths and temperatures into output file
C               "words".  Print same values into a plotting file named
C               by user.

      write(7,372)c1,decoll(c1)
372   format(/'COLUMN ',i3,' Decollement at: ',f5.2,' km')
      do 343, j=1,npts
      write(7,342)parcel(j)
342   format(//'Rock parcel originally at ',f6.2,' km:')

      do 377, i=1,tpts
      write(7,344)tprint(i),temp7(i,n3(j),c1),dprint(i,n3(j)),
     +xprint(i,n3(j))
344   format('at time ',f5.1,'my,  temp = ',f7.2,'  depth= ',f6.2, 'km
     +xdist= ',f6.2,' km')
377   continue

343   continue

        write(*,500)
500     format('What do you want to call the path data file?')
        read(*,501)string
501     format(a10)

      open(8,file=string,form='formatted')
      write(8,844)(tprint(i),(temp7(i,n3(j),c1),dprint(i,n3(j)),
     +j=1,4),i=1,tpts)
844   format(9(f7.2))

C       This loop for use with subroutine sgeoplot.f only.
      do 843,i=1,tpts
      do 445,j=1,4
      z(i,j)=temp7(i,n3(j),c1)
      y(i,j)=dprint(i,n3(j))
445   continue
843   continue

      close(8)

C     Loop to allow user to input new points and times
      write(*,407)
407   format('Input new points and times? 1=yes, 2=no')
      read(*,408)yorn
408   format(i1)
      write(7,411)
411   format(//)
      if (yorn.ne.2) go to 409
790   k=0.008

C       End of do loop started at beginning of program;  loop back to
C               beginning for the analysis of imbricate fault structures.
1     continue



C       Graphics output routines
```

```
      write(*,575)
575   format('Do you want graphics output? 1=yes, 2=no')
      read(*,576)answ
576   format(i1)
      if (answ.ne.1) go to 552

      write(*,577)
577   format('Do you want to plot rock paths(1) or geotherms(2)')
      read(*,578)answ
578   format(i1)
      if (answ.eq.1) go to 553
      write(*,180)
180   format('How many geotherms do you want to plot on one graph?')
        read(*,181)pl
181     format(i2)
        write(*,182)
182     format('Input column number of the geotherms and times')
        read(*,183)(c3(i),ctime(i),i=1,pl)
183     format(10(i2,f5.2))
        do 184,i=1,pl
        i5(i)=int(ctime(i)/dt)+1
184     continue

C       Create plotting file for geotherms

        open (4,file='plot.dat',form='formatted')
        do 841,j=1,increm+1
        write(4,840)depth(j,1),(temp(i5(i),j,c3(i)),i=1,pl)
840     format(11f7.2)
841     continue
        close(4)

        go to 430

C     Sorting routine to determine maximum depth and temperature for
C               scaling of rock path plot

553   tmax=0.0
      dmax=0.0

851   do 846,i=1,tpts
      if (z(i,1).gt.tmax) tmax=z(i,1)
      if (y(i,1).gt.dmax) dmax=y(i,1)
846   continue
      write(*,15)tmax,dmax,dx,tpts
15    format(4f7.2)

C     Call to plotting routine for rock paths
            call geopath(tmax,dmax,dx,tpts)

C     Call to geotherm plotting routine
430           call geoplot(tbase,x,dx,increm+1,pl)

552   close(7)
      close(11)
      end
```

A.2 Subroutine sgeoplot.f

This subroutine uses an internal data file produced by **formodel.f** to produce plots of geotherms at time intervals chosen by the user. The program includes calls to the subroutine **marker.f** listed below and to **penplot**, a graphics library available at MIT.

```
C       * * * * * * * * * * SUBROUTINE GEOPLOT * * * * * * * * * * * * *

C       This subroutine connects to the main program and uses an internal
C               data file created by formodel.f to generate plots of
C               geotherms at time intervals chosen by the user.

        subroutine geoplot(tmax,dmax,dx,inc,mnum)
        character*8 variable
        integer b,e,f,i,k,j,flag
        character*5 xaxis(15),yaxis(15)
        character*25 lab
        character*10 temp
        character*12 depth
        real r,c,g,sfine
        real x(75,10),y(75),xsm(75,10),ysm(75)
        open(unit=4,file='plot.dat',status='old')
        temp='TEMP. (C) '
        lab='PLOT OF GEOTHERMS'
        depth='DEPTH   (km)'

        do 100,i=1,15
        xaxis(i)=' '
        yaxis(i)=' '
100     continue

C       Calculation of parameters for tick marks
        b=int(tmax/100.0)
        if (b.lt.16) go to 5
        b=b*0.5
        flag=1
        go to 7
5       flag=0
7       r=380.0/b
        e=int(dmax/(dx*10.0))
        f=int(dmax/(dx*2.0))
        sfine=380.0/f

C       Call to the subroutine that creates labels for the axes
        call marker(b,e,xaxis,yaxis,flag)

C       Beginning of call sequence to penplot library.
        call terminal(7)
        call show(-225.,225.,-225.,225.)
        call pen(1)

C       Draw axes for the graph
        call move(-190.,190.)
        call draw(-190.,-190.)
        call move(-190.,190.)
        call draw(190.,190.)
```

```
C       Draw tick marks for the axes
        do 15,i=1,b
        c=real(i*r)
        call move(-190.0+c,193.)
        call draw(-190.0+c,190.)
        call move(-197.0+c,205.)
        call letter(2.5,0.5,0.0,0.0)
        call label(xaxis(i))
15      continue

        do 25,i=1,f
        g=real(i*sfine)
        if (mod(i,5).eq.0.0) go to 30
        call move(-192.0,190.0-g)
        call draw(-190.0,190.0-g)
        go to 35
30      j=i/5
        call move(-194.0,190.0-g)
        call draw(-190.0,190.0-g)
        call move(-210.0,192.0-g)
        if (yaxis(j).lt.'100') yaxis(j)=yaxis(j)(2:4)
        call label(yaxis(j))
35      k=1
25      continue

C       Label the axes
        call move(192.0,180.0)
        call letter(3.,0.7,0.0,0.0)
        call label(temp)
        call move(-224.0,35.0)
        call letter(3.,.7,-90.,0.)
        call label(depth)

        call move(-100.0,-220.0)
        call letter(3.,.7,0.,0.)
        call label(lab)

C       Read data from the file created by formodel.f
        do 45,k=1,inc
        read(unit=4,fmt='(10f7.2)',end=75)ysm(k),
     +(xsm(k,i),i=1,mnum)
75      l=1
45      continue

C       Plot the geotherms
21      do 26,i=1,mnum
19      do 20,k=1,inc
        x(k,i)=380.0*(xsm(k,i)/tmax)-190.0
        y(k)=-380.0*(ysm(k)/dmax)+190.0
        call plot(x(k,i),y(k))
20      continue
        call penup
26      continue


46      call tsend(7)

C       Program will become "hung" here to allow user to view graph.
C       Any character typed in from the keyboard will terminate the
C               program.
        read*, variable

        call endplt(7)
        stop
        end
```

A.3 Subroutine sgeopath.f

This program produces very crude and unlabelled plots of cooling paths of rocks. Plots like those produced in the text can only be done using the RS/1 graphics package. This program connects with **formodel.f** and includes calls to the **penplot** library of FORTRAN plotting routines.

```
      subroutine geopath(tmax,dmax,dx,j)
      character*8 variable
      integer b,e,f,i
      character*5 temp,depth
      character*25 lab
      real r,c,g,k,sfine
      real x(75),y(75),xsm(75),ysm(75)
      open(unit=8,file='path.dat',status='old')
      temp='temp '
      lab='P-T PATHS OF ROCKS'
      depth='depth'
      call terminal(7)
      call show(-200.,200.,-200.,200.)
      call pen(1)
      call move(-190.,190.)
      call draw(-190.,-190.)
      call move(-190.,190.)
      call draw(190.,190.)

      b=int(tmax/100.0)+1
      r=380.0/b

      do 15,i=1,b
      c=real(i*r)
      call move(-190.0+c,193.)
      call draw(-190.0+c,190.)
      call move(-190.0+c,194.)
15    continue

      f=int(dmax/dx)
      sfine=380.0/f

      do 25,i=1,f
      g=real(i*sfine)
      if (mod(i,e).eq.0.0) go to 30
      call move(-192.0,190-g)
      call draw(-190.0,190-g)
      go to 35
30    call move(-194.0,190-g)
      call draw(-190.0,190-g)
35    k=0.008
25    continue

      call move(195.0,180.0)
      call label(temp)
      call move(-198.0,50.0)
      call letter(3.,.7,-90.,0.)
      call label(depth)

40    read(unit=8,fmt='(f7.2,f7.2)',end=39)(xsm(i),ysm(i),i=1,j)
39    do 45,i=1,j
      x(i)=380.0*(xsm(i)/tmax)-190.0
      y(i)=-380.0*(ysm(i)/dmax)+190.0
```

```
      call plot(x(i),y(i))
45    continue

      call move(50.0,120.0)
      call letter(3.,.7,0.,0.)
      call label(lab)

46    call tsend(7)
      read*, variable

      call endplt(7)
      stop

      end
```

A.4 Subroutine marker.f

This subroutine is responsible for generating the labels on the graphs produced by **sgeoplot.f** and the independent program **indplot.f**. The program involves simply the conversion of the desired numerical labels to characters, a task that can only be accomplished by using the internal symbols of the FORTRAN library.

```
C       * * * * * * * * * * * SUBROUTINE MARKER * * * * * * * * * *

C       This subroutine connects to plotting programs and merely
C               generates the labels for the graphs.

        subroutine marker(ia,ib,taxis,daxis,ik)
        integer symbol,step,dig1,dig2,dig3
        real s
        character*5 taxis(15),daxis(15)
        integer i,j,int,ic

C       Conversion of integer to character values using compiler's
C               internal string conversion code

C       Labelling routine for temperature axis
        if (ik.ne.1) go to 5
        if (ik.eq.1) ic=2*ia
        step=2
        int=2
        go to 15

5       step=1
        int=1
        ic=ia

15      do 10,i=int,ic,step
        symbol=48+i
        if (ik.eq.1) j=i/2
        if (ik.ne.1) j=i
        if (i.ge.10 .and. i.lt.20) go to 30
        if (i.ge.20) go to 35
        taxis(j)=char(symbol)//char(48)//char(48)
        go to 25
30      symbol=38+i
        dig1=49
        go to 27
35      if (symbol.ge.58) symbol=28+i
        dig1=50
27      taxis(j)=char(dig1)//char(symbol)//char(48)//char(48)
25      write(*,20)taxis(i)
20      format(a5)
10      continue

C       Labelling routine for depth axis
        do 40,i=1,ib
        symbol=i*25
        s=real(symbol)
        if (mod(s,10.0).eq.0.0) dig3=48
```

```
      if (mod(s,10.0).ne.0.0) dig3=53
      if (s.ge.100.0) dig1=49
      if (s.lt.100.0) dig1=31
      do 50,j=1,15
      if (symbol.ge.(j*10) .and. symbol.lt.(j+1)*10) dig2=48+j
50    continue
      if (s.ge.100.0) dig2=dig2-10
      daxis(i)=char(dig1)//char(dig2)//char(dig3)
      write(*,60)daxis(i)
60    format(a5)
40    continue
      return

      end
```

A.5 Program fourier.f

This program does a summation of the first twenty Fourier terms for a geotherm that is at the base temperature throughout the entire lithospheric thickness and at 0°C on the surface. Output is to the file "fourie".

```
C       .....................PROGRAM  FOURIER.F.........................

C       Program to do simple thermal relaxation models by Fourier methods.

        real a,x,tbase,t,pi,dx,tsec,k
        real four(20,60),sum(60),temp(60)
        integer inc,i,n,j
        open(8,file='fourie',form='formatted')

        write(*,10)
10      format('Input lithosphere thickness, depth increment, and
     + base T:')
        read(*,20)x,dx,tbase
20      format(f6.1,f4.1,f6.1)

30      write(*,40)
40      format('At what time should the expression be evaluated?')
        read(*,50)t
50      format(f6.2)

        inc=int(x/dx)+1
        k=0.008
        tsec=3155.27
        pi=3.14159

        do 60,i=2,inc
        sum(i)=0.0
        do 70,n=1,20
        a=real(n)
        four(n,i)=1.0/a*sin(n*pi*(i-1)*dx/x)*exp(-(n**2)*(pi**2)*k
     +*tsec*t/(x**2))
        sum(i)=sum(i)+four(n,i)
70      continue
60      continue

        write(8,75)t
75      format(/'At time ',f5.2,' my after the initial state:')
        do 80,i=1,inc
        if (i.eq.1) go to 85
        temp(i)=tbase*(i-1)*dx/x+(2.0*tbase/pi)*sum(i)
85      temp(1)=0.0
        write(8,90)(i-1)*dx,temp(i)
90      format(f6.1,'km',5x,f7.2)
80      continue

        write(*,100)
100     format('Input a new time?  1=yes')
        read(*,110)j
110     format(i1)
        if (j.eq.1) go to 30

        close(8)
        end
```

A.6 Program splining.f

This program, though of limited usefulness, fits splines to depth-temperature and time-temperature points generated by the **formodel.f**. It also produces two auxiliary files that are named by the user and include quantitative information about the plots. The first derivative is probably the most useful of the generated quantities, as this permits comparison of the depth-temperature or time-temperature gradients between curves that have different characteristics. The program reads from files formatted for the plotting routines by **formodel.f**. The spline values can be transferred over to **RS/1** for plotting directly on the particle path graphs. The program includes calls to the NAG (Numerical Algorithms Group) subroutine package.

```
C       Program to do cubic spline calculations between points of
C               temperature-depth curves
C               This program includes several calls to the nag library
C               available on the Athena system and must be compiled with
C               the -lnag option for the Fortran 77 compiler.
C               It is important to note that the number of intervals
C               used to calculate the cubic spline may not exceed
C               the number of points in the data file - seven.
C               The complicated printout routines at the end of this
C               file are adapted versions of the example program texts
C               provided in the nag library manual, copyright 1978 by the
C               nag corporation.

        logical midpt
        double precision temp2(25,55,5),dept(25,55)
        double precision wt(26),ord(26),abc(26),wk1(26)
        double precision wk2(4,26),c(15),k1(15)
        double precision ssq,fit,xarg,s(4)
        integer i,j,n,ifal,pass,part,divi,r,r2,num2,l,left,yorn
        character*7 str,str2,str3,str4

        write(*,77)
77      format('What do you want to call the info. output file?')
        read(*,78)str2
        write(*,79)
79      format('Name of derivative output file?')
        read(*,78)str4
78      format(a7)
        open(4,file=str2,form='formatted')
        open(10,file=str4,form='formatted')

4       write(*,5)
5       format('File to be splined?')
        read(*,7)str
7       format(a7)
```

```
      open(8,file=str,form='formatted',status='old')
      num=14
      do 10, i=num,1,-1
      read(8,25)(temp2(i,j,1),dept(i,j),j=1,4)
25    format(4(f7.2,f7.2))
10    continue

C     Set weights for splining = one
      do 30,i=1,num
      wt(i)=1.0
30    continue

      write(*,40)
40    format('Particle path to fit with cubic spline, 1-4?')
      read(*,45)part
45    format(i1)

C     Initialize the abscissa and ordinate values of function
      do 50,i=1,num
      abc(i)=temp2(i,part,1)
      ord(i)=dept(i,part)
50    continue

      write(*,55)
55    format('Splines should be fit using how many intervals?')
      read(*,60)n
60    format(i1)
      pass=n+8

      divi=int(num/n)
      do 65,i=divi,num-1,divi
      k1(i/divi+4)=abc(i)
      if ((i/divi).gt.n) go to 75
      write(*,70)k1(i/divi+4),ord(i)
70    format(2(f9.2))
75    p=3
65    continue

      write(4,83)str,part
      write(10,83)str,part
83    format(//'Input path file is',a8,'; particle ',i3)

      write(4,87)
87    format(/1x,'Point no.',8x,'Abscissa X(m)',3x,'Ordinate X(m)')
      do 85,i=1,num
      write(4,90)i,abc(i),ord(i)
90    format(5x,i2,3x,2e20.5)
85    continue
      call e02baf(num,pass,abc,ord,wt,k1,wk1,wk2,c,ssq,ifal)
      write(4,80)ssq
80    format(/'Residual sum of squares is = ',e20.5/)
      j=1
      write(4,100)j,c(1)
      do 110, j=2,n+3
      j2=j+2
      write(4,105)j,k1(j2),c(j)
105   format(1x,i3,2e20.5)
110   continue
      write(4,100)n+4,c(n+4)
100   format(1x,i3,20x,e20.5)

      midpt=.false.
      num2=2*num-1
      r=0
      write(4,125)
125   format(//1x,'Point no.',3x,'Abscissa X',8x,'Approximation',7x,
```

```
     +'Residual'/)
        write(*,600)
600     format('What do you want to call the spline plot output file?')
        read(*,610)str3
610     format(a7)

        open(11,file=str3,form='formatted')
        do 300,r2=1,num2
          if (.not.midpt) go to 280
          xarg=0.5*(abc(r)+abc(r+1))
          ifal=1
          call e02bbf(pass,k1,c,xarg,fit,ifal)
          if (ifal.ne.0) go to 260
          write(4,115)xarg,fit
          write(11,120)xarg,fit
          go to 320
260       write(*,117)xarg
          go to 320
280       r=r+1
          ifal=1
          call e02bbf(pass,k1,c,abc(r),fit,ifal)
          if (ifal.ne.0) go to 310
          res=fit-ord(r)
          write(4,118)r,abc(r),fit,res
          write(11,120)abc(r),fit
          go to 320
310       write(*,119)r,xarg
320       midpt=.not.midpt
300     continue
120     format(2e20.5)
115     format(5x,2e20.5)
117     format(5x,e20.5,'argument not in range')
118     format(1x,i3,3e20.5)
119     format(1x,i3,e20.5,'argument not in range')

        write(4,96)
        write(10,98)
96      format(//5x,'X',20x,'SPLINE',4x,'1st Deriv',2x,
     +'2nd Deriv',2x,'3rd Deriv')
        do 400,i=1,num
          do 450,left=1,2
          ifal=1
          call e02bcf(pass,k1,c,abc(i),left,s,ifal)
          if (ifal.ne.0 .and. left.eq.1) write(4,94)abc(i),ifal
          if (ifal.ne.0 .and. left.ne.1) write(4,93)abc(i),ifal
          if (ifal.eq.0 .and. left.eq.1) write(4,92)abc(i),
     +(s(l),l=1,4)
          if (ifal.eq.0 .and. left.eq.1) write(10,98)i,
     +(s(l),l=1,4)
          if (ifal.eq.0 .and. left.ne.1) write(4,91)abc(i),
     +(s(l),l=1,4)
450       continue
400     continue

91      format(1x,e11.3,6x,'right',4e11.3)
92      format(1x,e11.3,6x,'left ',4e11.3)
93      format(1x,e11.3,12x,'right','fail',i4)
94      format(1x,e11.3,12x,'left ','fail',i4)
98      format(2i,10x,4e11.3)
        close(11)
        close(8)
        write(*,500)
500     format('Run again? 1=yes')
        read(*,510)yorn
510     format(i1)
        if (yorn.eq.1) go to 4
```

```
stop
end
```

Appendix B
Sample Program Output

The following is an example of the textual output provided by a run of **formodel.f**. The problem parameters input by the user are listed at the beginning of the file, followed by a simple graphical representation of the fault geometry, and any depth-temperature-time information requested by the user.

```
*    *    *    *    *    SAMPLE TEXT OUTPUT *    *    *    *    *

      0.    cal/sec cm**3 at   0.  km
     11.00 cal/sec cm**3 at   2.5 km
     11.00 cal/sec cm**3 at  20.0 km        X10E-13
      0.    cal/sec cm**3 at  22.5 km
      0.    cal/sec cm**3 at 125.0 km


Lithospheric thickness: 125.00
Grid spacing: 0.1my  by  2.5km
Total iteration time:  50.00my
% Extension above decollement:    0.     (gamma:  1.00)
% Extension below decollement:    0.     (beta:  1.00)
Extension between: 49.9 my  and 50.0 my
Total movement on fault (measured along horizontal):  25.0km
Movement along fault occurs between:  0.1 my and 25.0 my
```

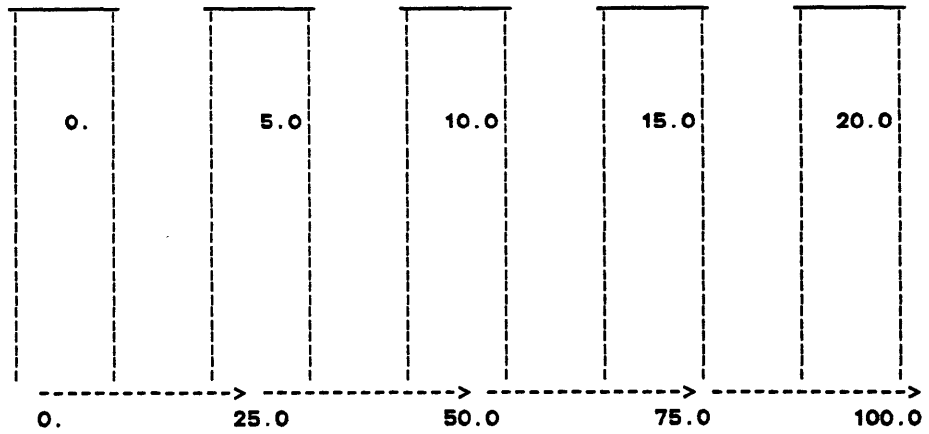


```
COLUMN   4 Decollement at: 15.00 km


Rock parcel originally at  15.00 km:
at time   0. my,  temp =  408.62  depth=  15.00km  xdist=  75.00 km
at time   1.0my,  temp =  384.37  depth=  15.00km  xdist=  76.00 km
at time   5.0my,  temp =  336.58  depth=  15.00km  xdist=  80.02 km
at time  10.0my,  temp =  313.45  depth=  15.00km  xdist=  85.04 km
```

```
at time  15.0my,  temp =  290.07  depth=  15.00km  xdist=  90.06 km
at time  20.0my,  temp =  268.31  depth=  15.00km  xdist=  95.08 km
at time  25.0my,  temp =  254.00  depth=  15.00km  xdist= 100.00 km
at time  30.0my,  temp =  231.93  depth=  15.00km  xdist= 100.00 km
at time  35.0my,  temp =  219.47  depth=  15.00km  xdist= 100.00 km
at time  49.9my,  temp =  278.54  depth=  15.00km  xdist= 100.00 km


Rock parcel originally at  20.00 km:
at time   0. my,  temp =  469.48  depth=  20.00km  xdist=  75.00 km
at time   1.0my,  temp =  459.00  depth=  19.80km  xdist=  75.00 km
at time   5.0my,  temp =  414.32  depth=  19.00km  xdist=  75.00 km
at time  10.0my,  temp =  385.12  depth=  17.99km  xdist=  75.00 km
at time  15.0my,  temp =  362.95  depth=  16.99km  xdist=  75.00 km
at time  20.0my,  temp =  341.51  depth=  15.98km  xdist=  75.00 km
at time  25.0my,  temp =  329.70  depth=  15.00km  xdist=  75.00 km
at time  30.0my,  temp =  306.84  depth=  15.00km  xdist=  75.00 km
at time  35.0my,  temp =  295.02  depth=  15.00km  xdist=  75.00 km
at time  49.9my,  temp =  278.54  depth=  15.00km  xdist=  75.00 km


Rock parcel originally at  50.00 km:
at time   0. my,  temp =  672.65  depth=  50.00km  xdist=  75.00 km
at time   1.0my,  temp =  673.37  depth=  49.80km  xdist=  75.00 km
at time   5.0my,  temp =  675.70  depth=  49.00km  xdist=  75.00 km
at time  10.0my,  temp =  673.09  depth=  47.99km  xdist=  75.00 km
at time  15.0my,  temp =  666.86  depth=  46.99km  xdist=  75.00 km
at time  20.0my,  temp =  659.39  depth=  45.98km  xdist=  75.00 km
at time  25.0my,  temp =  651.03  depth=  45.00km  xdist=  75.00 km
at time  30.0my,  temp =  642.92  depth=  45.00km  xdist=  75.00 km
at time  35.0my,  temp =  634.15  depth=  45.00km  xdist=  75.00 km
at time  49.9my,  temp =  611.57  depth=  45.00km  xdist=  75.00 km



COLUMN   2 Decollement at:  5.00 km


Rock parcel originally at  10.00 km:
at time   0. my,  temp =  311.38  depth=  10.00km  xdist=  25.00 km
at time   2.5my,  temp =  295.66  depth=   9.50km  xdist=  25.00 km
at time   5.0my,  temp =  289.97  depth=   9.00km  xdist=  25.00 km
at time  15.0my,  temp =  247.54  depth=   6.99km  xdist=  25.00 km
at time  25.0my,  temp =  216.39  depth=   5.00km  xdist=  25.00 km
at time  35.0my,  temp =  160.92  depth=   5.00km  xdist=  25.00 km
at time  45.0my,  temp =  155.80  depth=   5.00km  xdist=  25.00 km
at time  49.9my,  temp =  154.45  depth=   5.00km  xdist=  25.00 km


Rock parcel originally at  22.50 km:
at time   0. my,  temp =  478.89  depth=  22.50km  xdist=  25.00 km
at time   2.5my,  temp =  481.39  depth=  22.00km  xdist=  25.00 km
at time   5.0my,  temp =  478.11  depth=  21.50km  xdist=  25.00 km
at time  15.0my,  temp =  466.45  depth=  19.49km  xdist=  25.00 km
at time  25.0my,  temp =  440.88  depth=  17.50km  xdist=  25.00 km
at time  35.0my,  temp =  397.76  depth=  17.50km  xdist=  25.00 km
at time  45.0my,  temp =  382.86  depth=  17.50km  xdist=  25.00 km
at time  49.9my,  temp =  378.65  depth=  17.50km  xdist=  25.00 km


Rock parcel originally at  75.00 km:
at time   0. my,  temp =  866.97  depth=  75.00km  xdist=  25.00 km
at time   2.5my,  temp =  868.71  depth=  74.50km  xdist=  25.00 km
at time   5.0my,  temp =  870.39  depth=  74.00km  xdist=  25.00 km
at time  15.0my,  temp =  876.43  depth=  71.99km  xdist=  25.00 km
```

```
at time  25.0my,  temp =  880.57  depth=  70.00km  xdist=  25.00 km
at time  35.0my,  temp =  881.67  depth=  70.00km  xdist=  25.00 km
at time  45.0my,  temp =  879.11  depth=  70.00km  xdist=  25.00 km
at time  49.9my,  temp =  876.98  depth=  70.00km  xdist=  25.00 km
```

Acknowledgements

Funding for this project came from the Undergraduate Research Opportunities Program (UROP) during the summer of 1985. UROP paid the salary of the author during the period when the thermal-modelling program was in the initial stages of development. This study comprises the preliminary work for a project entitled "Thermal and Petrologic Effects of Uplift Related to Extensional Tectonics," funded by a National Science Foundation grant to Profs. Kip Hodges and Leigh Royden.

Several groups and individuals have helped in various aspects of this work. MIT's Project Athena and its employees, although a source of great frustration at times, deserve special acknowledgement; several employees of the Project have been particularly helpful, answering complicated queries on their own time, and, the free computing time, laser-printing, and graphics hard-copying offerred by Athena made this project a reality. Prof. Kip Hodges acted as unofficial advisor in the extended absence of Leigh Royden, and his willingness to answer questions, dispense advice, and read preliminary drafts of this thesis helped immeasurably. I am grateful for his patience, tolerance, and willingness to offer advice about various aspects of this study. Steve Recca also contributed technical advice to this project, offering excellent suggestions about troublesome programming and subroutine linkage problems. In addition, several MIT graduate students helped the author with practical questions about everything from using a microcomputer to producing final drafts of figures.

I would like to thank my parents who, during the past ten years, have made enormous sacrifices in all aspects of their lives for the sake of my education. I hope I can prove worthy of their investment in me. A. Bosh and especially P. Kim provided moral support and distractions throughout this past year, greeting a great deal of complaining with reassurances and optimism. P. Kim deserves special mention for having faithfully brought me lunch and words of encouragement during many ten and twelve hour stints in the computer room.

Finally, I gratefully acknowledge J. Hunt. She is almost solely responsible for my having continued to push forward academically, personally, and emotionally, and her friendship has sustained me through many tribulations and through the last harrowing weeks of finishing this thesis. It was she who assured me a year ago that I could, in fact, do this project, and she has fought unceasingly to boost my self-confidence and instill a sense of hope in me.